Spinal dI3 circuits in the modulation of skilled and corrective locomotor behaviours

Sarah Chiasson

A thesis submitted to the University of Ottawa in partial fulfillment of the requirements for the Master of Science in Biology

Department of Biology

Faculty of Science

University of Ottawa

Table of Contents

Abstract

Many spinal neurons integrate sensory input to adapt a wide array of movements. Prior research has shown that spinal dorsal interneuron 3 (dI3) neurons receive cutaneous and proprioceptive sensory input and that they project to motor circuits, most notably through excitation of motoneurons. We sought to better delineate the spinal circuits within which dI3 neurons operated. To reach this objective, we tested motor performance of transgenic mice where dI3s could be chemogenetically silenced by the DREADD receptor, *hM4Di*. Chemogenetic inhibition of dI3s was concomitant with drug treatments that putatively inhibited (mecamylamine) or enhanced (L-acetyl carnitine) recurrent motoneuron excitation of central targets such as Renshaw cells. In addition to these two cholinergic modulators, saline was also administered as a separate treatment to act as a control. Each of these three separate treatments were administered in combination with either JHU37160, an *hM4Di* agonist to silence dI3s, or a saline control to maintain dI3 activity. These mice were then tested on three behavioural tasks.

For performance related to fine motor control, balance, and coordination, mice were tested on a vibrating balance beam and horizontal ladder walking task. In both ladder and beam tasks, mice demonstrated an up to three-fold increase in the incidence of foot falls after dI3 inhibition with either L-acetyl carnitine or saline as a combined treatment. We also observed two- to three-fold increases in footfalls on the ladder and beam after mecamylamine administration, an antagonist of Renshaw cell excitation, in combination with dI3 silencing but also without dI3 silencing. Interestingly, ladder and beam tasks performed after a combined treatment that silenced both dI3s and Renshaw cell excitation did not appear to have a compounding effect in the observed motor deficits on these apparatuses; the increase in foot falls remained two to three-fold higher when comparing trials with and without dI3 silencing as combined with mecamylamine. Overall,

we observed an increase in motor deficits and difficulty when crossing both the ladder and beam after dI3 silencing and mecamylamine administration.

Additionally, mice were also tested on a treadmill apparatus wherein the hindlimb paw was either mechanically or electrically perturbed to attempt to trigger the stumbling corrective reaction. With L-acetyl carnitine and saline trials, dI3 silencing resulted in a significant reduction in the peak step height during a stumbling corrective response in comparison to trials without dI3 silencing. Conversely, the effects of dI3 inhibition and mecamylamine administration yielded a similar trend to the previous behavioural task, wherein step heights during the peak of the reflex were significantly reduced after dI3 silencing and/or mecamylamine administration compared to saline controls but were not statistically different when comparing trials with and without dI3 silencing if mecamylamine was also administered. While this reflex was not completely abolished, we observed significantly increased instances of failed attempts to clear the perturbation resulting in dragging and a significant blunting of the stumbling corrective response with both mecamylamine administration and dI3 silencing, both separately and together.

Overall, our findings support the hypothesis that dI3s are involved in the activation of the stumbling corrective response, wherein proprioceptive and cutaneous signals may be used to modulate the activation of muscles during locomotion. While there remains much to be understood about dI3 spinal circuits, it appears that a lack of dI3 signaling inhibits skilled locomotor behaviours. Our results suggest that dI3s are more involved in skilled and corrective motor behaviours than previously understood, as we suggest that Renshaw cells and dI3s may operate together within a type of neural comparator module to actively monitor sensory signals and rapidly adjust motor outputs. Our experiments begin to identify the spinal circuits within which dI3s operate to shape motor activity.

Résumé

De nombreux neurones spinaux intègrent des entrées sensorielles pour s'adapter à un large éventail de mouvements. Des recherches antérieures ont montré que les neurones spinaux interneurones dorsaux 3 (dI3) reçoivent des entrées sensorielles cutanées et proprioceptives et qu'ils se projettent dans les circuits moteurs, notamment par l'excitation des motoneurones. Nous avons cherché à mieux délimiter les circuits spinaux dans lesquels les neurones dI3 opéraient. Pour atteindre cet objectif, nous avons testé les performances motrices de souris transgéniques où les dI3 pouvaient être chimiogénétiquement réduits au silence par le récepteur DREADD, hM4Di. L'inhibition chimiogénétique des dI3 était concomitante à des traitements pharmacologiques qui inhibaient (mécamylamine) ou amélioraient (L-acétyl carnitine) l'excitation récurrente des motoneurones de cibles centrales telles que les cellules de Renshaw. En plus de ces deux modulateurs cholinergiques, une solution saline a également été administrée comme traitement séparé pour servir de contrôle. Chacun de ces trois traitements distincts a été administré en combinaison avec soit JHU37160, un agoniste hM4Di pour faire taire les dI3, soit un contrôle salin pour maintenir l'activité dI3. Ces souris ont ensuite été testées sur trois tâches comportementales.

Pour les performances liées au contrôle de la motricité fine, à l'équilibre et à la coordination, les souris ont été testées sur une poutre d'équilibre vibrante et une tâche de marche sur une échelle horizontale. Dans les deux tâches sur l'échelle et la poutre, les souris ont montré une augmentation jusqu'à trois fois de l'incidence des chutes de pieds après l'inhibition de dI3 avec soit de la L-acétyl carnitine soit une solution saline comme traitement combiné. Nous avons également observé une augmentation de deux à trois fois des chutes de pieds sur l'échelle et la poutre après l'administration de mécamylamine, un antagoniste de l'excitation des cellules de Renshaw, en combinaison avec la mise sous silence de dI3 mais aussi sans mise sous silence de

dI3. Il est intéressant de noter que les tâches sur l'échelle et la poutre effectuées après un traitement combiné qui a fait taire à la fois les dI3 et l'excitation des cellules de Renshaw ne semblent pas avoir d'effet aggravant sur les déficits moteurs observés sur ces appareils. L'augmentation des chutes de pieds est restée deux à trois fois supérieure lors de la comparaison des essais avec et sans silençage dI3 combiné à la mécamylamine. Dans l'ensemble, nous avons observé une augmentation des déficits moteurs et des difficultés à traverser l'échelle et la poutre après silençage dI3 et administration de mécamylamine.

De plus, les souris ont également été testées sur un appareil de tapis roulant dans lequel la patte du membre postérieur était perturbée mécaniquement ou électriquement pour tenter de déclencher la réaction corrective de trébuchement. Avec des essais à la L-acétyl carnitine et au sérum physiologique, le silençage dI3 a entraîné une réduction significative de la hauteur maximale de la marche lors d'une réponse corrective de trébuchement par rapport aux essais sans silençage dI3. À l'inverse, les effets de l'inhibition dI3 et de l'administration de mécamylamine ont donné lieu à une tendance similaire à la tâche comportementale précédente, dans laquelle les hauteurs de marche pendant le pic du réflexe ont été significativement réduites par rapport aux témoins salins, mais n'étaient pas statistiquement différentes lors de la comparaison des essais avec et sans silençage dI3 si la mécamylamine était également administrée. Bien que ce réflexe n'ait pas été complètement aboli, nous avons observé une augmentation significative des cas de tentatives infructueuses pour éliminer la perturbation et un affaiblissement significatif de la réponse corrective par trébuchement avec l'administration de mécamylamine et le silençage de dI3, à la fois séparément et ensemble.

Dans l'ensemble, nos résultats soutiennent l'hypothèse selon laquelle les dI3 sont impliqués dans l'activation de la réponse corrective par trébuchement, dans laquelle les signaux

proprioceptifs et cutanés peuvent être utilisés pour moduler l'activation des muscles pendant la locomotion. Bien qu'il reste beaucoup à comprendre sur les circuits spinaux dI3, il semble qu'un manque de signalisation dI3 inhibe les comportements locomoteurs qualifiés. Nos résultats suggèrent que les dI3 sont plus impliqués dans les comportements moteurs qualifiés et correctifs qu'on ne le pensait auparavant, car nous suggérons que les cellules de Renshaw et les dI3 peuvent fonctionner ensemble au sein d'un type de module de comparaison neuronale pour surveiller activement les signaux sensoriels et ajuster rapidement les sorties motrices. Nos expériences commencent à identifier les circuits spinaux dans lesquels les dI3 fonctionnent pour façonner l'activité motrice.

Acknowledgements

I would first like to extend my deepest gratitude to my supervisor, Dr. Tuan Bui, who has been the best mentor I could have asked for. I could not have succeeded without your patience, feedback, and support throughout all of the trials and tribulations of my research project. You were always available to help with troubleshooting and technical problems, and you gave me the opportunity to learn incredibly advanced skills that made me the scientist I am today. You have always fostered an immensely supportive and kind atmosphere in our lab, and I am truly grateful to have had so many memorable and enriching experiences during my time as a graduate student under your supervision.

I would also like to acknowledge the past and present members of the Bui lab, especially Dr. Alex Laliberte, Stephanie Gaudreau, Dr. Sara Goltash, Emine Topcu, Lauren Couvrette, Emam Khan, and Shariar Nasiri. Not only have my colleagues helped to teach me valuable skills and assisted with data collection, analysis and problem solving, but they have contributed significantly in shaping this thesis and my growth as a scientist. I consider myself very fortunate to have been surrounded by incredibly talented and knowledgeable people who have helped make my time in the Bui lab so special.

I also owe many thanks to the incredible staff at the Vanier animal care facility, particularly Julie Tremblay for always being so dependable and for providing excellent animal care. Special thanks to Kerstin Ure, the Behaviour Core, and Iroshan Hewage for assisting with many animal services and care.

I am beyond grateful to my fantastic thesis advisory committee, Dr. Emily Standen and Dr. John Lewis. I could not ask for more kind, insightful, and engaged committee members. The time

taken out of your busy schedules to invest in my project and attend meetings is greatly appreciated, and I am so thankful for your excellent advice and support throughout this journey.

I would also like to thank everyone in the Brownstone, Beato and Akay Lab (University College London, Dalhousie University) for working tirelessly over the past two years to collaborate on this project. Despite the distance, it has been incredibly rewarding to work with such knowledgeable and experienced scientists in this field and I have learned a great deal from all of you.

Beyond my colleagues and community in academia, I am sincerely thankful for my friends and family who have supported me endlessly throughout this endeavor. My partner, Dany, who did everything he could to make it as easy as possible for me to give my all to my research. My parents, who were always willing and eager to help with Python problems and keep me motivated. My siblings and close friends, whose unwavering support and interest in my research helped to continually inspire me along the way.

Finally, I would like to acknowledge the Canadian Institutes of Health Research for funding this project and all of the time and resources required to complete it. This research would not have been possible without the contributions of all of these individuals, to whom I am deeply indebted to. I would like to thank all of these people for supporting me and allowing for such an enriching experience as a graduate student that I will never forget.

Statement of Contributions

For this project, I would like to acknowledge that Alex Laliberte and Emam Khan helped with the data collection and analysis of treadmill, ladder and beam experiments. Tuan Bui contributed to the conceptualization, analysis, figure preparation, and writing. Additionally, as part of a collaborative work, our colleagues from the Brownstone, Beato, and Akay lab have contributed to the conceptualization of this project, specifically Robert Brownstone, Marco Beato, Turgay Akay, Gorkem Ozyurt, and Rémi Ronzano.

List of Tables

List of Figures

List of Abbreviations

AEP – Anterior extreme position

CPG – Central pattern generator

dI3 – Dorsal interneuron 3

DREADD – Designer Receptor Exclusively Activated by Designer Drugs

Elec. – Electrical

EMG – Electromyography

Isl1 – Islet Lim Homeobox 1

L-AC – L-acetyl carnitine

LTMR – Low-threshold mechanoreceptor

Mech. – Mechanical

MEC – Mecamylamine

MG – Medial gastrocnemius

MN – Motoneuron

PEP – Posterior extreme position

RC – Renshaw cell

SCR – Stumbling corrective response

SN – Sensory neuron

TA – Tibialis anterior

VGlut – Vesicular glutamate transferase

YFP – Yellow fluorescent protein

CHAPTER 1: GENERAL INTRODUCTION

1.1 Spinal interneurons

The spinal cord plays a major role in controlling motor output. In most mammals, there are four major segments to the spinal cord with nerve projections to various parts of the body below the neck. These four major segments comprise the cervical, thoracic, lumbar and sacral divisions of the spinal cord, each associated with various roles from regulating breathing, maintaining a rhythmic pattern of walking through central pattern generators, to initiating muscle reflexes in response to proprioceptive stimuli (DeVries & Goshgarian, 1989; Dietz, 2003; Quevedo et al., 2005a). To perform these roles, the spinal cord contains many populations of motoneurons and interneurons with diverse roles and functions. Spinal interneurons help to shape motor output through diverse microcircuits connecting the sensory periphery to the central nervous system; interneurons are also involved in generating motor rhythm, coordinating muscle activation during movement, as well as sending and receiving supraspinal commands (Chapman et al., 2024; Dougherty et al., 2013; Kwan et al., 2009; Talpalar et al., 2013; Zhang et al., 2014). In contrast to interneuron populations within the cortex and other brain structures, which are mostly inhibitory in nature, spinal interneurons present a greater neurotransmitter diversity with many populations being excitatory or inhibitory, glutamatergic or GABAergic (Brownstone & Bui, 2010; Bui et al., 2015).

Earlier studies of spinal interneurons have mostly defined their anatomy, location, dendritic morphology, and electrophysiological features (Eccles et al., 1954; P. J. Harrison et al., 1986; Hoover & Durkovic, 1992; Puskár & Antal, 1997). However, more recent characterization of the developmental origins of neurons has opened new avenues of studies of spinal neurons and the involvement of certain genes, notably transcription factors, in spinal neuron fates and function. In the dorsal horn, several classes of dorsal spinal interneurons, namely the dI1-dI6 subtypes, have

been described based on the progenitor domain from which they arise from during embryonic development (Gross et al., 2002; Müller et al., 2002, 2005; Nakada, Hunsaker et al., 2004; Nakada, Parab, et al., 2004; Pivetta et al., 2014). The identification of transcription factors that uniquely, or in combination with a discrete set of genes, define certain populations of spinal progenitor domains has allowed for the distinction and characterization of many postmitotic spinal neurons.

Transgenic and viral approaches that rely on these transcription factors have proven invaluable in providing unique approaches to studying spinal neuron function in sensory processing and motor control. Each progenitor pool is the result of the expression of certain sets of transcription factor, and this knowledge has enabled the use of genetic tools such as transgenic animal models where transgenes are expressed under the control of these transcription factors to study specific populations of dorsal spinal interneurons. For example, the investigation of the transcription factor *Math1* has been demonstrated to be required for the development of dI1 interneurons, which have been suggested to form distinct spinal tracts that relay sensory feedback to the cerebellum and govern the development of proprioceptive pathways (Bermingham et al., 2001). Similarly, the study of *Ptf1a* transcription factor has deepened our understanding of another group of dorsally derived and *Ptf1a*-derived spinal interneuron, dI4s, which have been found to give rise to GABAergic projections to sensory neurons in the spinal cord, and later mediate presynaptic inhibition (Betley et al., 2009). Other spinal neurons, like the *Lbx1*-expressing dI6 populations which migrate ventrally during development, are also thought to be involved in locomotor pattern generation. Studies performing dI6 ablation and electrophysiological characterization have demonstrated their rhythmic firing and potential role in stepping, thus suggesting they comprise an important part of the locomotor central pattern generator to modulate motor behaviour (Dyck et al., 2012; Griener et al., 2017). Although we have elucidated the

contributions of certain populations of spinal neurons, the interactions of each population and the circuits that they form to modulate sensory information or integrate motor commands remain poorly described.

1.2 dI3 neurons

Dorsal interneuron 3 (dI3) represents a population of dorsal spinal neurons whose roles in sensorimotor integration have been particularly insightful. Their circuitry is being progressively identified, and studies in the context of specific movements and reflexes are discovering newfound contribution from dI3s (Bui et al., 2013, 2016; Laliberte et al., 2022). dI3s are currently known to act as links within sensorimotor circuits that bridge communication between cutaneous and proprioceptive afferents and motoneurons (Bui et al., 2013, 2016; Laliberte et al., 2022). This group of interneurons comprises major populations residing within the cervical and lumbar regions of the spinal cord, with most located in intermediate laminae V-VII (Bui et al., 2013; Figure 1.1C). dI3s are distinguished from other spinal neuron populations due to the expression of Isl1 (Bui et al., 2016; Capelli et al., 2017), a LIM-homeodomain transcription factor that is shared amongst spinal motoneurons and sensory neurons of the dorsal root ganglia but is exclusively expressed in dI3s within the intermediate spinal cord (Liem et al., 1997). Through anatomical and electrophysiological studies, dI3s have been found to receive direct inputs from both proprioceptive and cutaneous low-threshold mechanosensitive inputs (Figure 1.1A), while ipsilaterally projecting glutamatergic synapses expressing the glutamate transporter vGlut2 to motoneurons (Bui et al., 2013; Figure 1.1B) and putatively to spinal locomotor circuits (Bui et al., 2016; Figure 1.1G). These neurons are more likely to synapse on motoneurons innervating the limb muscles, particularly the more distal muscles (Goetz et al., 2015).

When manipulating dI3 activity in transgenic mice strains, wherein dI3s are functionally silenced through disruption of their glutamate release, it has been observed that more complex tasks like hanging, gripping, and crossing a ladder were impaired in the absence of dI3 signaling (Bui et al., 2013, 2016; Figure 1.1F). Moreover, dI3 neurons appear to mediate the cutaneous control of paw grasp wherein the silencing of dI3s results in loss of the ability to maintain grip strength, demonstrating their importance in spinal circuits that integrate cutaneous signals and reflexes (Bui et al., 2013; Figure 1.1F).

Furthermore, dI3 neurons have demonstrated involvement in locomotion in other contexts beyond grasping, such as motor system plasticity after injury. Genetically silencing dI3 neurotransmitter release impairs the activation of spinal locomotor networks by stimulation of sensory inputs in ex-vivo settings in comparison to control spinal cords (Bui et al., 2016). These findings indicate that dI3 output can contribute to the activation of spinal locomotor circuits (Bui et al., 2016). Remarkably, genetically silencing dI3s greatly impairs recovery of locomotor function after spinal cord injury in mice, thus indicating the role of dI3s as a significant substrate for locomotor plasticity after injury (Bui et al., 2016). Additional studies have also observed synaptic changes to dI3s and a general circuit remodelling of dI3s to motoneurons after acute and chronic spinal cord injury (Goltash et al., 2023). This influence on recovery from dI3s may be related to their significant input from cutaneous and proprioceptive inputs, both of which have been shown to be crucial for recovery of locomotor function in animal models of spinal cord injury (Bouyer & Rossignol, 2003; Takeoka et al., 2014).

Currently, the role of dI3s in locomotion in intact animals appears to be less distinct than after injury, as dI3 silencing results in mostly subtle changes in locomotion (Bui et al., 2016).

Although dI3s are not necessary for normal locomotor function, disruption of their activity leads to alterations in hindlimb movement and gait; the absence of dI3 activity appears to lead to longer stance times and shorter swing phases during treadmill walking (Bui et al., 2016). Interestingly, electrophysiological recordings of dI3s have found that they appear to demonstrate phasic firing, with preference during either the swing or stance phase of the walking cycle (Bui et al., 2016; Figure 1.1D, E). Based on their known sensory inputs and connectivity to spinal motoneurons, it is possible that dI3s may play a role in reflex adaptation of locomotor behaviour (Figure 1.1).

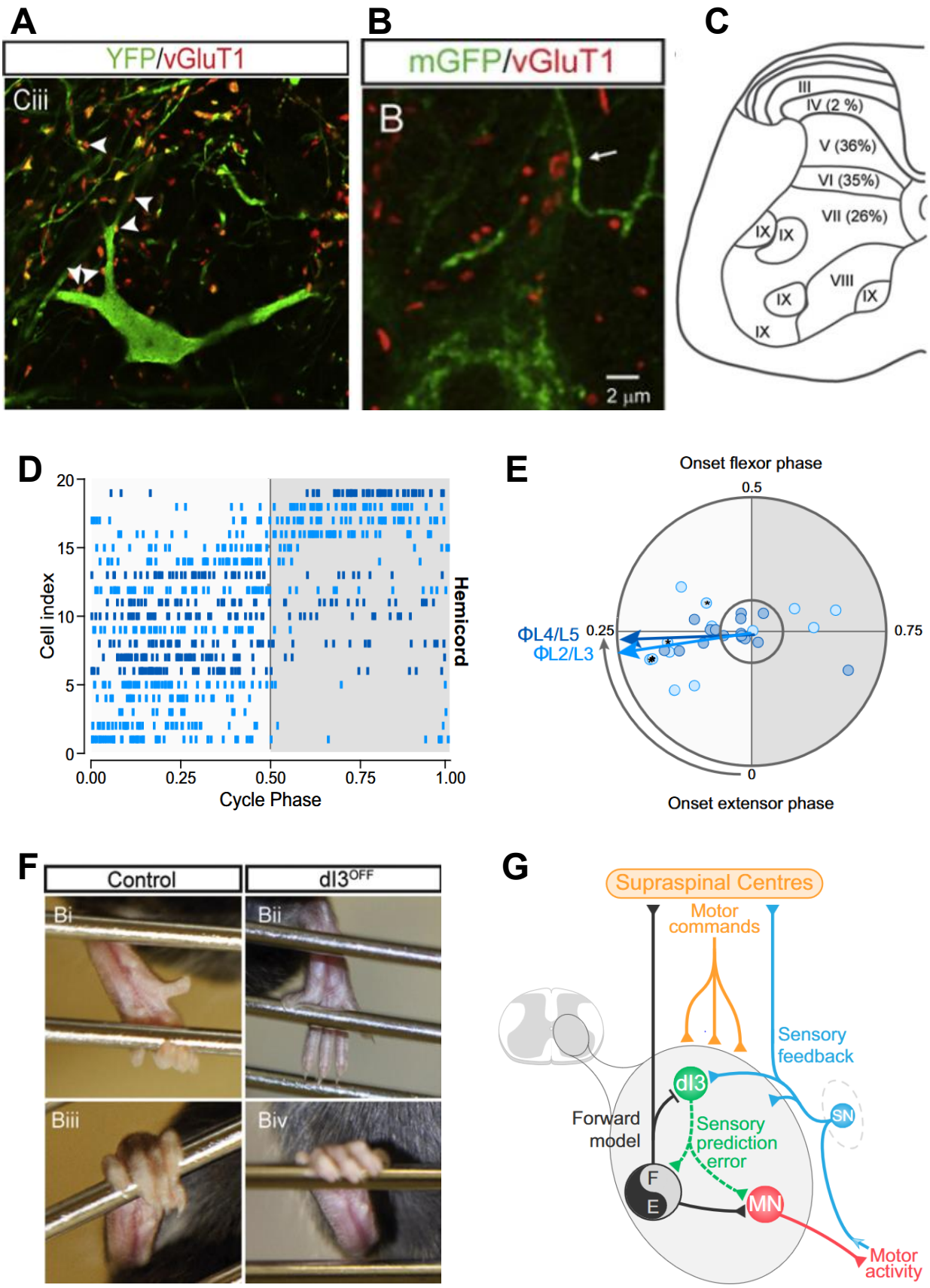
A
YFP/vGluT1
Ciii
B
mGFP/vGluT1
B
2 µm
C
III
IV (2 %)
V (36%)
VI (35%)
VII (26%)
IX
IX
VIII
IX
IX
IX
D
Cell index
Hemicord
Cycle Phase
0.00
0.25
0.50
0.75
1.00
E
Onset flexor phase
0.5
ΦL4/L5
ΦL2/L3
0.25
0.75
0
Onset extensor phase
F
Control
dI3OFF
Bi
Bii
Biii
Biv
G
Supraspinal Centres
Motor commands
Sensory feedback
dI3
Forward model
Sensory prediction error
SN
F
E
MN
Motor activity

Figure 1.1 Major physiological and functional features of dI3s as a candidate spinal neuron for the involvement in cutaneous reflexes and corrective behaviours (adapted from Bui et al., 2013, 2016). A. Labelling in Isl1-YFP mice demonstrating anatomical evidence of sensory afferents (vGlut1+ boutons, indicated by arrowheads) projecting to dI3s (YFP+) in a transected spinal cord. B. Labelling in Isl1-YFP mice demonstrating dI3 projections (YFP+ boutons, indicated by arrow) to motoneurons (YFP+). C. The laminar distribution of dI3s, based upon cell counts, within the spinal cord at L4 and L5 sections. D. Raster plot demonstrating the phasic firing of dI3s within L2-L5 sections of the spinal cord during the extensor and flexor phase of the walking cycle, wherein cycle phases 0.00 to 0.5 represent the extensor phase and 0.50 to 1.00 represent the flexor phase. E. Polar plot demonstrating the rhythmic activity of dI3s between L2-L5, with points representing the average phase at which cells demonstrated the most spiking between the extensor and flexor phase. F. Hindlimb grip comparison between mice before and after dI3 silencing. G. Schematic demonstrating the relationship between dI3s and movement generation; sensory neurons (SN) send sensory input to dI3s, which then project to motoneurons (MN) and potentially to locomotor circuits (i.e., CPGs) to mediate rhythm and pattern of locomotion.

1.3 Stumbling corrective response

One particular reflex of interest involved with locomotion is the stumbling corrective response (SCR). The SCR is a well-documented reflex in many mammals that occurs during the walking cycle to allow animals to avoid unexpected perturbations or obstacles in their environment that might otherwise disrupt movement and locomotion (Figure 1.2). More specifically, a stimulus to the paw dorsum that is detected during the swing phase of the walking cycle triggers a short-latency activation of flexor muscles in the hindlimb to lift the paw or limb (Forssberg, 1979).

Early work observing this reflex was conducted with intact and spinalized cats and demonstrated that mechanical stimulation of the dorsum region of the paw was enough to elicit this flexor response of the hindlimb, thus confirming this reflex as a cutaneous-mediated response (Forssberg et al., 1977; Quevedo et al., 2005a). This corrective response has also been investigated and found to be present in humans, demonstrating similar properties and features of muscle activation to what has been documented in cats (Berger et al., 1984; Dietz et al., 1984; Lam et al., 2003). The reflex was also discovered to be phase-dependent, however, such that the perturbation must occur during the swing phase of the step cycle to initiate the typical muscle flexion (Forssberg, 1979). Using electromyography (EMG) recordings directly from various hindlimb muscles, the most significant activity preceding and succeeding the response appears to be found in the semitendinosus, tibialis anterior, iliopsoas, biceps femoris, and lateral/medial gastrocnemius muscles (Forssberg et al., 1977). Similar work has been performed to confirm the presence of this reflex in walking mice and has shown that the response can be initiated through electrical stimulation of the predominantly cutaneous saphenous nerve alone without mechanical perturbation of the paw (Mayer & Akay, 2018). Few studies have investigated this reflex with respect to specific populations of spinal neurons, however some have hypothesized that there may

be only one or two distinct spinal neurons, likely excitatory, involved in mediating this corrective response (Quevedo et al., 2005b). While the muscles involved, the sequence of their activation, the implicated sensory modalities and nerves are well described, the exact neural circuitry underlying this reflex has yet to be identified.

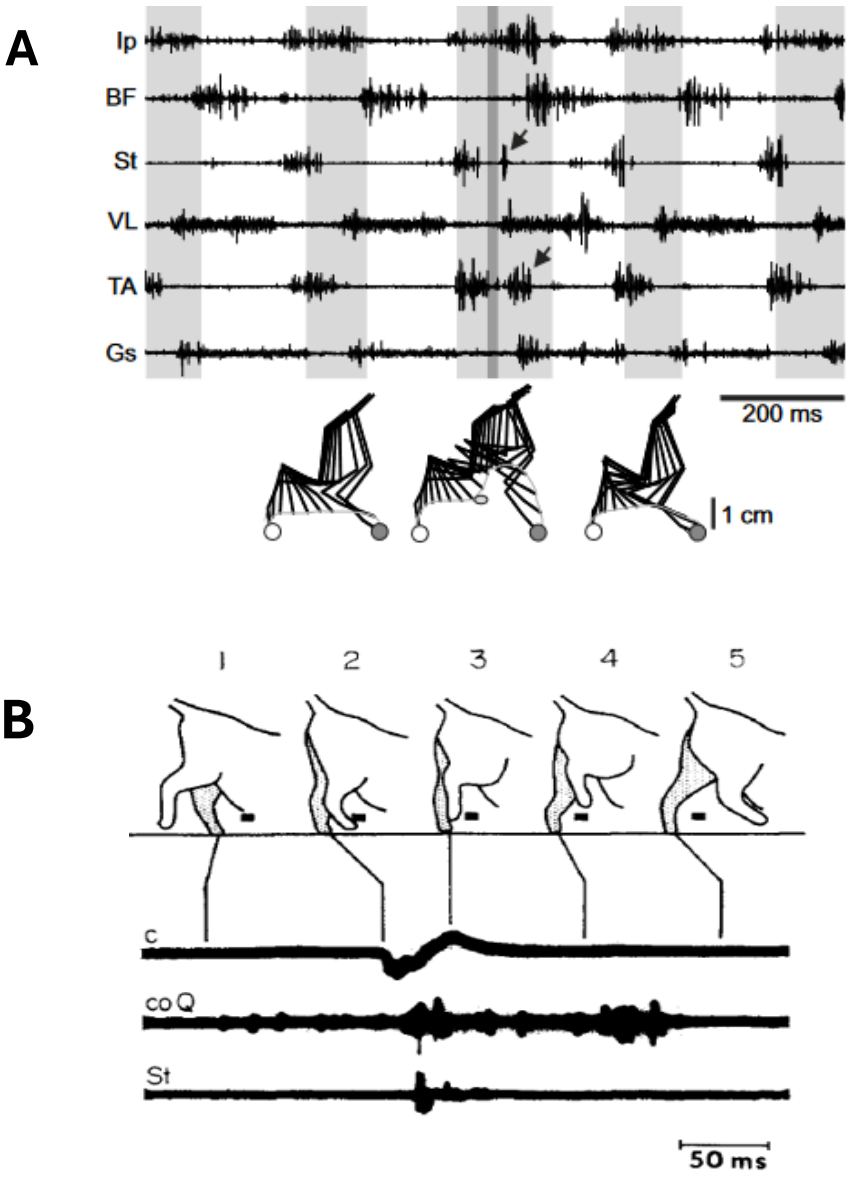

Figure 1.2 Different representations of the stumbling corrective response in mammalian models (adapted from Grillner et al., 1977; Mayer & Akay, 2018). A. Electromyographic responses of various hindlimb muscles (flexors and extensors) involved in the stumbling corrective reflex in the mouse; stick plot reconstructions of the hindlimb swing phase of the step before, during, and after the stumble reflex are represented below muscle recordings. B. Visual representation of the stumbling corrective response in the cat, where phases 1-2 demonstrate the unperturbed swing phase and phases 3-5 demonstrate the perturbed swing with added flexion to clear the object. Traces below demonstrate electromyographical recordings of several key muscles associated with the activation of the stumbling corrective reflex.

1.4 Reflex pathways and dI3s

Several characteristics of the SCR and properties of dI3s strongly suggest that the latter could mediate the SCR. Firstly, the strong input from cutaneous afferents to dI3s infers the possibility of involvement in this cutaneous-mediated reflex triggered by detection of touch stimuli to the foot dorsum. With direct excitatory projections to motoneurons of the hindlimb muscles, and putatively to spinal locomotor circuits as well, dI3s are a likely population of neurons that may modulate the activation of this rapid reflex. Additionally, recordings of dI3s in isolated spinal cord fictive locomotion experiments suggest that most dI3s are rhythmically active during locomotion. Many have preferred firing activity during either the stance phase or during the swing phase (Bui et al., 2016), much like the phasic nature of firing seen during walking and in key hindlimb muscles of the stumbling corrective response (Forssberg, 1979). Furthermore, the increased stimulation threshold to induce locomotion in isolated spinal cord preparations of dI3-silenced mice was found to be connected to spinal locomotor circuits (Bui et al., 2016) that could control the limb movements needed to clear obstacles during the stumbling corrective response. Thus, we can postulate that dI3s may not only be involved in adaptive reflexes like the stumble reflex, but also perhaps other corrective behaviours that involve rapid modulation of motor output.

1.5 Potential coordination of Renshaw cells and dI3s in corrective motor circuits

Another population of spinal neurons that has been linked to rapid adaptation of motor outputs are Renshaw cells. Located in the most ventral regions of the spinal cord where motoneurons also reside, Renshaw cells (RCs) are a unique population of inhibitory spinal neurons with direct connections to and from motoneurons (Alvarez et al., 1999; Cullheim & Kellerth, 1981; Eccles et al., 1954). RCs have inhibitory synapses on motoneurons that release GABA and glycine

(Cullheim & Kellerth, 1981). In turn, RCs receive cholinergic contacts from motoneurons which increase excitation through either acetylcholine or glutamate release (Alvarez et al., 1999). This recurrent inhibitory circuitry between RCs and motoneurons may allow RCs to play a significant role in rapid feedback processing, as many studies using electrophysiological recordings have described this negative feedback loop specifically as a recurrent circuit, wherein RCs receive direct excitatory outputs from motoneurons and project back to motoneurons through their inhibitory synapses (Eccles et al., 1961; Granit et al., 1957; Renshaw, 1946). RCs are thus primed to quickly adjust motoneuron firing through their inhibitory effects (Bhumbra et al., 2014) and Hultborn and colleagues have proposed that the function of these recurrent circuits optimizes the contraction of various muscle groups through the adjustment of motoneuron excitation (Hultborn et al., 1979). However, convincing evidence of the involvement of RCs in the control of movement remains lacking.

We suggest that RCs, like dI3s, may also play a role in modulating motor output for fast and adaptive motor behaviours. Although behavioural research studies on RCs in murine models are lacking in the literature, it has been shown through fictive locomotion that RCs influence motoneuron firing, specifically disrupting rhythmicity of motoneuron firing when RC activity is depressed (Noga et al., 1987). With the capacity to limit firing rates of motoneurons and potentially influence step cycle dynamics, RC activity may also contribute to locomotion beyond basic adjustment of muscle activation. With their extensive connections to motoneurons and expansive axonal projections between various motor pools, they are suggested to both monitor motor output and exert feedback through modulation of motoneuron excitability (Fyffe, 1991; Maltenfort et al., 2004; Renshaw, 1946).

Additionally, through emerging research and an ongoing collaboration with the Brownstone and Beato lab at the University College London, new projections have been identified between populations of RCs and dI3s within the cervical and lumbar spinal segments, revealing inhibitory synapses to dI3s that may modulate dI3 firing through RC activity (unpublished, personal communication). Until now, the connections between dI3s and other spinal interneuron populations have been poorly understood, thus the presence of axonal projections from RCs directly to dI3s demonstrates exciting new evidence suggesting a more significant role for dI3s within corrective motor circuits, and perhaps even within motor learning.

Given our current knowledge of motor learning modules within the cerebellum, for example, we can suggest that dI3s may operate within a neuronal network similar to those in the cerebellum responsible for error prediction and learning (Brownstone et al., 2015). Within the cerebellum, many complex motor circuits comprise a central controller to translate motor intention, which then communicates to effectors to drive motor activity (Brownstone et al., 2015; Freeman & Steinmetz, 2011). As is necessary for complex motor behaviours, many circuits require additional processing in order to predict error and actively adjust motor output; to achieve this, motor networks often have connections to a neuronal comparator which acts to receive and relay predictive input and instructive feedback on motor output (Brownstone et al., 2015). The complex circuitry of a comparator module is crucial for rapid motor correction and learning, wherein the integration of both outgoing motor command and active sensory feedback can be used to calculate and predict motor error (Figure 1.3; Brownstone et al., 2015). The key components of comparator module circuitry comprise a controller to command motor output, effectors to conduct the movement, sensors to relay active sensory information, and a comparator that uses motor commands with sensory input to calculate motor error (Figure 1.3). The sum of these connections thus allows for

correction and motor learning by performing both error prediction and motor instruction, processes that are critical to reflexive and adaptive behaviours.

While it appears that comparator modules exist within the brain and cerebellum (Freeman & Steinmetz, 2011), it is possible that they may be present throughout the spinal cord as well, existing as their own complex circuits processing motor correction almost entirely within the spinal cord. Although there remains much to be investigated on spinal motor learning, there are some populations of interneurons whose synaptic connections and functions may suggest their role as spinal comparators such as α-motoneurons or RCs (Brownstone et al., 2015). Given what we know about dI3 neural connections and function, we propose that this spinal population may be a likely candidate for comparator neurons. As both dI3 and RC neuron populations project directly to motoneurons with the capacity to excite or inhibit their motoneuron targets, the identification of RC inhibition of dI3s suggests that dI3s receive a copy of motor output through RC signaling. If dI3 circuitry does resemble a true comparator module then motoneurons would act as the controller to motor output, meanwhile RCs send a copy of motor command to dI3s as they simultaneously receive active sensory feedback from their sensory afferent connections. Thus, dI3s would have the necessary feedforward and feedback information to then predict motor error and actively adjust motor command through their connections to motoneurons. Given these newfound connections between spinal interneurons, we suggest that dI3s may use both motor and sensory information to form a type of spinal comparator module that is partly responsible for triggering reflexive and corrective motor behaviours.

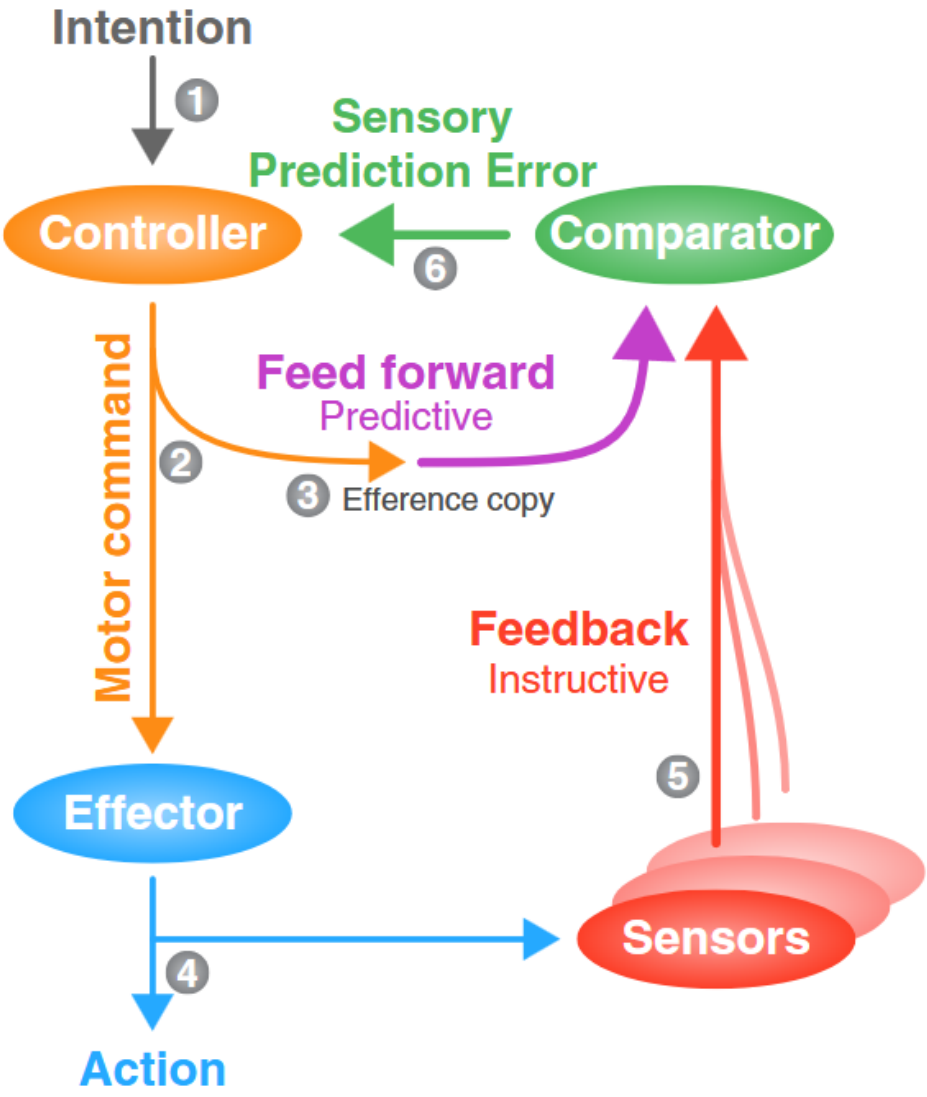

Figure 1.3 Feedback and feed forward concepts of a comparator module involved in corrective motor behaviour initiation (adapted from Brownstone, Bui & Stifani, 2015). Within comparator module circuitry, outgoing motor command is sent to the comparator as the efference copy of movement, meanwhile sensory input is also sent to the comparator as the copy of active feedback. The comparator utilizes the predictive (feed-forward) and instructive (feedback) information to then estimate sensory error and provide rapid adjustment to motor output through the controller.

1.6 Hypothesis and thesis overview

Overall, dI3s have been described as important neurons within several spinal pathways that play a key role in mediating information between sensory inputs and motor circuits. We hypothesized that spinal circuits comprising dI3s contribute to the initiation and activation of the stumbling corrective response, as well as other corrective and skilled locomotor behaviours. We predicted that the inhibition of dI3 signaling would result in a blunted stumbling corrective response during locomotion, and possibly blunted performance during additional complex tasks such as a horizontal ladder and beam walk in a mouse model. The investigation of these potential spinal circuits would allow us to further understand the neural substrate of this well characterized reflex that enables locomotion to adapt to obstacles. Through these experiments, we hope to better delineate the role of dI3s with respect to the control of mammalian locomotion.

Additionally, our investigation will allow us to advance our understanding of which spinal neuron populations are responsible for various reflexes and corrective behaviours. Considering the newfound connections from RCs to dI3s, we sought to determine if these two groups of spinal neurons act together in some capacity to actively integrate sensory inputs and rapidly modulate motor outputs. Thus, we hypothesized that a spinal circuit exists wherein dI3s and RCs project sensory information to one another to compare both proprioceptive and cutaneous sensory information to actively adjust motoneuron excitation for fast adjustments to motor behaviour. We predicted that the reduced activation of RCs would have a similar impact to dI3 silencing, such that corrective behaviours and the stumbling reflex would be blunted or impaired, with even greater impairment when RC and dI3 silencing were combined. Conversely, we predicted that enhancement of RC excitation would result in recovery of any lost function from dI3 silencing in terms of successful corrective behaviours.

To test our hypotheses, we aimed to investigate the stumbling corrective response in freely walking mice with and without dI3 activity, as well as compare the locomotor performance of two different corrective behaviour tasks with and without dI3 signaling. Rapid and transient silencing of dI3s would be achieved through chemogenetic silencing via the activation of inhibitory Designer Receptors Exclusively Activated by Designer Drugs (DREADDs). Simultaneously, we also aimed to observe the role of RCs in these corrective behaviours and how their projections to dI3s might impact the execution of motor corrections. Specifically, we planned to investigate the potential RC-dI3 circuit dynamics through excitation and depression of cholinergic signaling to alter RC excitability. Therefore, through chemogenetic inhibition of dI3s and pharmacological modulation of RC activity, we will observe the potential outcomes on various behavioural tasks testing corrective locomotion. Through these experiments, we hope to begin to understand how dI3 spinal circuits are involved in fast, adaptive behaviours and if RCs play a significant role in relaying additional sensory information to dI3s for smoother motor adaptation.

CHAPTER 2: MATERIALS AND METHODS

2.1 Animals

All animal procedures performed were approved by the University of Ottawa's Animal Care Committee and conform to the guidelines put forth by the Canadian Council for Animal Care (protocol number *BLe-3945*). All mice used were adult age, ranging from 5 weeks old at the first surgical procedure to 14 weeks old at the end of behavioural testing. We used two transgenic lines of mice to allow for temporary dI3 IN silencing. About half of the mice used (n=7) were Isl1-Cre; Vglut2-Flp; CreON-FlpON-hM4Di which allowed for the expression of the inhibitory Designer Receptor Exclusively Activated by Designer Drugs (DREADD) receptor *hM4Di* in dI3 neurons; the other subset of mice (n=5) were Isl1-Cre; Vglut2-Flp mice that received lumbar intraspinal injections in three sites on each side of the cord (L2-L4 segments) of AAV-CreON-FlpON-*hM4Di* to induce *hMD4i* receptor expression (see below for surgical details) . All mice were housed individually in a reverse light-cycle room with 12 hours of light from 7pm to 7am; all behavioural testing was performed in simulated darkness using red LED and infrared lighting between the hours of 8am and 5pm. Mice of either sex were used in experiments, with a total of 8 females and 4 males.

2.2 EMG electrode and implant fabrication

To record muscle activity and electrically stimulate afferent fibers in the hindlimb during treadmill walking, custom EMG muscle and nerve cuff electrodes were made following the protocols described in previous mouse studies (Akay et al., 2006; Mayer & Akay, 2018; Pearson et al., 2005). For muscle implant electrodes, stainless steel wire was stripped, twisted together, and knotted in the middle to create a paired-wire bipolar electrode; a 27G needle was attached to one end of the electrode wires to allow for smooth muscle insertion, while gold pins were soldered to

the opposite end of the electrode wires to be inserted into the head piece connector. The nerve cuff electrode was fabricated in a similar fashion; rather than a 27G needle, one end of the electrode wire was inserted through a silicone cuff to be slipped around the saphenous nerve and tied shut with a silk suture running through the silicone cuff. Individual electrode implants were attached to a central head piece connector by inserting the soldered gold pins into a female connector; each head piece connector contained a total of 4 muscle electrodes and 1 nerve cuff electrode attached. The plastic housing of the connector was then coated in a thin layer of biocompatible gel Epoxy (opaque 5-Minute Epoxy Gel, Devcon) to ensure a smooth and rounded finish to avoid potential irritation of the skin tissue upon implantation. After allowing the Epoxy coating to cure completely for at least 24 hours, implants were then sterilized prior to surgery in 3% hydrogen peroxide solution followed by a water wash in sterile water to remove any residual hydrogen peroxide. Implants were fabricated one week prior to implantation surgeries, with sterilization performed immediately before surgical intervention.

2.3 Surgical details of intraspinal injection, nerve cuff and electrode implantation

At 5 weeks old, 5 of the 12 mice (Isl1-Cre, Vglut2-Flp mice specifically) received an intraspinal injection of an adeno-associated virus (AAV) carrying the gene construct for *hM4Di*. Mice were given 0.1mg/kg of buprenorphine HCl 1 hour before surgery, then placed under isoflurane anesthesia throughout the procedure. Using a stereotaxic frame and micro-injector, a volume of 0.3uL of virus was administered at each of the three injection sites into the right and left laminar spaces between T11, T12, T13, and L1 vertebral segments of the spine (Harrison et al., 2013) for a total of 6 injections (between L2-L4 spinal cord segments). Animals were given analgesic (Buprenorphine, Ceva Animal Health) for 2 days and antibiotics in drinking water

(Baytril, Elanco) for 7 days post-operation, and allowed to recover for 7 days prior to the next surgical procedure.

Following recovery after intraspinal injection, surgical implantation of 4 muscle electrodes and 1 nerve cuff was performed for all 12 mice. Once again, mice were given 0.1mg/kg of buprenorphine HCl 1 hour before surgery, then placed under isoflurane anesthesia for the procedure. A set of 4 bipolar EMG electrodes were implanted into the ankle flexor and extensor muscles, the tibialis anterior (TA) and medial gastrocnemius (MG) muscles respectively, of both right and left hindlimbs. Additionally, one nerve stimulation cuff electrode was placed around the saphenous nerve (SN) of the left hindlimb. Electrodes were implanted following the surgical procedures as described in previous hindlimb EMG recording research in freely walking mice (Akay, 2014; Akay et al., 2006). Incisions were made in the upper neck region and in the skin of the hindlimbs to expose the target muscles and saphenous nerve. The electrodes were drawn through the neck incision down to the target muscle regions and inserted into the tissue, parallel to the muscle fibers. The nerve cuff electrode was placed around the saphenous nerve, to allow for electrical stimulation of cutaneous afferent fibers of the anterior portion of the distal hindlimb. A head piece connector was secured into the skin of the dorsal neck region to allow for EMG recordings and electrical stimulation from external equipment; the neck and leg incisions were then closed, and anesthesia was discontinued. Mice were placed in a warmed incubator set to 36 degrees Celsius and analgesics were administered subcutaneously (0.1mg/kg Buprenorphine) 6 hours post-operation; a local anesthetic (2% transdermal Bupivacaine Hydrochloride, Chiron Compounding Pharmacy Inc) was applied topically to all incisions to prevent irritation. Buprenorphine and bupivacaine were then administered at a 12-hour interval for 48-hours post-surgery. Mice were individually housed in cages placed on a heating pad for the first 2 days post-

surgery, then returned to their original mouse rack. A broad-spectrum antibiotic (Baytril, Elanco) was administered *ad libitum* via drinking water for 1 week following surgery. Mice were given at least 1 week to recover before any acclimation or training sessions began prior to behavioural testing.

2.4 Behavioural testing and training regimen

Following recovery after electrode implantation surgeries, all mice were given 2 weeks of training and acclimation to the testing apparatuses and behavioural testing room. The first week consisted of strictly treadmill training, which involved a daily 5-minute session of slow walking on the treadmill at a speed of approximately 0.01-0.02m/s. The second week combined both treadmill training and acclimation of the other testing apparatuses. Mice first performed a 5-minute session walking on the treadmill at an increased speed of 0.03-0.04m/s, followed by acclimation to the horizontal ladder and balance beam. Mice were placed on a horizontal ladder with all ladder rungs in place and evenly spaced, and were provided food rewards to encourage 5 successful passes across the ladder. Mice were then placed on the balance beam, without vibration, and were provided food rewards to encourage 5 successful passes across the balance beam. Mice were kept in the testing room for approximately 1 hour per day to acclimate to the testing environment, then returned to their original housing room.

After two weeks of training and acclimation, mice were tested on three different behavioural tasks to examine the effects of dI3 silencing on various skilled and corrective locomotor behaviours. Testing sessions included a treadmill task in which mechanical (rod) or electrical perturbations (stimulation via the nerve cuff electrode) were induced, followed by a

horizontal ladder task in which random ladder rungs were removed and spaced irregularly, and ended with a vibrating balance beam task. For treadmill trials, mice were placed on a horizontal treadmill set to 0.04m/s and walked for approximately 5 minutes. For half of the total behavioural sessions, electrical perturbations were triggered at the onset of the swing phase via electrical stimulation of the saphenous nerve. Treadmill trials were then repeated for the remaining half of behavioural sessions with mechanical perturbation with the use of a thin metal rod to physically perturb the swing of the hindlimb during walking. The two different methods (i.e., mechanical or electrical stimulation) were used to perturb the limb as each demonstrated unique advantages; mechanical manipulation of the limb is most reflective of a true SCR in real-world circumstances, however electrical perturbation of the limb prevented mice from predicting when a perturbation would be applied through visual or whisker feedback. Both electrical and mechanical perturbations were performed pseudo-randomly, as they were either induced electrically at the onset of the swing phase or mechanically through physical manipulation of the walking cycle.

Electrical stimulation of the saphenous nerve was performed using live EMG recordings of the TA muscle from a custom closed-loop Axoscope protocol (Molecular Devices), wherein threshold detection of bursting activity from the TA muscle triggered an electrical pulse sent to the saphenous nerve cuff implanted in the left hindlimb (0.2ms duration, 100Hz, ranging from 0.1-0.3mA). Stimulus intensity of the pulse to the saphenous nerve was determined individually for each mouse as 1.2 times the required current to elicit a small response from the TA muscle at rest. Throughout the duration of treadmill trials, muscle activity from TA and MG hindlimb muscles were recorded simultaneously with Axoscope software (Molecular Devices, 10 kHz sampling frequency), while high-speed video was recorded at 100 frames per second (fps).

Mice were then tested on tasks requiring more skilled and adaptive locomotion with the horizontal ladder and balance beam tests. In each testing session, mice performed 5-10 attempts at successfully crossing the ladder (60cm length, 3.5cm width) and beam (60cm length, 0.9cm width) from one end to the other. To increase the difficulty of these tasks, the horizontal ladder was set up with unevenly spaced rungs and the balance beam was equipped with a vibrating motor to reduce stability of the beam. The horizontal ladder rungs were uniquely rearranged prior to each testing session to prevent a learning effect. High-speed video was recorded at 100 fps for each attempt for ladder and beam trials, and video footage was then analyzed and scored to assess the number of footfalls when crossing the ladder and beam.

All video recordings were analyzed with DeepLabCut Python software (Version: 2.3.10; Mathis et al., 2018; Nath et al., 2019) to label and track the joints of the hindlimb, and to extract automated hindlimb coordinate data to assess stepping and gait kinematics. Pose estimation data from DeepLabCut was then analyzed with the ALMA toolbox Python software (Automated Limb Motion Analysis; Version: 1.1.0; Aljovic et al., 2022) to score the number of paw slips for each attempt across the horizontal ladder and balance beam, as well as to extract various kinematic parameters of stepping on the treadmill.

2.5 Pharmaceutical interventions for dI3 circuit silencing/activation

To manipulate dI3 neuron activity, mice were given a subcutaneous injection of the designer drug JHU37160, which acts as an *hM4Di* receptor agonist to transiently inhibit dI3s, as demonstrated in previous work with developing mice (Laliberte et al., 2022). To induce a “dI3 OFF” state, JHU37160 (dihydrochloride, DREADD ligand, Hello Bio) was administered

subcutaneously at a dosage of 0.5mg/kg. For a control "dI3 ON" state, the equivalent dosage/volume was administered as saline subcutaneously. To determine if dI3 neurons receive inputs from Renshaw cells, a population of inhibitory spinal neurons excited by motoneuron axon collaterals through cholinergic neurotransmission, two additional treatments were given to manipulate Renshaw cell activity. Mecamylamine (hydrochloride, Cayman Chemical), a nicotinic acetylcholine receptor antagonist, was administered intraperitoneally at a dosage of 5mg/kg to effectively reduce Renshaw cell activation, as demonstrated in previous research in a cat and rodent model (Kaneko et al., 2022; Noga et al., 1987). Conversely, acetyl-L-carnitine (chloride, Cayman Chemical), a central cholinergic compound, was administered intraperitoneally at a dosage of 100mg/kg to putatively increase Renshaw cell activation, as previously demonstrated in spasticity models (Mazzocchio et al., 1990). The two additional drug treatments, mecamylamine and acetyl-L-carnitine, were used in combination with either JHU37160 or saline to create 6 major treatment conditions, listed as follows: dI3 ON + mecamylamine, dI3 ON + acetyl-L-carnitine, dI3 ON + saline, dI3 OFF + mecamylamine, dI3 OFF + acetyl-L-carnitine, and dI3 OFF + saline. All behavioural sessions and drug administrations were separated by at least 48 hours to allow for complete drug metabolism and to prevent *hM4Di* receptor desensitization.

2.6 Statistical analysis

GraphPad Prism (Version: 10.3.1) was used to perform all statistical analyses. Data are reported as mean ± SD. For all tests, the level of significance is set to $p < 0.05$ and is indicated by asterisks in all figures. Comparisons involving all means across mice *and* drug treatments (e.g., step heights between dI3 ON vs dI3 OFF during the stumble reflex) were made using two-way ANOVA followed by Tukey's multiple comparisons test or Sidak's multiple comparisons test to

compare means between pairs of groups (e.g., dI3 ON + mecamylamine vs dI3 OFF + mecamylamine). For comparisons of all means between one group to another (e.g., dI3 ON vs dI3 OFF), repeated-measures one-way ANOVA was performed followed by Tukey's multiple comparison's test.

CHAPTER 3: RESULTS

3.1.1 Chemogenetic manipulations and transient silencing of dI3 activity

Prior to behavioural testing and data collection, twelve mice underwent the surgical implantation of saphenous nerve cuff and EMG recording electrodes, 5 of which received intraspinal injection of an AAV to induce expression of the inhibitory DREADD *hM4Di* in lumbar dI3 neurons. The remaining 7 mice expressed the *hM4Di* receptor in dI3s through conditional transgenic expression and selective breeding (Isl1-Cre; Vglut2-Flp; CreON-FlpON-hM4Di mice). All 12 mice (8 females, 4 males; average weight = 24.4 +/- 2.7 g) were trained in three different behavioural tasks including a balance beam walk, a horizontal ladder walk, and basic treadmill walking. Prior to each task, mice were given one of six unique combinations of three different pharmacological compounds on separate days to temporarily silence dI3 activity and/or manipulate Renshaw cell activity (Table 3.1). Over the course of the study, all mice were administered all six combinations. Treadmill task data from 6 of the 12 mice were excluded due to treadmill equipment complications.

Pharmacological treatments	Physiological effects
"dI3 OFF + Saline" *JHU37160 and saline*	Transient silencing of dI3 activity only.
"dI3 OFF + L-AC" *JHU37160 and L-acetyl carnitine*	Transient silencing of dI3 activity and increased Renshaw cell activation through increased cholinergic function.
"dI3 OFF + MEC" *JHU37160 and mecamylamine*	Transient silencing of dI3 activity and reduced Renshaw cell activation through nicotinic receptor antagonism.
"dI3 ON + Saline" *Saline*	No physiological manipulation (control).
"dI3 ON + L-AC" *Saline and L-acetyl carnitine*	Increased Renshaw cell activation.
"dI3 ON + MEC" *Saline and mecamylamine*	Reduced Renshaw cell activation.

Table 3.1 Pharmacological treatment combinations administered to manipulate dI3 spinal circuitry. Six distinct combinations of three different compounds were administered on separate days prior to behavioural testing to assess the impact of altered dI3 neuron activity on corrective behaviours. Treatments include two compounds influencing cholinergic activity to alter activation of Renshaw cells (i.e., mecamylamine and L-acetyl carnitine) and the DREADD agonist JHU37160 to excite inhibitory *hM4Di* receptors to suppress dI3 neuron activation.

3.2.1 dI3 silencing increases paw dragging upon perturbation and blunting of the stumble reflex

We first sought to investigate the involvement of dI3s in reflex behaviours, specifically the stumbling corrective response (SCR). To determine the potential role of dI3s in the SCR, mice walked on a treadmill while we applied either mechanical perturbation of the ventral aspect of the lower hindlimb or electrical stimulation of the saphenous nerve (Fig. 3.1, 3.2; Supplemental SCR videos: dI3_ON_Saline_Electrical_SCR_1.mp4, dI3_ON_Saline_Mechanical_SCR_1.mp4). We observed that the hindlimb appeared to demonstrate a blunted SCR in response to perturbation during active stepping for both electrical and mechanical perturbation on the treadmill with dI3 OFF mice (Fig. 3.1, 3.2; Supplemental SCR videos: dI3_OFF_Saline_Electrical_SCR.mp4, dI3_OFF_Saline_Mechanical_SCR_1.mp4). While the SCR was not eliminated completely with the absence of dI3 activity, we observed incidences of failed SCRs (Fig. 3.3), which we termed as paw dragging events. During paw dragging, the paw failed to reflexively clear the obstacle, specifically within mechanically perturbed treadmill trials when dI3s were silenced (Supplemental SCR videos: dI3_OFF_Saline_Mechanical_drag.mp4).

Between the three treatments in dI3 ON sessions, the incidence of dragging was low and statistically similar between L-AC and saline trials while MEC treatment was significantly different with a greater incidence of dragging (Table 3.2; $N = 6$; Tukey's test, $p \leq 0.05$ (L-AC vs MEC), $p \leq 0.01$ (MEC vs saline), $p > 0.05$ (L-AC vs saline). After dI3 silencing, L-AC and saline treatment trials presented significant increases in the incidence of dragging while MEC treatment was not significantly changed (Fig. 3.4; $N = 6$; Tukey's test, $p > 0.05$ for MEC mechanical SCR trials, $p \leq 0.0001$ for saline mechanical SCR trials and $p \leq 0.05$ for L-AC mechanical SCR trials). When comparing dI3 ON to dI3 OFF treatment in saline and L-AC treadmill trials, there was a significant increase in the percentage of perturbation attempts that resulted in dragging events

rather than paw clearance or an SCR (Fig. 3.4B; $N = 6$; Tukey's test, $p \leq 0.0001$ for saline mechanical SCR trials and $p \leq 0.05$ for L-AC mechanical SCR trials). While the percentage of dragging demonstrated an eight-fold increase on average when comparing dI3 ON to dI3 OFF for saline trials (811.1 ± 375.2%), this effect was seen to a lesser extent in L-AC trials where the percentage of dragging quadrupled on average (447.2 ± 187.3%) There was a small increase in the percentage of dragging in MEC treatment trials (42.8% ± 20.8%,), however the difference between dI3 ON to dI3 OFF in this treatment group was not statistically significant and the average incidence of dragging remained comparable (Fig. 3.4; $N = 6$; Tukey's test, $p > 0.05$). Because the number of dragging events in dI3 ON mice seemed to be greater in the MEC treatment group, which would affect the percent increase, we calculated the net increase in the percentage of trials that resulted in dragging from dI3 ON to dI3 OFF. This net increase in the percentage of trials was greatest in saline treatment trials and lowest in MEC trials (Fig. 3.4B; $N = 6$; Tukey's test, $p > 0.05$ for MEC trials, $p \leq 0.05$ for L-AC trials, $p \leq 0.0001$ for saline trials). All p-values from Tukey's multiple comparisons test are presented below in Table 3.2.

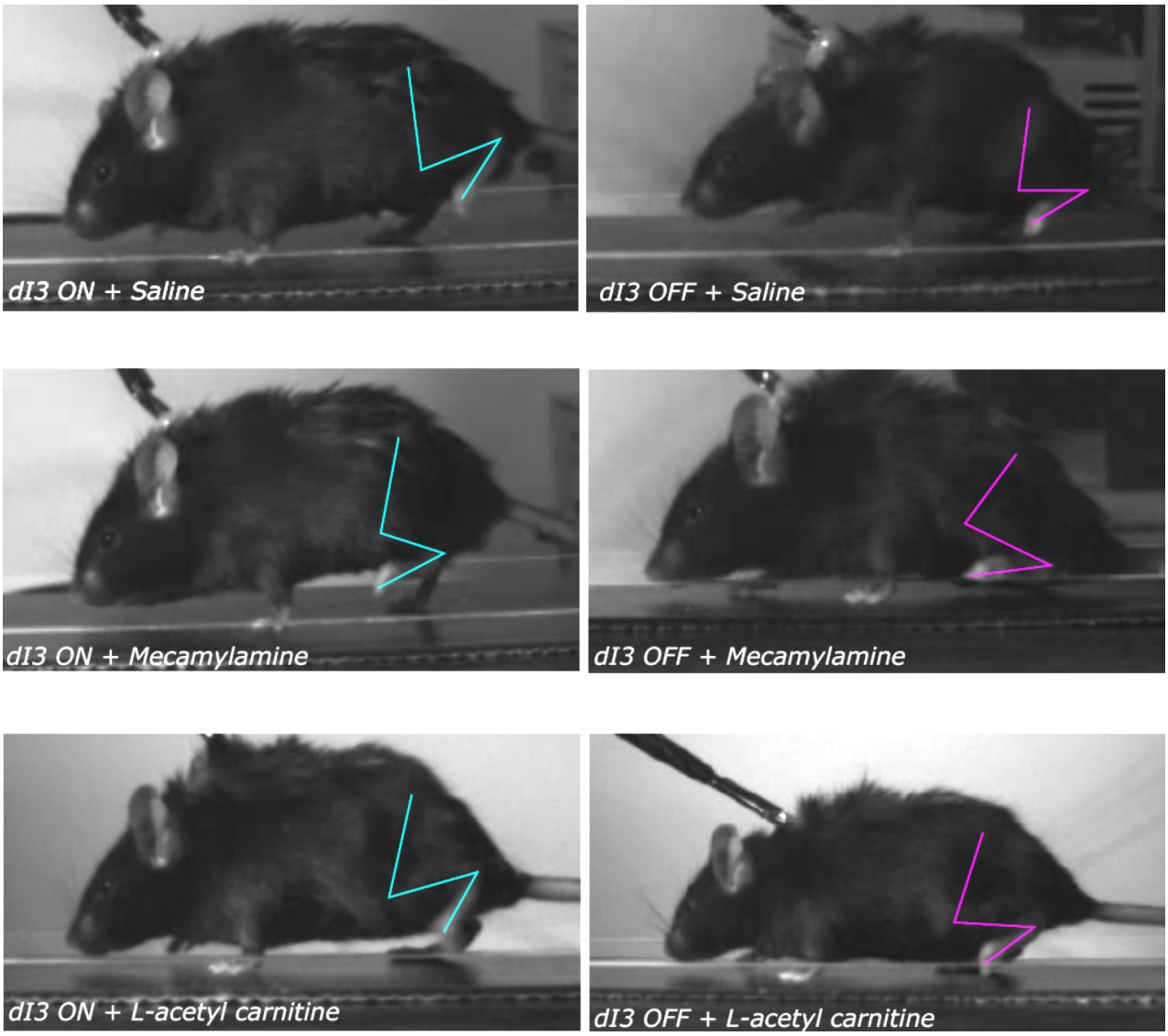

Figure 3.1 Images capturing the SCR induced by electrical perturbation across all 6 treatment combinations. Cyan-colored kinematic hindlimb skeletons represent dI3 ON conditions; magenta-colored kinematic skeletons represent dI3 OFF conditions.

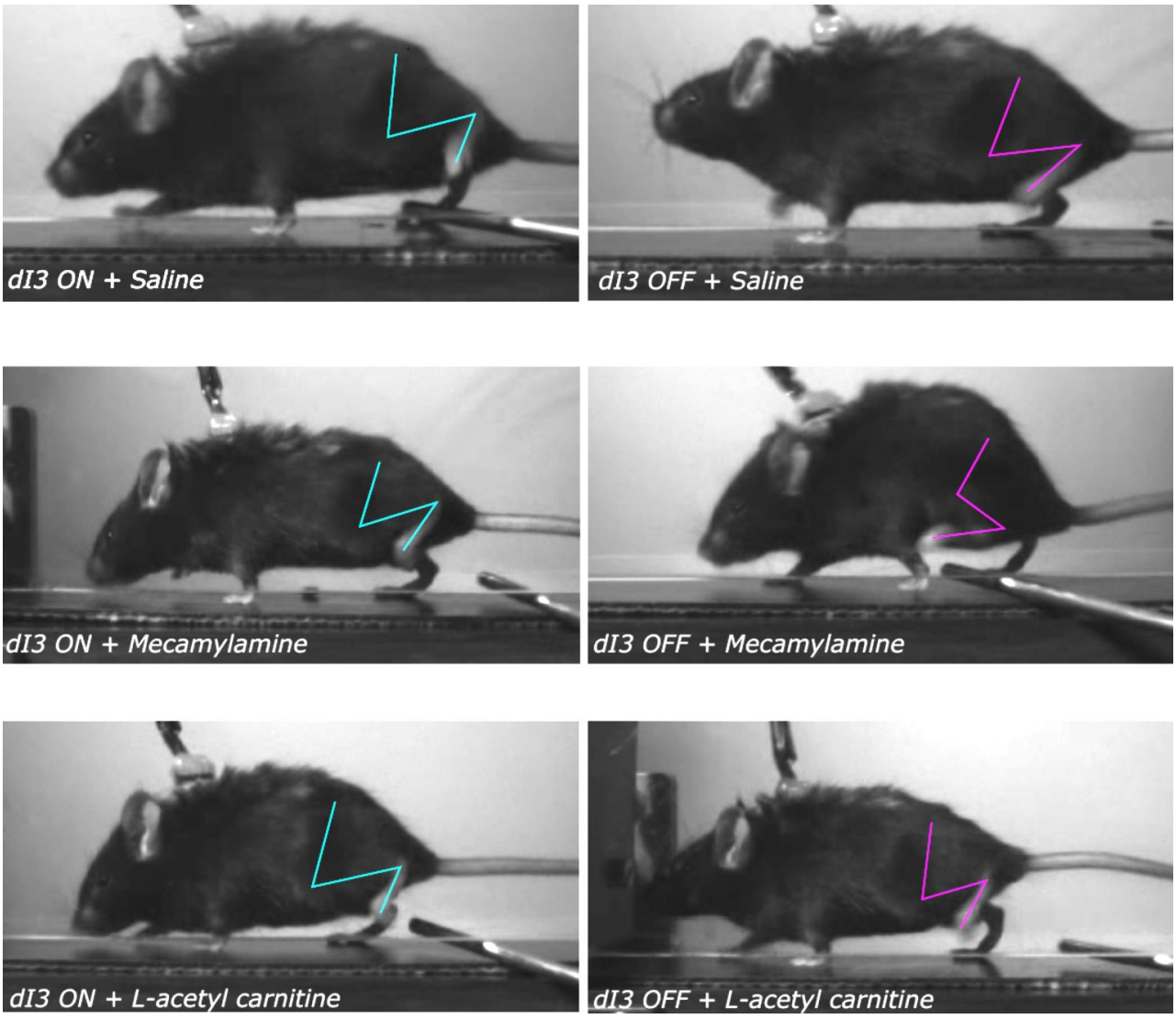

Figure 3.2 Images capturing the SCR induced by mechanical perturbation across all 6 treatment combinations. Cyan-colored kinematic hindlimb skeletons represent dI3 ON conditions; magenta-colored kinematic skeletons represent dI3 OFF conditions.

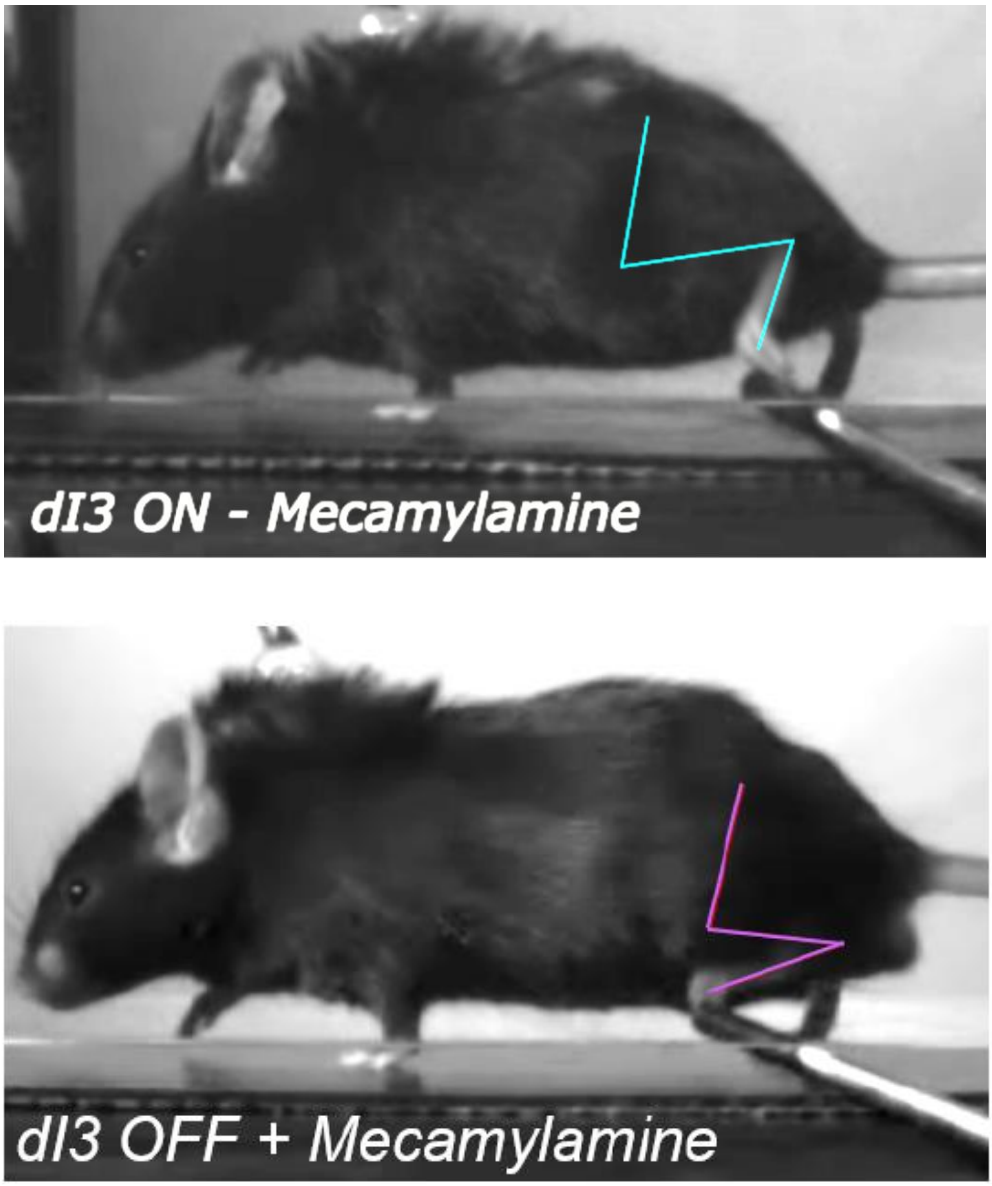

Figure 3.3 Images capturing a dragging event (i.e., failed SCR) induced by mechanical perturbation in mecamylamine trials both with and without dI3 silencing. Cyan-colored kinematic hindlimb skeletons represent dI3 ON conditions; magenta-colored kinematic skeletons represent dI3 OFF conditions.

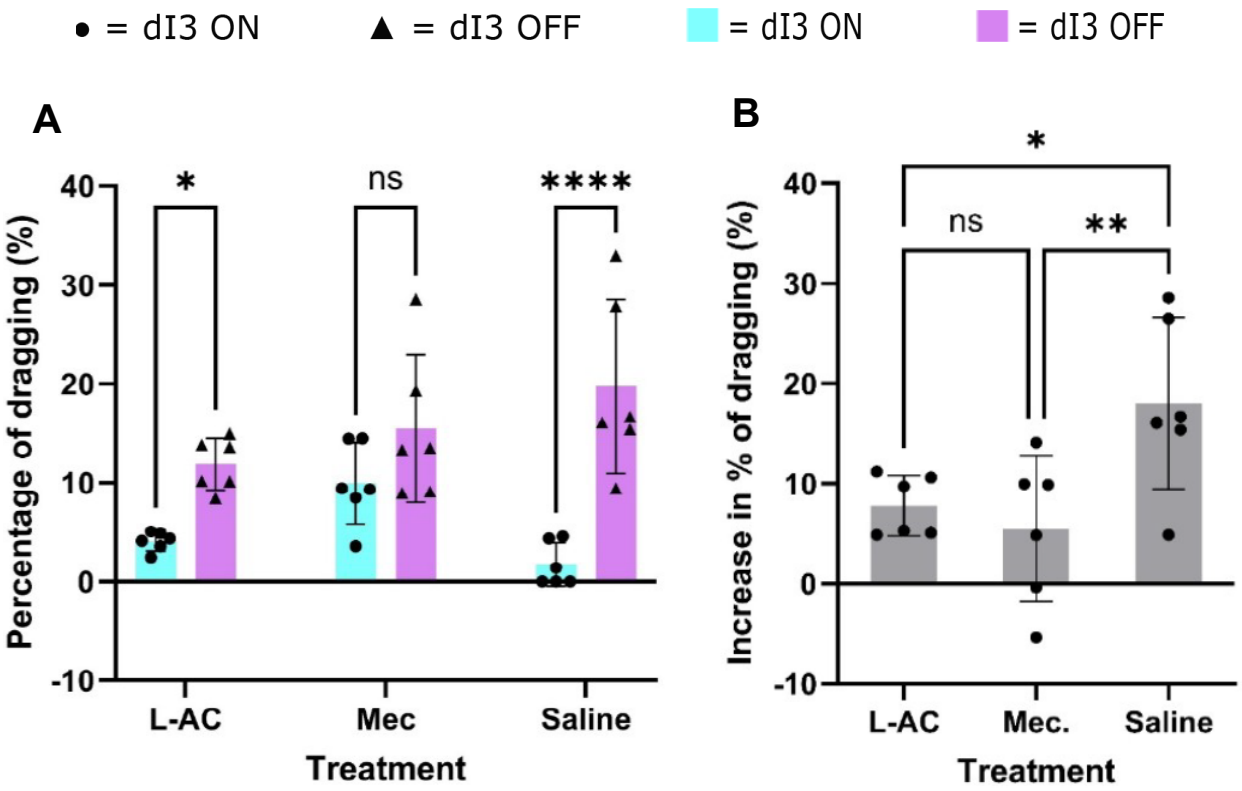

Figure 3.4 The increased incidence of dragging events (i.e., failed SCR) between dI3 ON and dI3 OFF treatment trials resulting from mechanical perturbation attempts in the treadmill task. A) Percentage of SCR trials resulting in dragging events. Bars colored in cyan with circular data points represent dI3 ON trials while bars colored in magenta with triangular data points represent dI3 OFF trials. B) The net increase in the percentage of SCR trials resulting in dragging. Grey colored bars and circular data points represent the mean increase in drags from dI3 ON to dI3 OFF trials. Data are presented as means ± SD. $N = 6$. The net increase in the incidence of dragging events between dI3 ON and dI3 OFF treatment trials, as well as between the three combined treatments, was analyzed using a two-way ANOVA and Sidak's multiple comparisons test: *$p \leq 0.05$, **$p \leq 0.01$, ****$p \leq 0.0001$.

A) Comparisons between dI3 ON and dI3 OFF	P-Value	Significance
dI3 ON + L-AC vs. dI3 OFF + L-AC	0.0370	*
dI3 ON + MEC vs. dI3 OFF + MEC	0.1788	ns
dI3 ON + Saline vs. dI3 OFF + Saline	<0.0001	****
dI3 ON + L-AC vs. dI3 ON + MEC	0.0415	*
dI3 ON + L-AC vs. dI3 ON + Saline	0.0651	ns
dI3 ON + MEC vs. dI3 ON + Saline	0.0012	**
dI3 OFF + L-AC vs. dI3 OFF + MEC	0.3905	ns
dI3 OFF + L-AC vs. dI3 OFF + Saline	0.0939	ns
dI3 OFF + MEC vs. dI3 OFF + Saline	0.2842	ns
B) Comparisons between treatments	**P-Value**	**Significance**
L-AC vs. MEC	0.6450	ns
L-AC vs. Saline	0.0357	*
MEC vs. Saline	0.0082	**

Table 3.2 Table of *p*-value results of Tukey's multiple comparisons test after a two-way ANOVA comparing the incidence of dragging events from attempted mechanical perturbations. A) Statistical test results (*p*-values) testing the difference between the average percentage of dragging events from dI3 ON to dI3 OFF treatment, as well as between the three treatments (L-AC, MEC, and saline) in *mechanical* SCR treadmill trials. B) *p*-values represent the difference in increased dragging after dI3 silencing between the three treatments (L-AC, MEC, and saline). $N = 6$. *$p \leq 0.05$, ** $p \leq 0.01$, ****$p \leq 0.0001$.

3.2.2 dI3s modulate limb trajectory during the stumbling corrective response

In addition to lower step heights and increased incidence of failed SCRs/drags, we also observed differences in the trajectory of the hindlimb during the execution of this corrective reflex. For both mechanically and electrically induced SCRs, all three dI3 OFF treatment trials (i.e., saline, L-AC, and MEC) displayed a relatively blunted SCR trajectory demonstrating lower toe heights and less severe angular changes of the knee and ankle in comparison to those of dI3 ON trials with saline, L-AC, and MEC (Fig. 3.5 – 3.8). The trajectory of dragging events on the mechanical treadmill task also appeared to demonstrate hindlimb trajectories similar to those of blunted SCRs as demonstrated in dI3 OFF trials (Fig. 3.5 – 3.8). Moreover, the effects of MEC administration appeared to somewhat resemble those of JHU37160 to turn off dI3s, where even dI3 ON + MEC treadmill trials demonstrated SCR trajectories and dragging events similar to those of dI3 OFF trials (Fig. 3.6, Fig. 3.7). With L-AC treatment, both electrical and mechanical SCR trajectories in dI3 OFF trials still appear relatively blunted in comparison to dI3 ON trials (Fig. 3.8).

A) dl3 ON + Saline

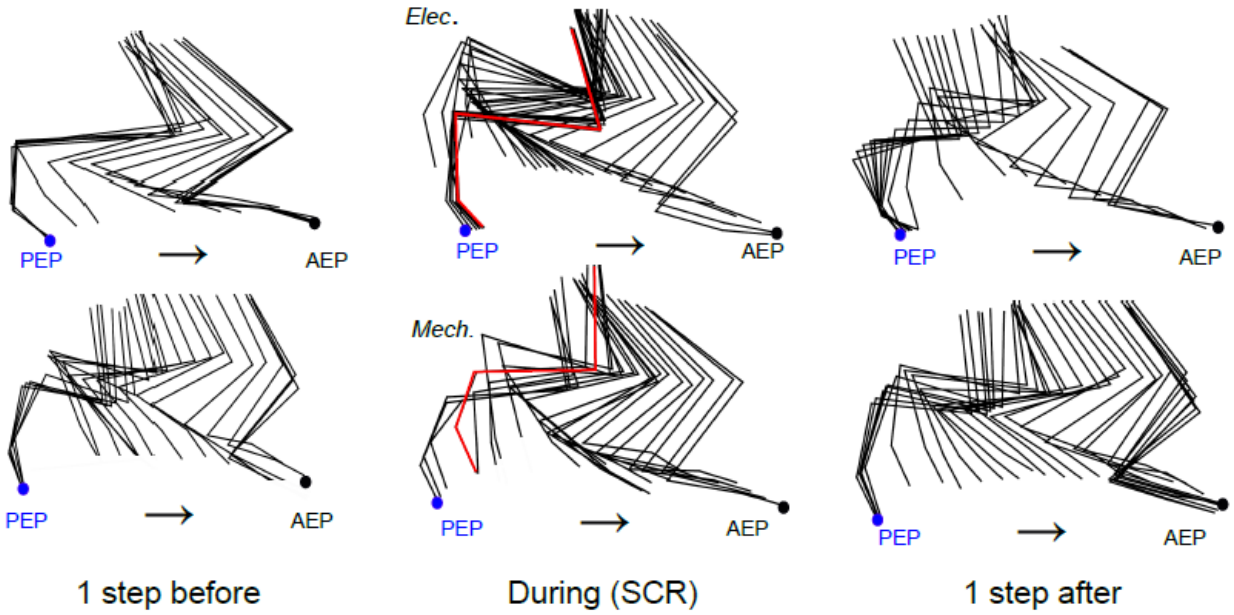

B) dl3 OFF + Saline

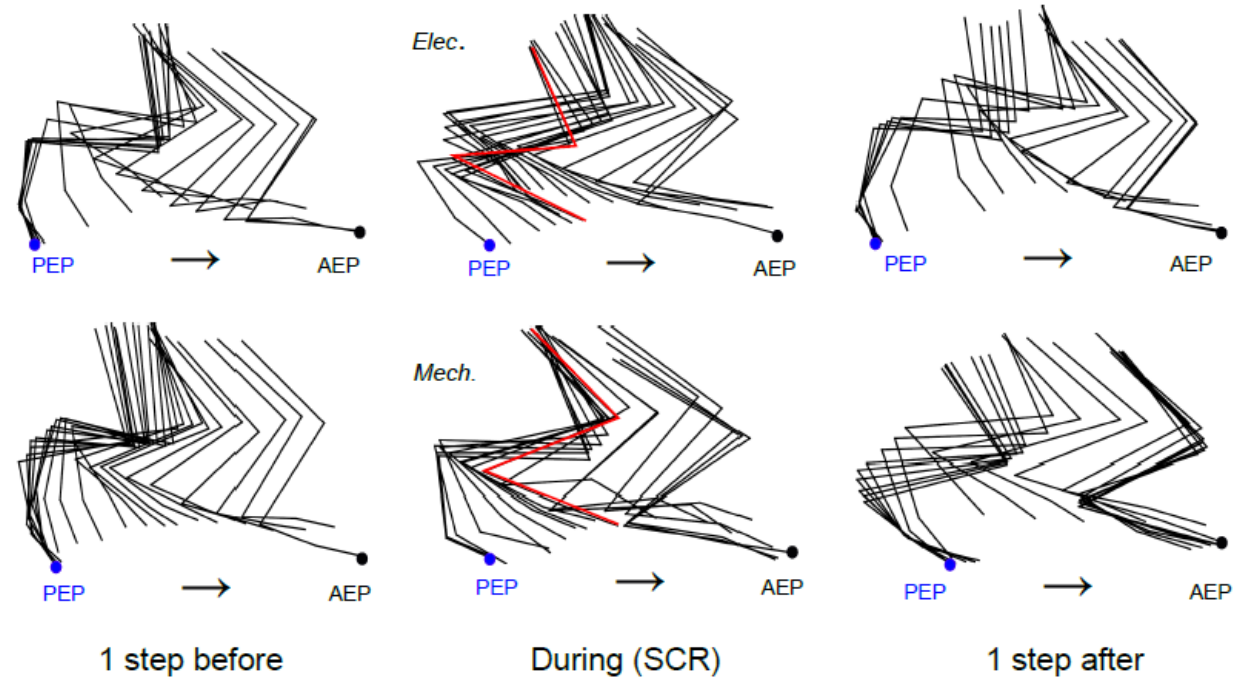

Figure 3.5 Stick plots from an individual mouse demonstrating the hindlimb trajectory during the step preceding, during and after the SCR in dI3 ON vs dI3 OFF treatment trials. *Elec.* represents the SCR elicited by electrical perturbation; *Mech*. represents the SCR elicited by mechanical perturbation. PEP, posterior extreme position (blue filled circles); AEP, anterior extreme position (black filled circles). Sticks highlighted in red indicate the timing of perturbation to the hindlimb.

A) dl3 ON + Mecamylamine

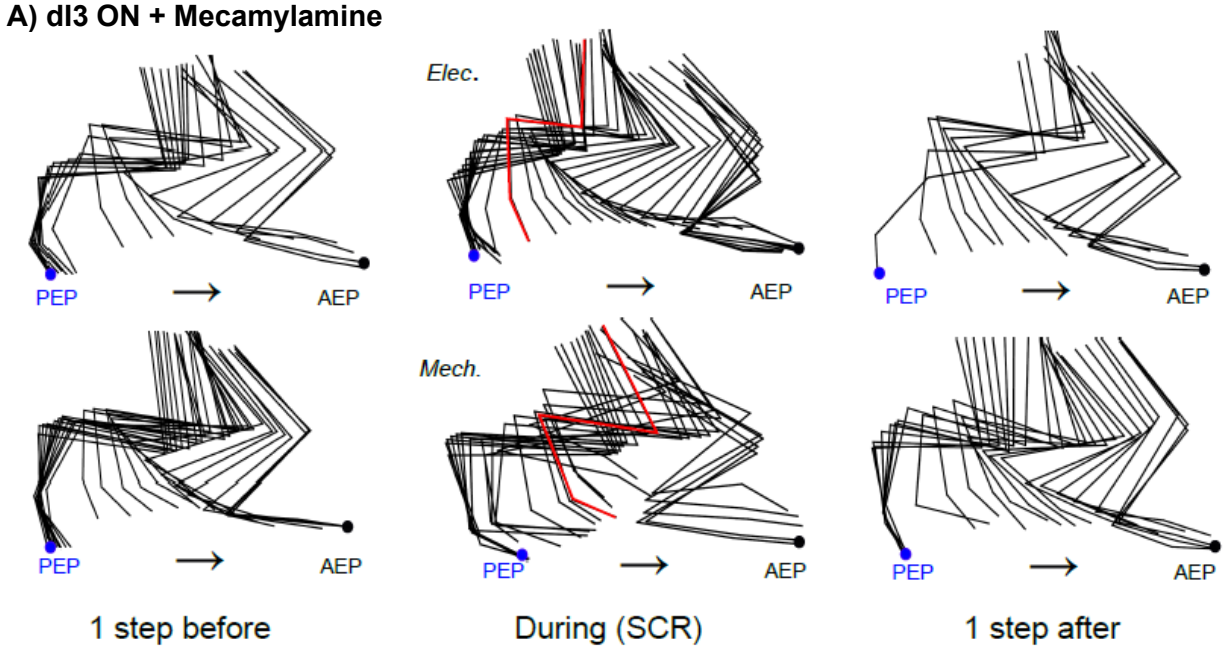

B) dl3 OFF + Mecamylamine

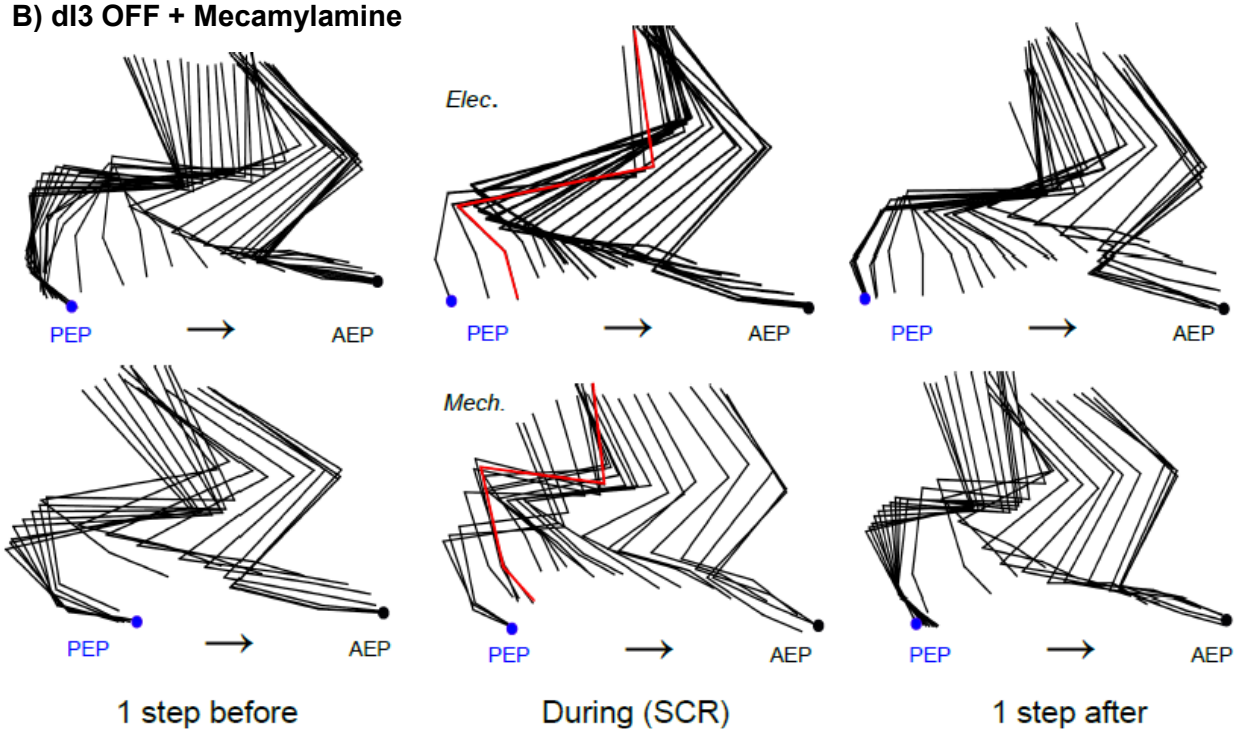

Figure 3.6 Stick plots from an individual mouse demonstrating the hindlimb trajectory during the step preceding, during and after the SCR in dI3 ON vs dI3 OFF treatment trials with mecamylamine. *Elec*. represents the SCR elicited by electrical perturbation; *Mech*. represents the SCR elicited by mechanical perturbation. PEP, posterior extreme position (blue filled circles); AEP, anterior extreme position (black filled circles). Sticks highlighted in red indicate the timing of perturbation to the hindlimb.

A) dl3 ON + L-acetyl carnitine

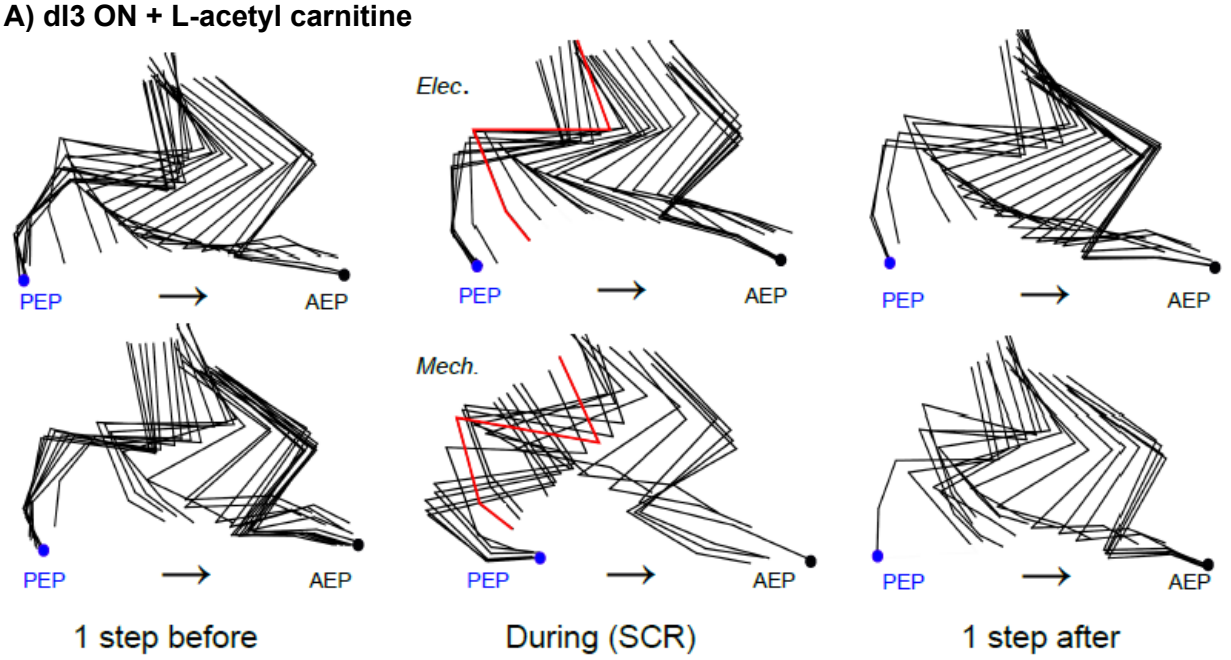

B) dl3 OFF + L-acetyl carnitine

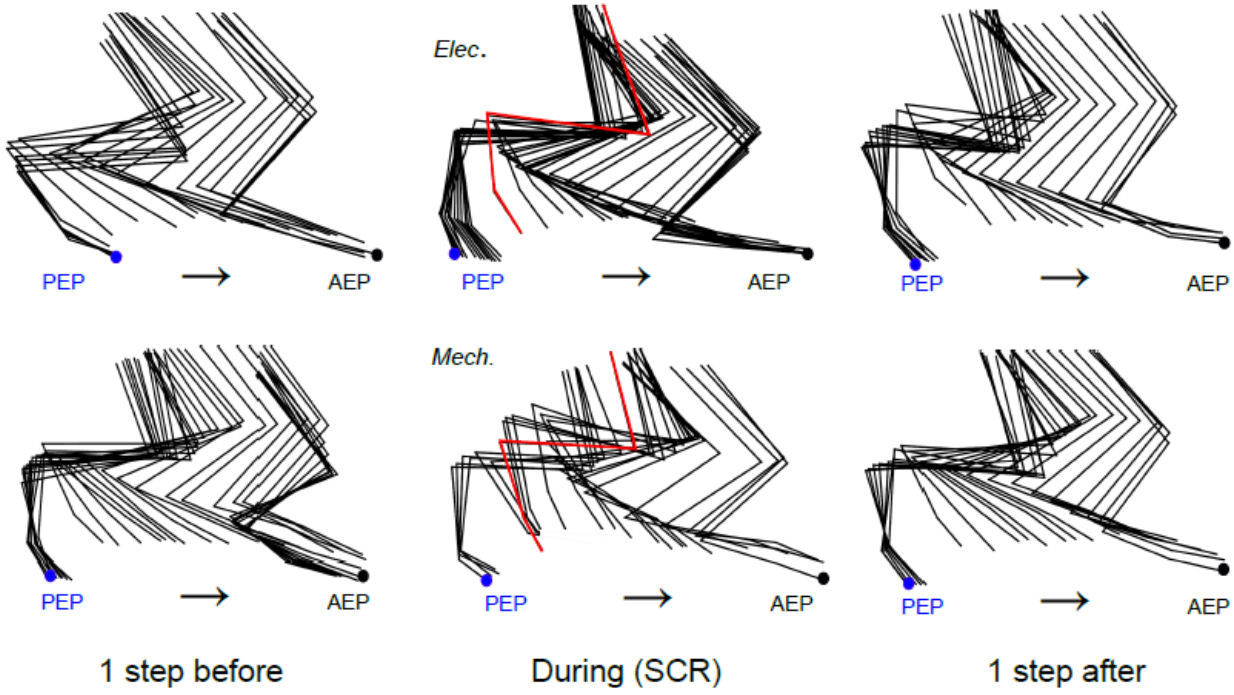

Figure 3.7 Stick plots from an individual mouse demonstrating the hindlimb trajectory during the step preceding, during and after the SCR in dI3 ON vs dI3 OFF treatment trials with L-acetyl carnitine. *Elec*. represents the SCR elicited by electrical perturbation; *Mech*. represents the SCR elicited by mechanical perturbation. PEP, posterior extreme position (blue filled circles); AEP, anterior extreme position (black filled circles). Sticks highlighted in red indicate the timing of perturbation to the hindlimb.

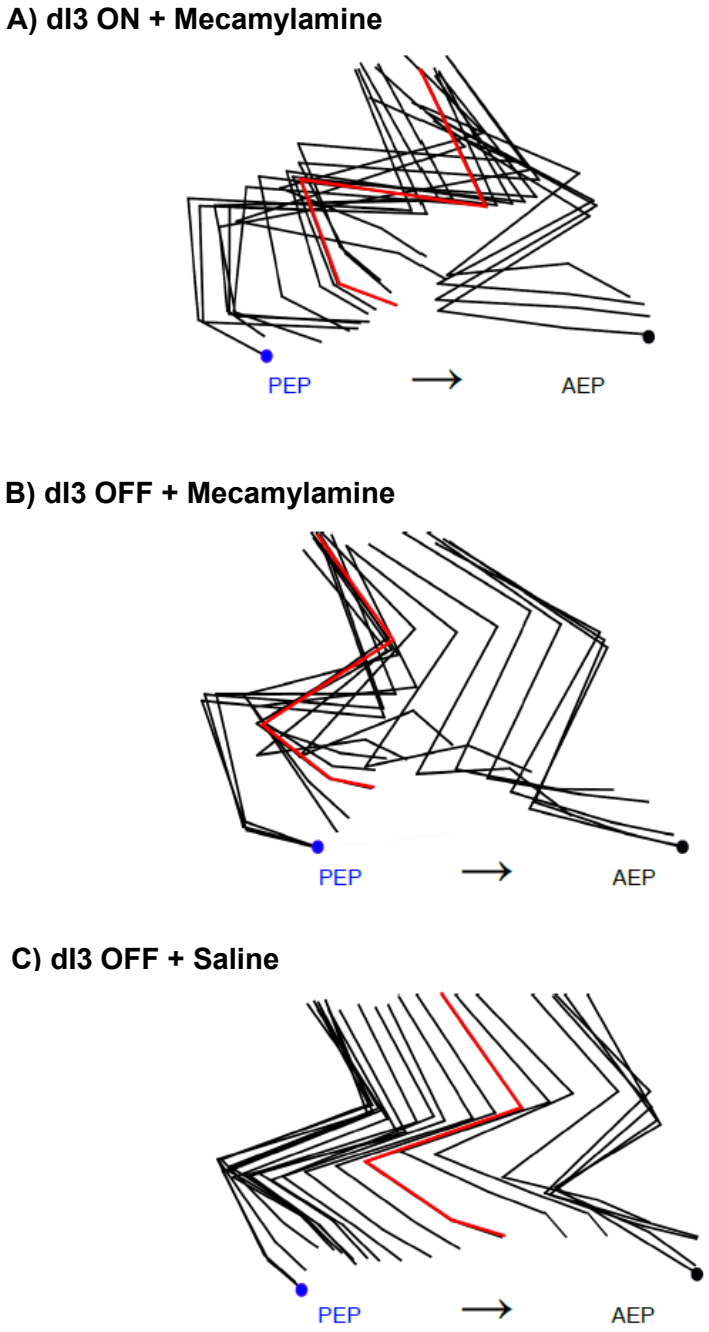

Figure 3.8 Stick plots from an individual mouse demonstrating the hindlimb trajectory during a dragging event (i.e., failed SCR) in dI3 ON vs dI3 OFF treatment trials with mecamylamine and saline. Drags were elicited by mechanical perturbation with a metal bar. PEP, posterior extreme position (blue filled circles); AEP, anterior extreme position (black filled circles). Sticks highlighted in red indicate the timing of perturbation to the hindlimb.

3.2.3. dI3s modulate step height of the stumbling corrective response

To confirm our qualitative assessment of the kinematics of the hindlimbs during SCR, we next examined the height of paw flexion when attempting to clear a perturbation. While the SCR was not eliminated completely with the absence of dI3 activity, we observed a significant reduction in the peak step height of the SCR when elicited by both mechanical and electrical stimulation when comparing dI3 ON + saline control trials to dI3 OFF + saline trials (Fig. 3.9, Fig. 3.10; N = 6; Tukey's test, $p \leq 0.05$ for electrical SCR trials and $p \leq 0.01$ for mechanical SCR trials). In contrast, when comparing SCR step heights after administration of MEC treatment, we observed no significant difference between dI3 ON and dI3 OFF trials, with peak step heights remaining consistent (Fig. 3.9, Fig. 3.10; N = 6; Tukey's test, $p > 0.05$ for both mechanical and electrical SCR).

Combined treatments with L-AC also resulted in a significant reduction in peak SCR step height from dI3 ON to dI3 OFF but only for mechanically stimulated perturbations (Fig. 3.9, Fig. 3.10; N = 6; Tukey's test, $p \leq 0.01$ for mechanical SCR trials and $p > 0.05$ for electrical SCR trials). While there were no significant changes in the step height of steps preceding the SCR elicited mechanically or electrically in any of the treatment groups, we did observe a significant reduction in the average step height immediately following the mechanically evoked SCR in dI3 OFF + saline trials compared to dI3 ON + saline trials (Fig. 3.9, Fig. 3.10; N = 6; Tukey's test, $p \leq 0.01$ for mechanical SCR trials and $p > 0.05$ for electrical SCR trials). After MEC combined treatments, average step heights preceding, during, and following the SCR remained comparable between dI3 ON and dI3 OFF trials when both mechanically and electrically stimulated (Fig. 3.9, Fig. 3.10; N = 6; Tukey's test, $p > 0.05$). All p-values from Tukey's multiple comparisons tests are presented below in Tables 3.3 – 3.8.

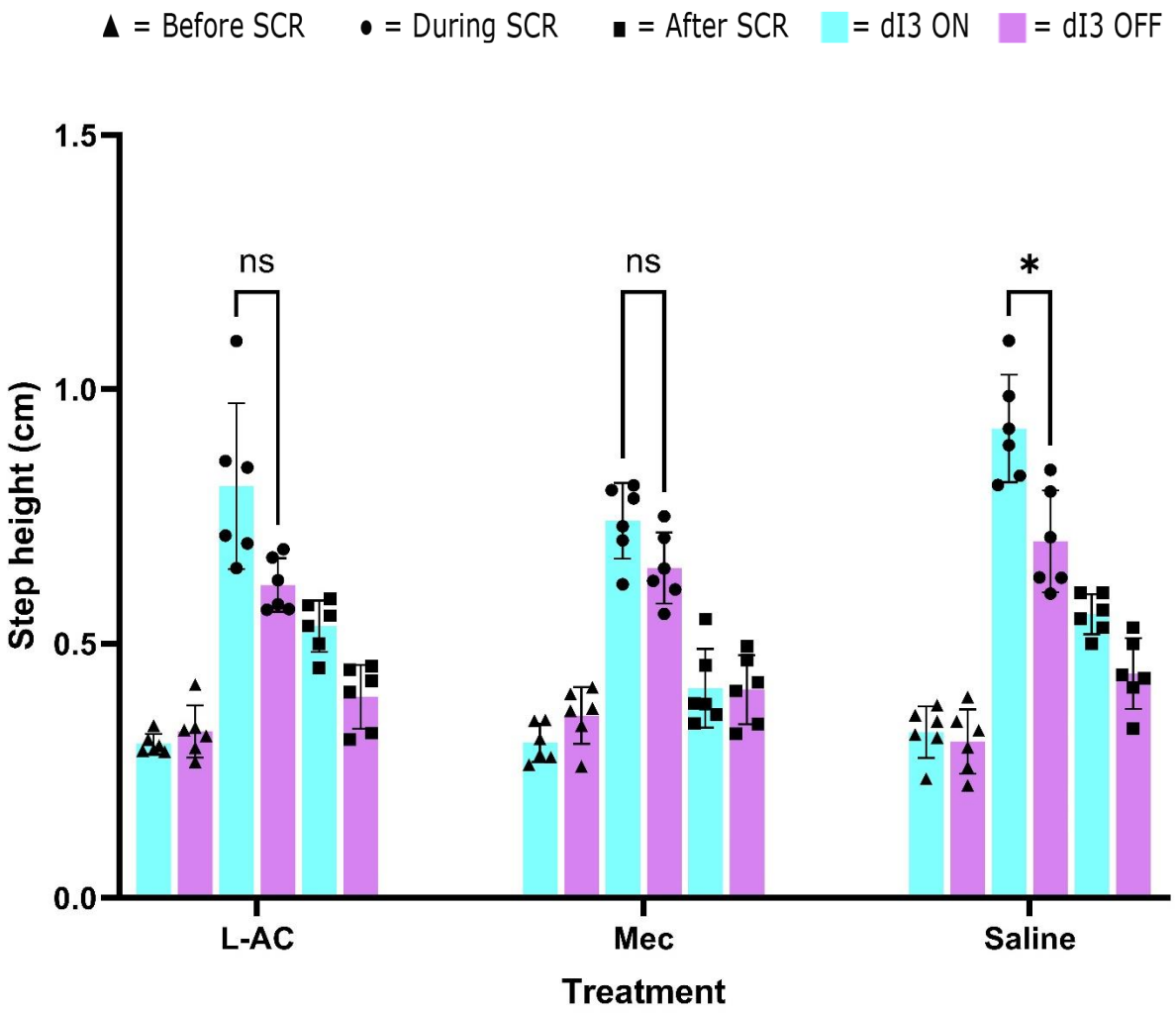

Figure 3.9 Peak toe height of the step before, during and after the SCR when elicited by electrical perturbation. Average step heights were calculated for each of the three different pharmacological treatments, with a total of 6 unique treatment conditions. Bars colored in cyan represent dI3 ON trials while bars colored in magenta represent dI3 OFF trials; triangular data points represent the step preceding the SCR, circular points represent the step during the SCR, and square data points represent the step immediately after. Data are presented as means ± SD; $N = 6$. *$p \leq 0.05$ (Tukey's multiple comparison test following two-way ANOVA).

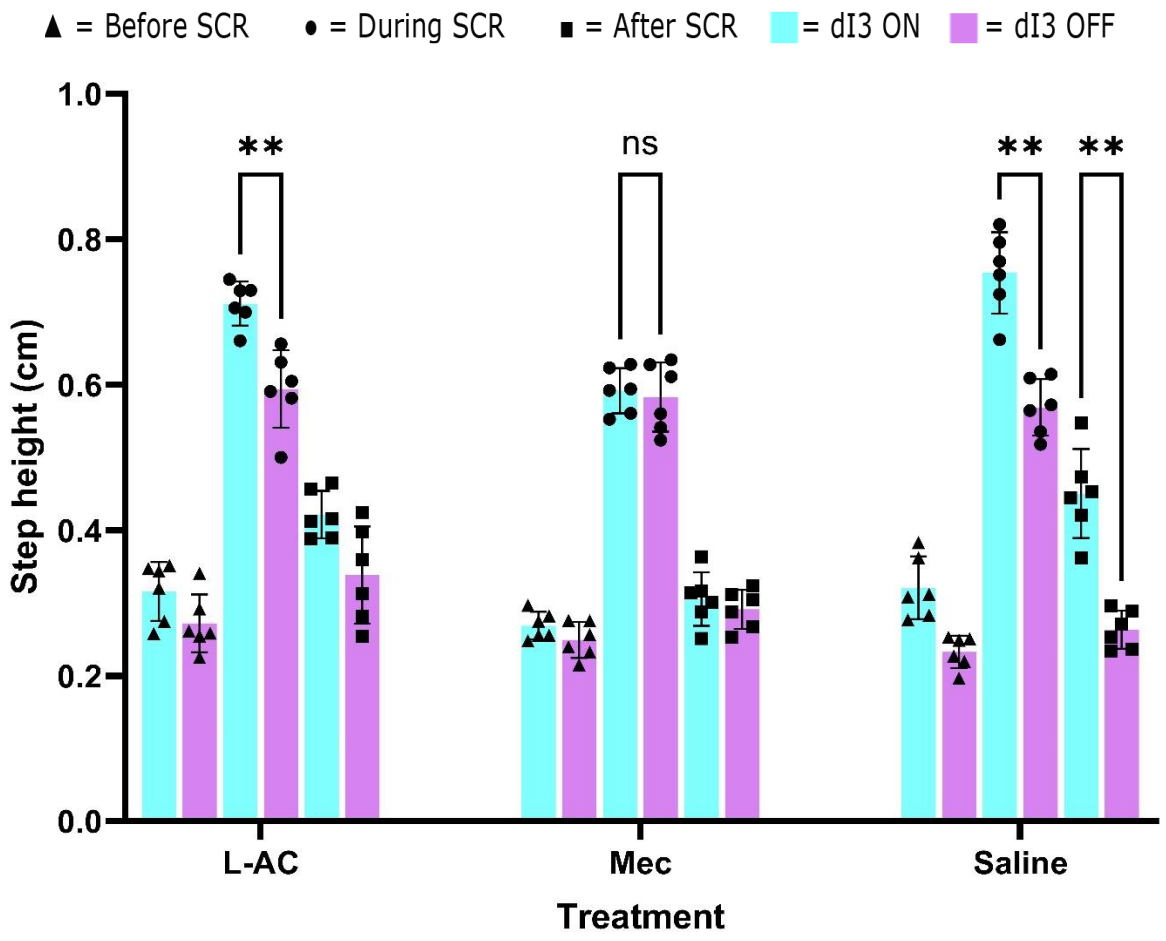

Figure 3.10 Peak toe height of the step before, during and after the SCR when elicited by mechanical perturbation. Average step heights were calculated for each of the three different pharmacological treatments, with a total of 6 unique treatment conditions. Bars colored in cyan represent dI3 ON trials while bars colored in magenta represent dI3 OFF trials; triangular data points represent the step preceding the SCR, circular points represent the step during the SCR, and square data points represent the step immediately after. Data are presented as means ± SD; $N = 6$. $^{**}p \leq 0.01$ (Tukey's multiple comparison test following two-way ANOVA).

Comparisons with L-acetyl carnitine	P-Value	Significance
Before SCR - dI3 ON vs. Before SCR - dI3 OFF	0.8789	Ns
Before SCR - dI3 ON vs. During SCR - dI3 ON	0.0043	**
Before SCR - dI3 ON vs. During SCR - dI3 OFF	0.0005	***
Before SCR - dI3 ON vs. After SCR - dI3 ON	0.0002	***
Before SCR - dI3 ON vs. After SCR - dI3 OFF	0.1539	Ns
Before SCR - dI3 OFF vs. During SCR - dI3 ON	0.0012	**
Before SCR - dI3 OFF vs. During SCR - dI3 OFF	<0.0001	****
Before SCR - dI3 OFF vs. After SCR - dI3 ON	0.0177	*
Before SCR - dI3 OFF vs. After SCR - dI3 OFF	0.2739	Ns
During SCR - dI3 ON vs. During SCR - dI3 OFF	0.0930	Ns
During SCR - dI3 ON vs. After SCR - dI3 ON	0.0981	Ns
During SCR - dI3 ON vs. After SCR - dI3 OFF	0.0072	**
During SCR - dI3 OFF vs. After SCR - dI3 ON	0.3523	Ns
During SCR - dI3 OFF vs. After SCR - dI3 OFF	0.0002	***
After SCR - dI3 ON vs. After SCR - dI3 OFF	0.0794	Ns

Table 3.3 Table of *p*-value results of Tukey's multiple comparisons test after a two-way ANOVA comparing electrical SCR step heights. Statistical test results (*p*-values) represent the difference between comparisons of the average step heights of the step before, during and after the *electrically* stimulated SCR in combined L-AC treatment trials. $N = 6$. *$p \leq 0.05$, **$p \leq 0.01$, ***$p \leq 0.001$, ****$p \leq 0.0001$.

Comparisons with mecamylamine	P-Value	Significance
Before SCR - dI3 ON vs. Before SCR - dI3 OFF	0.4125	Ns
Before SCR - dI3 ON vs. During SCR - dI3 ON	0.0002	***
Before SCR - dI3 ON vs. During SCR - dI3 OFF	0.0006	***
Before SCR - dI3 ON vs. After SCR - dI3 ON	0.0806	ns
Before SCR - dI3 ON vs. After SCR - dI3 OFF	0.1210	ns
Before SCR - dI3 OFF vs. During SCR - dI3 ON	0.0017	**
Before SCR - dI3 OFF vs. During SCR - dI3 OFF	<0.0001	****
Before SCR - dI3 OFF vs. After SCR - dI3 ON	0.8578	ns
Before SCR - dI3 OFF vs. After SCR - dI3 OFF	0.2099	ns
During SCR - dI3 ON vs. During SCR - dI3 OFF	0.3953	ns
During SCR - dI3 ON vs. After SCR - dI3 ON	0.0005	***
During SCR - dI3 ON vs. After SCR - dI3 OFF	0.0103	*
During SCR - dI3 OFF vs. After SCR - dI3 ON	0.0379	*
During SCR - dI3 OFF vs. After SCR - dI3 OFF	0.0003	***
After SCR - dI3 ON vs. After SCR - dI3 OFF	>0.9999	ns

Table 3.4 Table of *p*-value results of Tukey's multiple comparisons test after a two-way ANOVA comparing electrical SCR step heights. Statistical test results (*p*-values) represent the difference between comparisons of the average step heights of the step before, during and after the *electrically* stimulated SCR in combined MEC treatment trials. $N = 6$. *$p \leq 0.05$, **$p \leq 0.01$, ***$p \leq 0.001$, ****$p \leq 0.0001$.

Comparisons with saline	P-Value	Significance
Before SCR - dI3 ON vs. Before SCR - dI3 OFF	0.9963	ns
Before SCR - dI3 ON vs. During SCR - dI3 ON	0.0006	***
Before SCR - dI3 ON vs. During SCR - dI3 OFF	0.0078	**
Before SCR - dI3 ON vs. After SCR - dI3 ON	0.0032	**
Before SCR - dI3 ON vs. After SCR - dI3 OFF	0.2503	ns
Before SCR - dI3 OFF vs. During SCR - dI3 ON	0.0003	***
Before SCR - dI3 OFF vs. During SCR - dI3 OFF	0.0020	**
Before SCR - dI3 OFF vs. After SCR - dI3 ON	0.0001	***
Before SCR - dI3 OFF vs. After SCR - dI3 OFF	0.0562	ns
During SCR - dI3 ON vs. During SCR - dI3 OFF	0.0200	*
During SCR - dI3 ON vs. After SCR - dI3 ON	0.0022	**
During SCR - dI3 ON vs. After SCR - dI3 OFF	0.0027	**
During SCR - dI3 OFF vs. After SCR - dI3 ON	0.1540	ns
During SCR - dI3 OFF vs. After SCR - dI3 OFF	0.0045	**
After SCR - dI3 ON vs. After SCR - dI3 OFF	0.0957	ns

Table 3.5 Table of *p*-value results of Tukey's multiple comparisons test after a two-way ANOVA comparing electrical SCR step heights. Statistical test results (*p*-values) represent the difference between comparisons of the average step heights of the step before, during and after the *electrically* stimulated SCR in combined saline treatment trials. $N = 6$. *$p \leq 0.05$, **$p \leq 0.01$, ***$p \leq 0.001$.

Comparisons with L-acetyl carnitine	P-Value	Significance
Before SCR - dI3 ON vs. Before SCR - dI3 OFF	0.5072	ns
Before SCR - dI3 ON vs. During SCR - dI3 ON	<0.0001	****
Before SCR - dI3 ON vs. During SCR - dI3 OFF	0.0001	***
Before SCR - dI3 ON vs. After SCR - dI3 ON	0.0031	**
Before SCR - dI3 ON vs. After SCR - dI3 OFF	0.9697	ns
Before SCR - dI3 OFF vs. During SCR - dI3 ON	<0.0001	****
Before SCR - dI3 OFF vs. During SCR - dI3 OFF	0.0018	**
Before SCR - dI3 OFF vs. After SCR - dI3 ON	0.0110	*
Before SCR - dI3 OFF vs. After SCR - dI3 OFF	0.2834	ns
During SCR - dI3 ON vs. During SCR - dI3 OFF	0.0010	**
During SCR - dI3 ON vs. After SCR - dI3 ON	<0.0001	****
During SCR - dI3 ON vs. After SCR - dI3 OFF	0.0005	***
During SCR - dI3 OFF vs. After SCR - dI3 ON	0.0015	**
During SCR - dI3 OFF vs. After SCR - dI3 OFF	0.0051	**
After SCR - dI3 ON vs. After SCR - dI3 OFF	0.2176	ns

Table 3.6 Table of *p*-value results of Tukey's multiple comparisons test after a two-way ANOVA comparing mechanical SCR step heights. Statistical test results (*p*-values) represent the difference between comparisons of the average step heights of the step before, during and after the *mechanically* stimulated SCR in combined L-AC treatment trials. $N = 6$. *$p \leq 0.05$, **$p \leq 0.01$, ***$p \leq 0.001$, ****$p \leq 0.0001$.

Comparisons with mecamylamine	P-Value	Significance
Before SCR - dI3 ON vs. Before SCR - dI3 OFF	0.1525	ns
Before SCR - dI3 ON vs. During SCR - dI3 ON	<0.0001	****
Before SCR - dI3 ON vs. During SCR - dI3 OFF	<0.0001	****
Before SCR - dI3 ON vs. After SCR - dI3 ON	0.2588	ns
Before SCR - dI3 ON vs. After SCR - dI3 OFF	0.4784	ns
Before SCR - dI3 OFF vs. During SCR - dI3 ON	<0.0001	****
Before SCR - dI3 OFF vs. During SCR - dI3 OFF	<0.0001	****
Before SCR - dI3 OFF vs. After SCR - dI3 ON	0.0544	ns
Before SCR - dI3 OFF vs. After SCR - dI3 OFF	0.2003	ns
During SCR - dI3 ON vs. During SCR - dI3 OFF	0.9986	ns
During SCR - dI3 ON vs. After SCR - dI3 ON	<0.0001	****
During SCR - dI3 ON vs. After SCR - dI3 OFF	<0.0001	****
During SCR - dI3 OFF vs. After SCR - dI3 ON	0.0016	**
During SCR - dI3 OFF vs. After SCR - dI3 OFF	<0.0001	****
After SCR - dI3 ON vs. After SCR - dI3 OFF	0.9839	ns

Table 3.7 Table of *p*-value results of Tukey's multiple comparisons test after a two-way ANOVA comparing mechanical SCR step heights. Statistical test results (*p*-values) represent the difference between comparisons of the average step heights of the step before, during and after the *mechanically* stimulated SCR in combined MEC treatment trials. $N = 6$. $^{**}p \leq 0.01$, $^{****}p \leq 0.0001$.

Comparisons with saline	P-Value	Significance
Before SCR - dI3 ON vs. Before SCR - dI3 OFF	0.0876	ns
Before SCR - dI3 ON vs. During SCR - dI3 ON	<0.0001	****
Before SCR - dI3 ON vs. During SCR - dI3 OFF	0.0007	***
Before SCR - dI3 ON vs. After SCR - dI3 ON	0.0060	**
Before SCR - dI3 ON vs. After SCR - dI3 OFF	0.0410	*
Before SCR - dI3 OFF vs. During SCR - dI3 ON	<0.0001	****
Before SCR - dI3 OFF vs. During SCR - dI3 OFF	<0.0001	****
Before SCR - dI3 OFF vs. After SCR - dI3 ON	0.0083	**
Before SCR - dI3 OFF vs. After SCR - dI3 OFF	0.4490	ns
During SCR - dI3 ON vs. During SCR - dI3 OFF	0.0029	**
During SCR - dI3 ON vs. After SCR - dI3 ON	<0.0001	****
During SCR - dI3 ON vs. After SCR - dI3 OFF	<0.0001	****
During SCR - dI3 OFF vs. After SCR - dI3 ON	0.0620	ns
During SCR - dI3 OFF vs. After SCR - dI3 OFF	<0.0001	****
After SCR - dI3 ON vs. After SCR - dI3 OFF	0.0031	**

Table 3.8 Table of *p*-value results of Tukey's multiple comparisons test after a two-way ANOVA comparing mechanical SCR step heights. Statistical test results (*p*-values) represent the difference between comparisons of the average step heights of the step before, during and after the *mechanically* stimulated SCR in combined saline treatment trials. $N = 6$. *$p \leq 0.05$, **$p \leq 0.01$, ***$p \leq 0.001$, ****$p \leq 0.0001$.

3.2.4 dI3s modulate ankle flexor activation during the stumbling corrective response

We next analyzed the electromyographic (EMG) activity during the SCR to assess any differences in muscle activation in the presence or absence of dI3 activity as well as Renshaw cell activity. Muscle activation of the ankle flexor, tibialis anterior (TA), during the SCR appeared to demonstrate subtle changes after dI3 silencing on the treadmill (Fig. 3.11, 3.12). Raw EMG traces recorded from the ankle flexor (i.e., the TA) across the 6 different treatments demonstrated subtle visual differences with respect to duration and amplitude when compared to typical TA bursts during an SCR in control conditions (i.e., dI3 ON + saline). These small changes are observed in both the mechanical and electrical perturbation tasks, yet are most apparent in dI3 OFF trials with MEC and saline treatment during the electrical perturbation task specifically (Fig. 3.11, 3.12).

To quantify TA activity during the SCR, we examined TA burst duration and amplitude. We found that during SCRs elicited in the early-to-mid swing phase, TA bursts demonstrated a small, non-significant, increase in burst duration in mechanical SCR trials and a significant increase in electrical SCR trials between dI3 ON and dI3 OFF animals (Fig. 3.13; $N = 6$ for electrical SCR, $N = 3$ for mechanical SCR; Tukey's test, $p \leq 0.05$ in saline mechanical SCR trials and $p \leq 0.01$ for differences between dI3 ON and dI3 OFF in combination with L-AC, MEC, and saline in electrical SCR trials). Average burst duration demonstrated a greater increase in electrical SCR trials after dI3 silencing, with an average increase of 42.71 ± 15.32, 58.09 ± 17.91, and 66.55 ± 13.45 ms in trials with L-AC, MEC, and saline treatments, respectively (Fig. 3.13A; $N = 6$). These increases were statistically significantly greater than TA burst duration in dI3 ON trials for all three treatments. For mechanical SCR trials, TA burst duration increased on average by 36.22 ± 20.47, 39.95 ± 22.39, and 48.19 ± 18.93 ms in dI3 OFF trials with L-AC, MEC, and saline treatments respectively (Fig. 3.13B; $N = 3$). Only the increase seen in saline trials between dI3 ON

and OFF was significantly greater. EMG data from mechanical SCR trials for 3 of the 6 mice were excluded from analysis due to experimental error when collecting EMG recordings. All *p*-values from Tukey's multiple comparisons test are presented below in Table 3.9.

We also observed subtle differences in TA EMG burst amplitude during early-to-mid swing SCRs between dI3 ON and dI3 OFF with the saline treatment, where the average peak amplitude of TA bursts was slightly but non-significantly reduced after dI3 silencing in mechanical SCR trials and significantly reduced in electrical SCR trials (Fig. 3.14; $N = 6$ for electrical SCR, $N = 3$ for mechanical SCR; Tukey's test, $p \leq 0.05$ for dI3 ON to OFF in saline mechanical SCR trials, and $p \leq 0.05$ and $p \leq 0.01$ for dI3 ON to OFF in MEC and saline electrical SCR trials). Average TA burst amplitude demonstrated a greater reduction in electrical SCR trials by 0.40 ± 0.45, 2.59 ± 0.78, and 3.04 ± 0.77 in dI3 OFF + L-AC, MEC and saline treatments (Fig. 3.14A; $N = 6$). The reduction in TA burst amplitude between dI3 ON and dI3 OFF was significantly different in MEC and saline treatments. Comparatively, in dI3 OFF trials, TA burst amplitude was reduced on average by 1.51 ± 0.99, 1.62 ± 0.89, and 2.90 ± 0.72 units in L-AC, MEC, and saline treatments, respectively, in the mechanical SCR task in comparison to dI3 ON trials (Fig. 3.14B; $N = 3$). Only the reduction in TA burst amplitude between dI3 ON and dI3 OFF in the saline treatment was statistically significant. Overall, TA EMG activity demonstrated significant changes to burst duration and amplitude after dI3 silencing in electrical SCR trials and mechanical SCR trials (Fig. 3.14; $N = 6$ for electrical SCR, $N = 3$ for mechanical SCR). All *p*-values from Tukey's multiple comparisons test are presented below in Table 3.10.

In contrast, activity in the ankle extensor, the medial gastrocnemius (MG), demonstrated no significant differences in extensor activation or bursting activity between dI3 ON and dI3 OFF

trials, as well as between the three different treatments (i.e., saline, L-AC, and MEC). Treatment comparisons of mean burst durations and burst amplitudes of MG activity throughout the SCR revealed no statistically significant differences between the 6 total treatment combinations following a two-way ANOVA and Tukey's multiple comparisons test. Overall, EMG activity from the MG demonstrated no overt differences qualitatively or statistically (Fig. 3.15, 3.16, 3.17; Table 11, 12; $N = 6$, electrical SCR analysis; $N = 4$, mechanical SCR analysis).

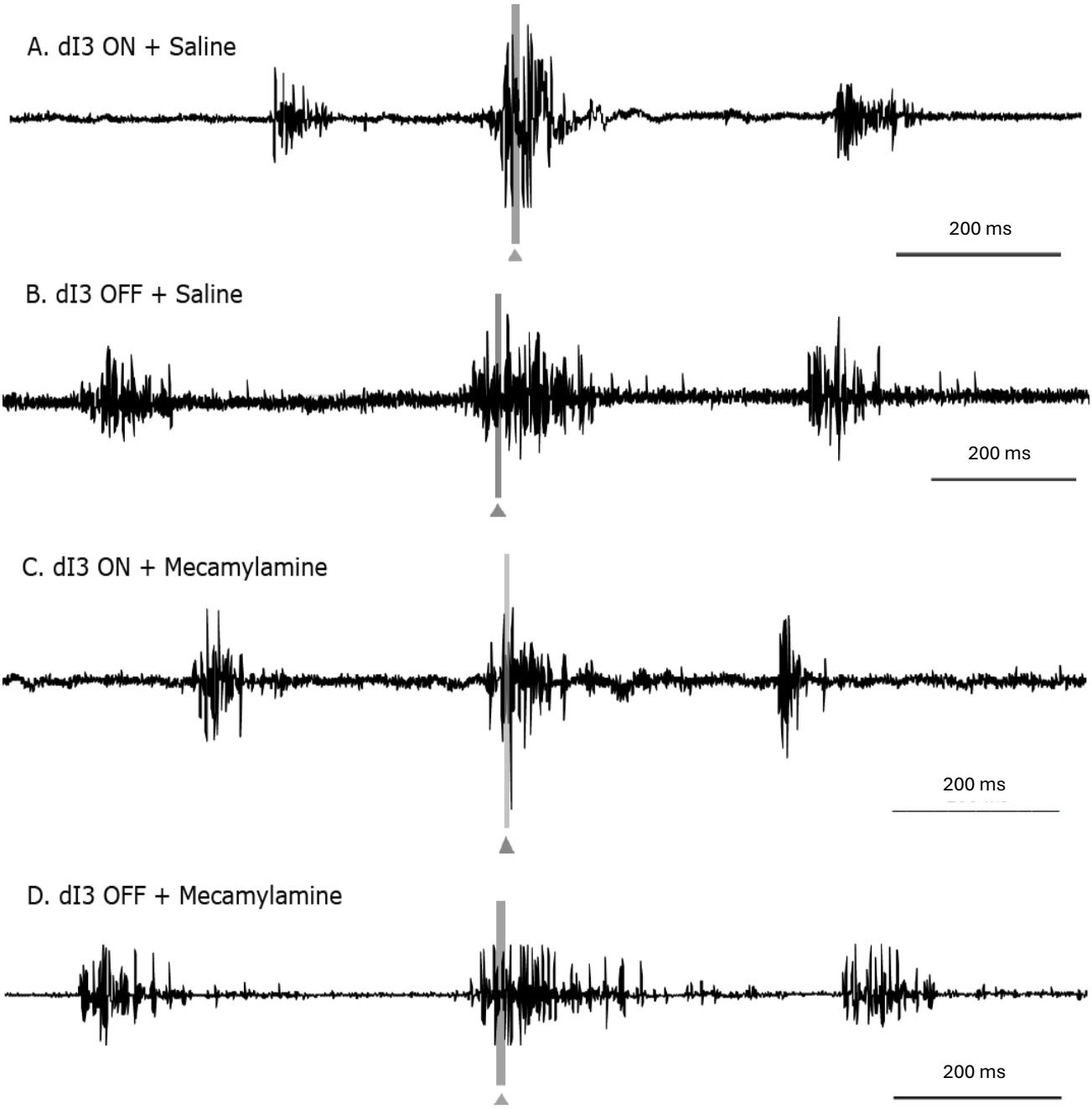

Figure 3.11 Raw EMG traces from the tibialis anterior hindlimb muscle of an individual mouse, demonstrating ankle flexor activation one step before, during and after electrical perturbation (SCR). Grey bars and triangles indicate the timing of electrical stimulus sent to the saphenous nerve to induce perturbation of the hindlimb. Scale bars represent 200ms.

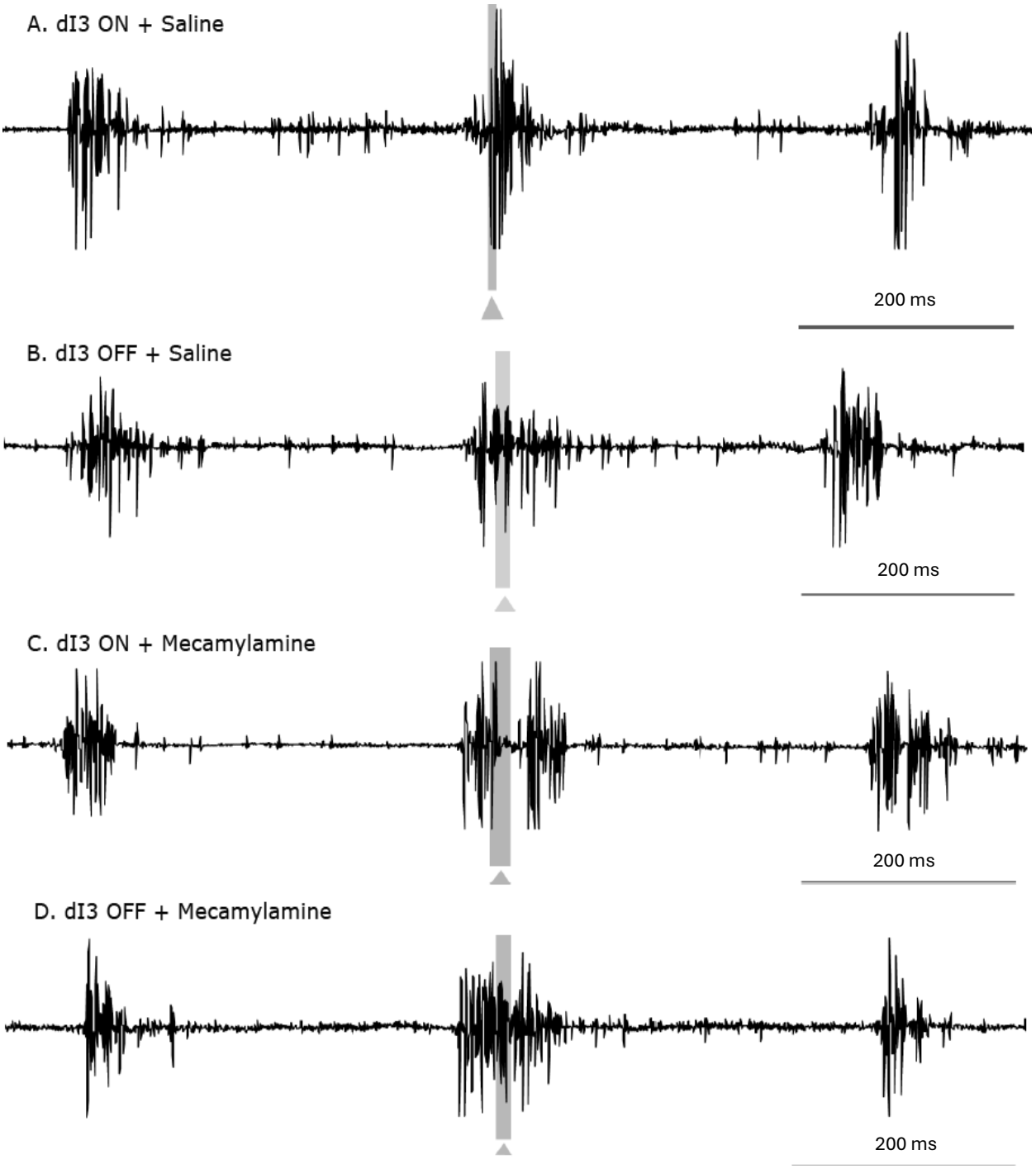

Figure 3.12 Raw EMG traces from the tibialis anterior hindlimb muscle of an individual mouse, demonstrating ankle flexor activation one step before, during and after mechanical perturbation (SCR). Grey bars and triangles indicate the moment of contact between the hindlimb paw and metal bar (i.e., perturbation). Scale bars represent 200ms.

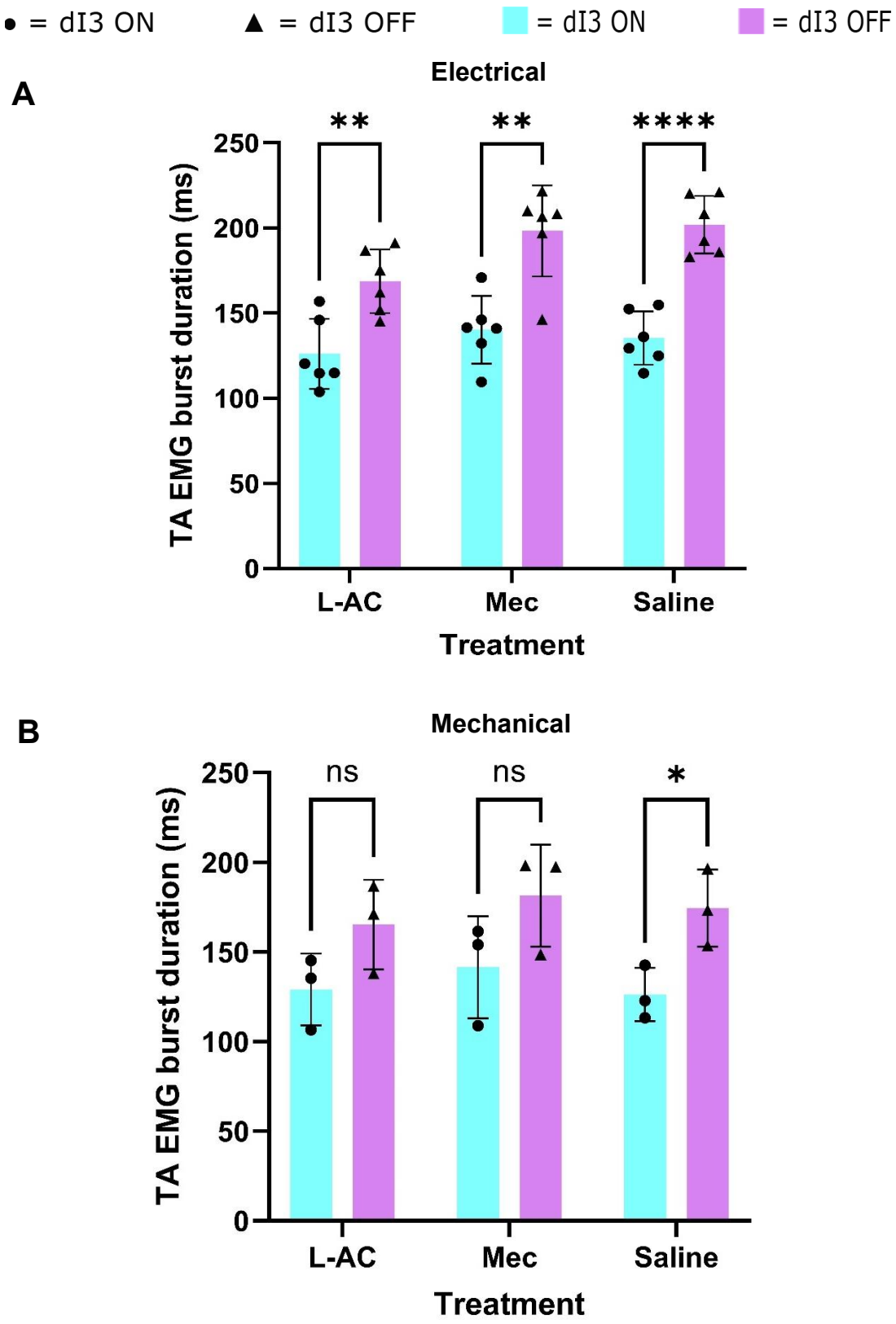
● = dI3 ON
▲ = dI3 OFF
= dI3 ON
= dI3 OFF
A
Electrical
**
**
****
250
200
150
100
50
0
TA EMG burst duration (ms)
L-AC
Mec
Saline
Treatment
B
Mechanical
ns
ns
*
250
200
150
100
50
0
TA EMG burst duration (ms)
L-AC
Mec
Saline
Treatment

Figure 3.13 The average burst duration of TA muscle activity from SCRs elicited during early-to-mid swing phase. A) Average EMG burst duration in the TA during electrical perturbation ($N = 6$). B) Average EMG burst duration in the TA during mechanical perturbation ($N = 3$). Data are presented as means ± SD. Bars colored in cyan with circular data points represent dI3 ON trials, while bars colored in magenta with triangular data points represent dI3 OFF trials. The observed increase in burst duration between dI3 ON and dI3 OFF treatment trials was analyzed using a two-way ANOVA and Tukey's multiple comparisons test: *$p \leq 0.05$, **$p \leq 0.01$, ****$p \leq 0.0001$.

A) Comparisons between dI3 ON and dI3 OFF	P-Value	Significance
dI3 ON + L-AC vs. dI3 OFF + L-AC	0.0038	**
dI3 ON + MEC vs. dI3 OFF + MEC	0.0020	**
dI3 ON + Saline vs. dI3 OFF + Saline	<0.0001	****
dI3 ON + L-AC vs. dI3 ON + MEC	0.5456	ns
dI3 ON + L-AC vs. dI3 ON + Saline	0.5621	ns
dI3 ON + MEC vs. dI3 ON + Saline	0.8680	ns
dI3 OFF + L-AC vs. dI3 OFF + MEC	0.1644	ns
dI3 OFF + L-AC vs. dI3 OFF + Saline	0.0496	*
dI3 OFF + MEC vs. dI3 OFF + Saline	0.9396	ns
B) Comparisons between dI3 ON and dI3 OFF	**P-Value**	**Significance**
dI3 ON + L-AC vs. dI3 OFF + L-AC	0.1248	ns
dI3 ON + MEC vs. dI3 OFF + MEC	0.1614	ns
dI3 ON + Saline vs. dI3 OFF + Saline	0.0390	*
dI3 ON + L-AC vs. dI3 ON + MEC	0.2380	ns
dI3 ON + L-AC vs. dI3 ON + Saline	0.8749	ns
dI3 ON + MEC vs. dI3 ON + Saline	0.4613	ns
dI3 OFF + L-AC vs. dI3 OFF + MEC	0.8532	ns
dI3 OFF + L-AC vs. dI3 OFF + Saline	0.2491	ns
dI3 OFF + MEC vs. dI3 OFF + Saline	0.9669	ns

Table 3.9 Table of *p*-value results from Tukey's multiple comparisons test after a two-way ANOVA comparing ankle flexor EMG burst duration during electrical and mechanical perturbation. A) *p*-values from electrical SCR TA burst duration data ($N = 6$). B) *p*-values from mechanical SCR TA burst duration data ($N = 3$). Statistical test results (*p*-values) represent the difference between the average TA burst duration during treadmill SCRs from dI3 ON to dI3 OFF treatment, as well as between combined treatments (i.e., L-AC, MEC, and saline). *$p \leq 0.05$, **$p \leq 0.01$, ****$p \leq 0.0001$.

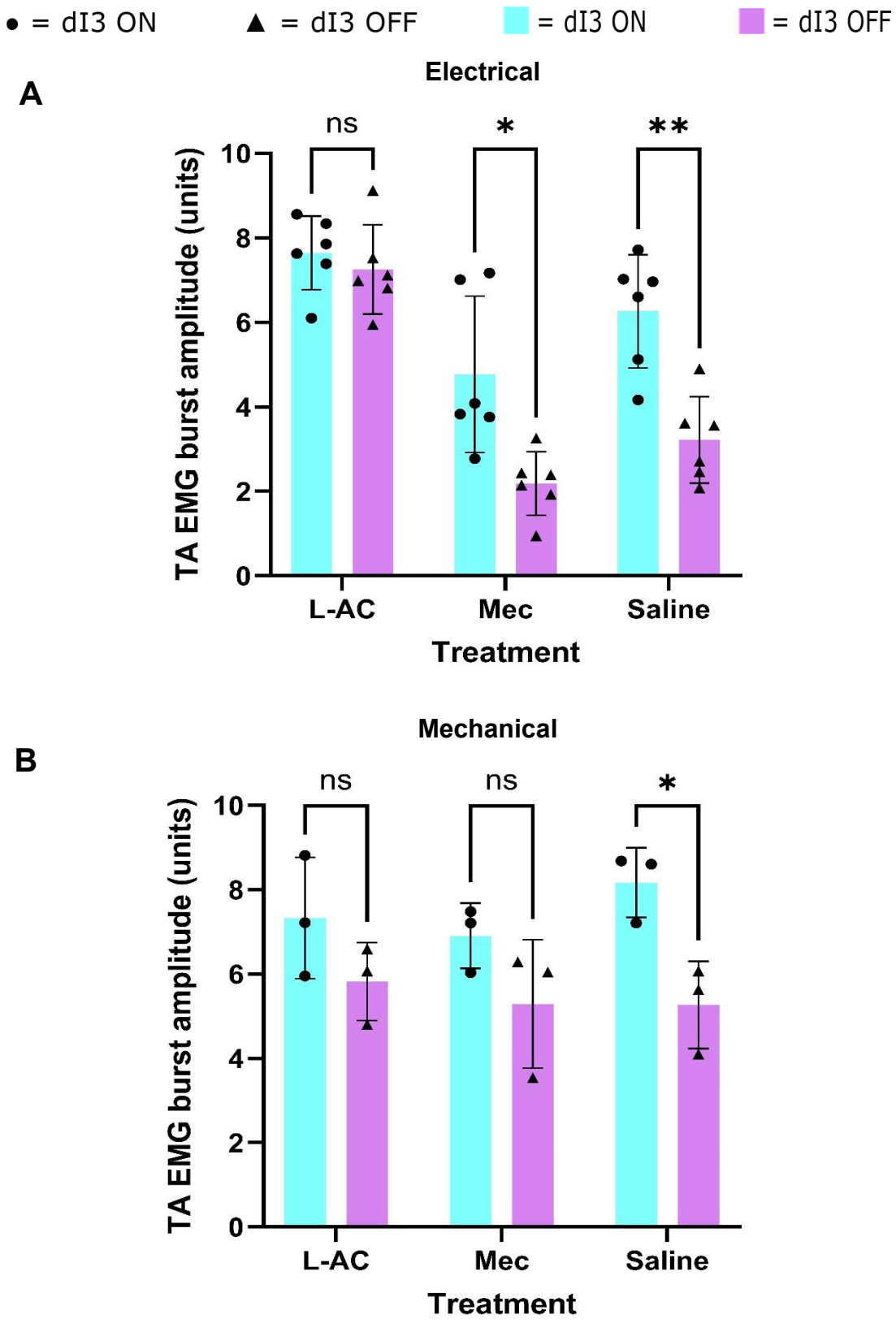
● = dI3 ON
▲ = dI3 OFF
= dI3 ON
= dI3 OFF
A
Electrical
ns
*
**
TA EMG burst amplitude (units)
10
8
6
4
2
0
L-AC
Mec
Saline
Treatment
B
Mechanical
ns
ns
*
TA EMG burst amplitude (units)
10
8
6
4
2
0
L-AC
Mec
Saline
Treatment

Figure 3.14 The average burst amplitude of TA muscle activity from SCRs elicited during early-to-mid swing phase. A) Average peak amplitude of TA bursts during electrical perturbation ($N = 6$). B) Average peak amplitude of TA bursts during mechanical perturbation ($N = 3$). Data are presented as means ± SD. Bars colored in cyan with circular data points represent dI3 ON trials, while bars colored in magenta with triangular data points represent dI3 OFF trials. The observed decrease in burst amplitude between dI3 ON and dI3 OFF treatment trials was analyzed using a two-way ANOVA and Tukey's multiple comparisons test: $*p \leq 0.05$, $**p \leq 0.01$.

A) Comparisons between dI3 ON and dI3 OFF	P-Value	Significance
dI3 ON + L-AC vs. dI3 OFF + L-AC	0.5008	ns
dI3 ON + MEC vs. dI3 OFF + MEC	0.0170	*
dI3 ON + Saline vs. dI3 OFF + Saline	0.0015	**
dI3 ON + L-AC vs. dI3 ON + MEC	0.0232	*
dI3 ON + L-AC vs. dI3 ON + Saline	0.0260	*
dI3 ON + MEC vs. dI3 ON + Saline	0.1881	ns
dI3 OFF + L-AC vs. dI3 OFF + MEC	0.0007	***
dI3 OFF + L-AC vs. dI3 OFF + Saline	0.0068	**
dI3 OFF + MEC vs. dI3 OFF + Saline	0.3451	ns
B) Comparisons between dI3 ON and dI3 OFF	**P-Value**	**Significance**
dI3 ON + L-AC vs. dI3 OFF + L-AC	0.2125	ns
dI3 ON + MEC vs. dI3 OFF + MEC	0.2004	ns
dI3 ON + Saline vs. dI3 OFF + Saline	0.0210	*
dI3 ON + L-AC vs. dI3 ON + MEC	0.8781	ns
dI3 ON + L-AC vs. dI3 ON + Saline	0.6812	ns
dI3 ON + MEC vs. dI3 ON + Saline	0.0051	**
dI3 OFF + L-AC vs. dI3 OFF + MEC	0.4742	ns
dI3 OFF + L-AC vs. dI3 OFF + Saline	0.0328	*
dI3 OFF + MEC vs. dI3 OFF + Saline	0.9964	ns

Table 3.10 Table of *p*-value results from Tukey's multiple comparisons test after a two-way ANOVA comparing ankle flexor EMG burst amplitude during electrical and mechanical perturbation. A) *p*-values from electrical SCR TA burst amplitude data ($N = 6$). B) *p*-values from mechanical SCR TA burst amplitude data ($N = 3$). Statistical test results (*p*-values) represent the difference between the average TA burst amplitude during treadmill SCRs from dI3 ON to dI3 OFF treatment, as well as between combined treatments (i.e., L-AC, MEC, and saline). *$p \leq 0.05$, **$p \leq 0.01$, ***$p \leq 0.001$.

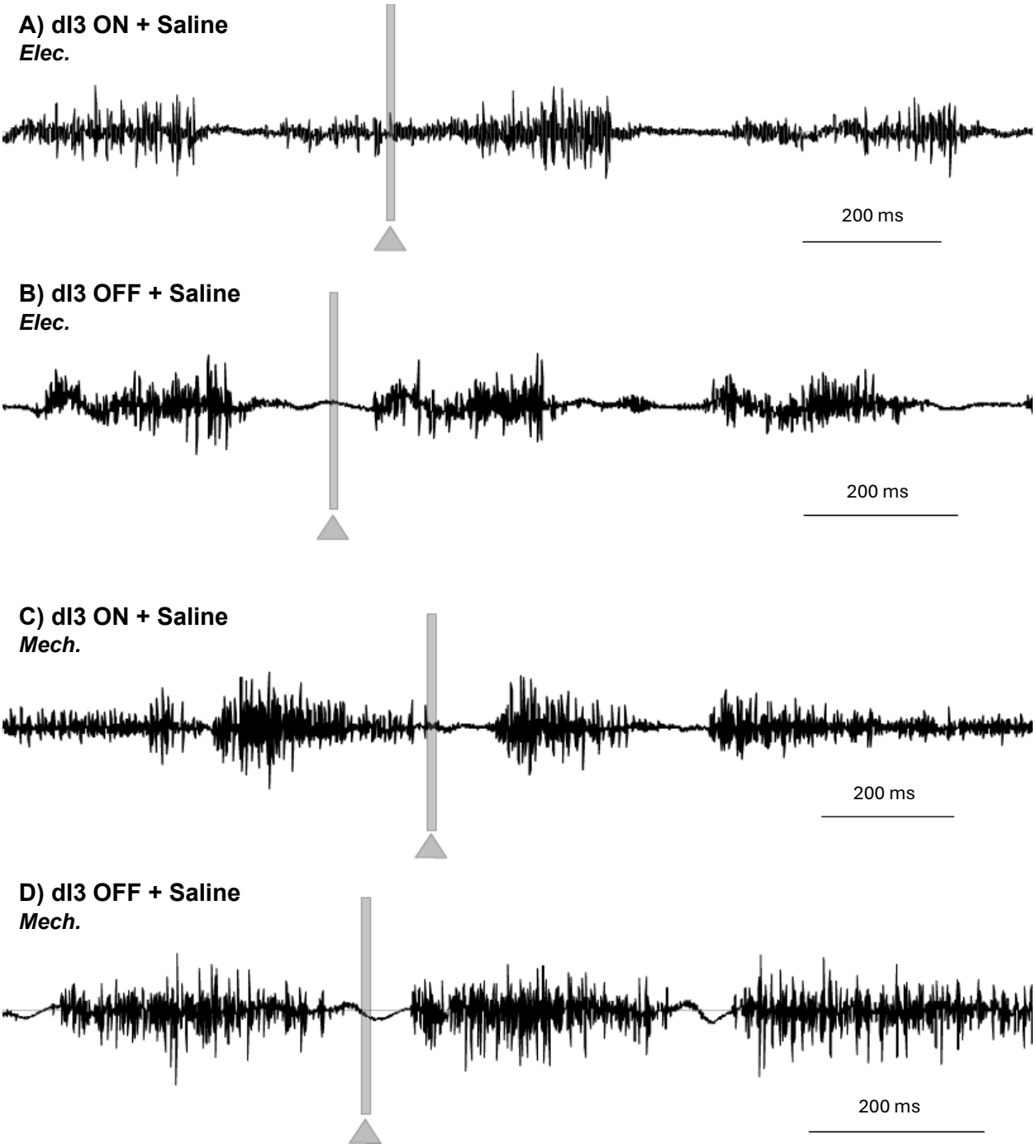

Figure 3.15 Raw EMG traces from the medial gastrocnemius hindlimb muscle of an individual mouse, demonstrating ankle extensor activation during the step before and after electrical (*elec.*) and mechanical (*mech.*) perturbation (SCR). Grey bars and triangles indicate the moment of contact between the hindlimb paw and perturbation (electrical pulse or metal bar). Scale bars represent 200ms.

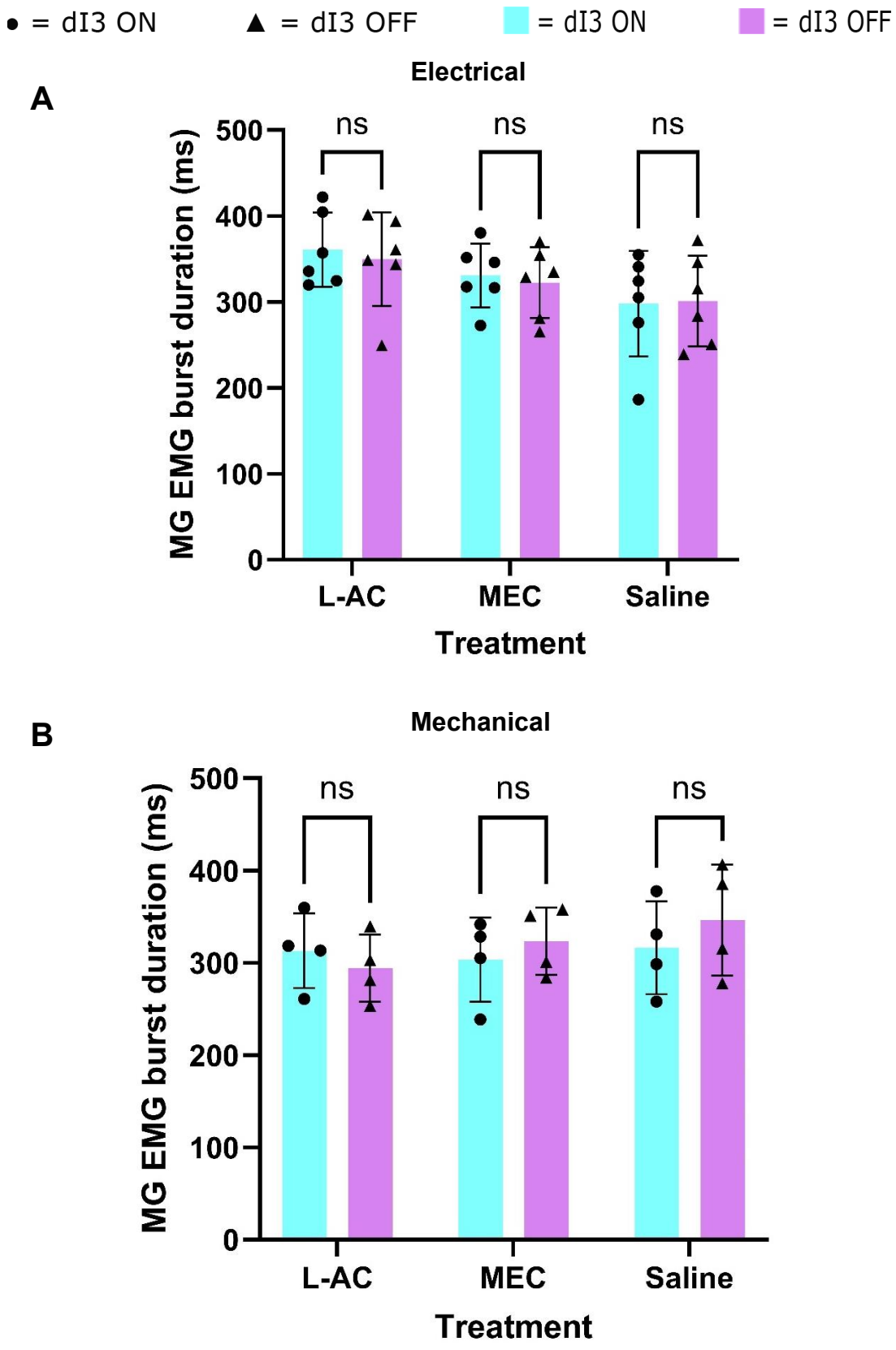
● = dI3 ON
▲ = dI3 OFF
= dI3 ON
= dI3 OFF
A
Electrical
MG EMG burst duration (ms)
500
400
300
200
100
0
ns
ns
ns
L-AC
MEC
Saline
Treatment
B
Mechanical
MG EMG burst duration (ms)
500
400
300
200
100
0
ns
ns
ns
L-AC
MEC
Saline
Treatment

Figure 3.16 The average burst duration of MG muscle activity from SCRs elicited during early-to-mid swing phase. A) Average EMG burst duration in the MG in the first burst after electrical perturbation (N = 6). B) Average EMG burst duration in the MG in the first burst after mechanical perturbation (N = 4). Data are presented as means ± SD. Bars colored in cyan with circular data points represent dI3 ON trials, while bars colored in magenta with triangular data points represent dI3 OFF trials. The change in burst duration between dI3 ON and dI3 OFF treatment trials was analyzed using a two-way ANOVA and Tukey's multiple comparisons test: ns indicates $p > 0.05$.

A) Comparisons between dI3 ON and dI3 OFF	P-Value	Significance
dI3 ON + L-AC vs. dI3 OFF + L-AC	0.7068	ns
dI3 ON + MEC vs. dI3 OFF + MEC	0.7198	ns
dI3 ON + Saline vs. dI3 OFF + Saline	0.9243	ns
dI3 ON + L-AC vs. dI3 ON + MEC	0.6527	ns
dI3 ON + L-AC vs. dI3 ON + Saline	0.4170	ns
dI3 ON + MEC vs. dI3 ON + Saline	0.3947	ns
dI3 OFF + L-AC vs. dI3 OFF + MEC	0.8296	ns
dI3 OFF + L-AC vs. dI3 OFF + Saline	0.5436	ns
dI3 OFF + MEC vs. dI3 OFF + Saline	0.6264	ns
B) Comparisons between dI3 ON and dI3 OFF	**P-Value**	**Significance**
dI3 ON + L-AC vs. dI3 OFF + L-AC	0.5176	ns
dI3 ON + MEC vs. dI3 OFF + MEC	0.5182	ns
dI3 ON + Saline vs. dI3 OFF + Saline	0.4759	ns
dI3 ON + L-AC vs. dI3 ON + MEC	0.9399	ns
dI3 ON + L-AC vs. dI3 ON + Saline	0.9962	ns
dI3 ON + MEC vs. dI3 ON + Saline	0.9591	ns
dI3 OFF + L-AC vs. dI3 OFF + MEC	0.1051	ns
dI3 OFF + L-AC vs. dI3 OFF + Saline	0.3564	ns
dI3 OFF + MEC vs. dI3 OFF + Saline	0.7078	ns

Table 3.11 Table of *p*-value results from Tukey's multiple comparisons test after a two-way ANOVA comparing ankle extensor EMG burst duration after electrical and mechanical perturbation. A) *p*-values from electrical SCR MG burst duration data ($N = 6$). B) *p*-values from mechanical SCR MG burst duration data ($N = 4$). Statistical test results (*p*-values) represent the difference between the average MG burst duration after treadmill SCRs from dI3 ON to dI3 OFF treatment, as well as between combined treatments (i.e., L-AC, MEC, and saline). ns indicates $p > 0.05$.

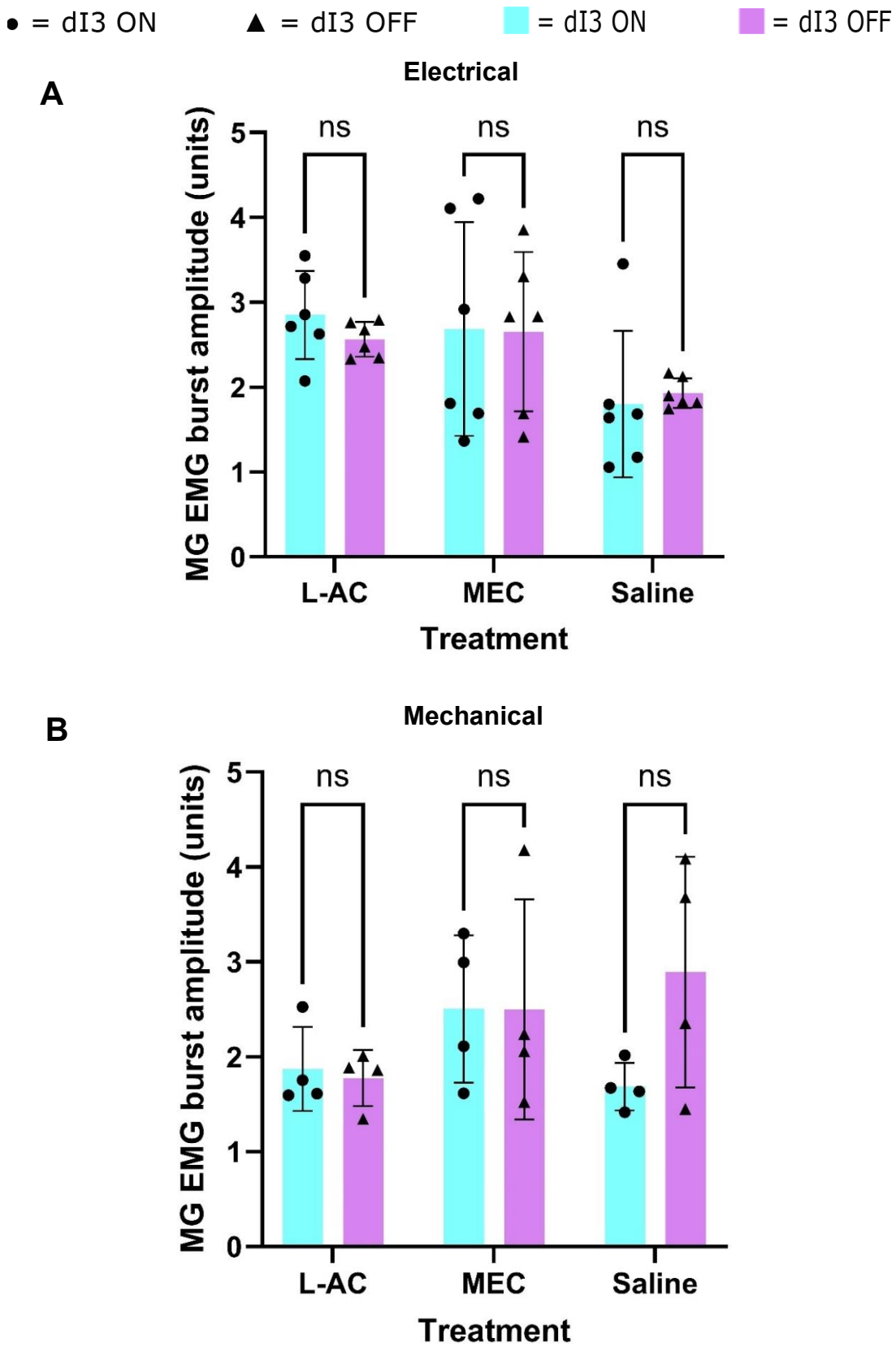
● = dI3 ON
▲ = dI3 OFF
= dI3 ON
= dI3 OFF
A
Electrical
MG EMG burst amplitude (units)
ns
ns
ns
0
1
2
3
4
5
L-AC
MEC
Saline
Treatment
B
Mechanical
MG EMG burst amplitude (units)
ns
ns
ns
0
1
2
3
4
5
L-AC
MEC
Saline
Treatment

Figure 3.17 The average burst amplitude of MG muscle activity from SCRs elicited during early-to-mid swing phase. A) Average EMG burst amplitude in the MG in the first burst after electrical perturbation (N = 6). B) Average EMG burst amplitude in the MG in the first burst after mechanical perturbation (N = 4). Data are presented as means ± SD. Bars colored in cyan with circular data points represent dI3 ON trials, while bars colored in magenta with triangular data points represent dI3 OFF trials. The change in burst amplitude between dI3 ON and dI3 OFF treatment trials was analyzed using a two-way ANOVA and Tukey's multiple comparisons test: ns indicates $p > 0.05$.

A) Comparisons between dI3 ON and dI3 OFF	P-Value	Significance
dI3 ON + L-AC vs. dI3 OFF + L-AC	0.2539	ns
dI3 ON + MEC vs. dI3 OFF + MEC	0.9632	ns
dI3 ON + Saline vs. dI3 OFF + Saline	0.7310	ns
dI3 ON + L-AC vs. dI3 ON + MEC	0.9453	ns
dI3 ON + L-AC vs. dI3 ON + Saline	0.1165	ns
dI3 ON + MEC vs. dI3 ON + Saline	0.1426	ns
dI3 OFF + L-AC vs. dI3 OFF + MEC	0.9752	ns
dI3 OFF + L-AC vs. dI3 OFF + Saline	0.0044	**
dI3 OFF + MEC vs. dI3 OFF + Saline	0.2654	ns
B) Comparisons between dI3 ON and dI3 OFF	**P-Value**	**Significance**
dI3 ON + L-AC vs. dI3 OFF + L-AC	0.7310	ns
dI3 ON + MEC vs. dI3 OFF + MEC	0.9943	ns
dI3 ON + Saline vs. dI3 OFF + Saline	0.1392	ns
dI3 ON + L-AC vs. dI3 ON + MEC	0.5328	ns
dI3 ON + L-AC vs. dI3 ON + Saline	0.4815	ns
dI3 ON + MEC vs. dI3 ON + Saline	0.2426	ns
dI3 OFF + L-AC vs. dI3 OFF + MEC	0.5142	ns
dI3 OFF + L-AC vs. dI3 OFF + Saline	0.3788	ns
dI3 OFF + MEC vs. dI3 OFF + Saline	0.9298	ns

Table 3.12 Table of *p*-value results from Tukey's multiple comparisons test after a two-way ANOVA comparing ankle extensor EMG burst amplitude after electrical and mechanical perturbation. A) *p*-values from electrical SCR MG burst amplitude data ($N = 6$). B) *p*-values from mechanical SCR MG burst amplitude data ($N = 4$). Statistical test results (*p*-values) represent the difference between the average MG burst amplitude after treadmill SCRs from dI3 ON to dI3 OFF treatment, as well as between combined treatments (i.e., L-AC, MEC, and saline). $^{**}p \leq 0.01$, ns indicates $p > 0.05$.

3.3.1 dI3 silencing increases paw slipping during tasks requiring balance and coordination

We next sought to determine if dI3s were involved in other behavioural tasks requiring motor skill and fast correction. Twelve mice were trained and tested on a vibrating balance beam and horizontal ladder walk task after receiving the 6 different treatments to determine if dI3 circuit manipulation would result in corrective behaviour changes (Fig. 3.18; Supplemental ladder and beam videos: dI3 OFF Saline_Beam slip.mp4, dI3 OFF Mec_Ladder slip.mp4). In the vibrating beam task, we observed very few slips on average per attempt in dI3 ON sessions with L-AC and saline treatment, with an average number of slips per attempt of 0.43 ± 0.32 and 0.36 ± 0.32, respectively (Fig. 3.19; N = 12). Control trials with MEC treatment, however, demonstrated a greater average number of slips of 1.35 ± 0.46 slips per attempt (Fig. 3.19; N = 12).

After dI3 silencing, we observed that MEC treatment resulted in the largest number of average slips per attempt in dI3 OFF trials, with an average number of slips of 2.70 ± 0.65 per attempt (Fig. 3.19A; N = 12). Conversely, L-AC and saline treatment during dI3 OFF sessions resulted in smaller slip numbers with an average of 1.93 ± 0.56 and 2.24 ± 0.54 slips per attempt (Fig. 3.19A; N = 12). For all treatment groups, silencing dI3s increased the average number of paw slips off the beam two- to three-folds with the average number of slips per attempt increasing significantly by 1.96 ± 0.38, 1.42 ± 0.47, and 2.33 ± 0.55 in L-AC, MEC, and saline treatment trials, respectively (Fig. 3.19A; N = 12; Tukey's multiple comparisons test, $p \leq 0.0001$ for L-AC, MEC, and saline treatments). The absolute difference in slips from dI3 ON to dI3 OFF trials was comparable between MEC and saline treatment, as well as between L-AC and saline, with no statistical difference observed between these groups (Fig. 3.19B; Table 3.13; N = 12). Overall, MEC trials demonstrated the smallest increase and saline trials demonstrated the largest increase

in slips after dI3 silencing (Fig. 3.19B; $N = 12$). All p-values from Tukey's multiple comparisons test are presented below in Table 3.13.

Similar motor changes were observed during the horizontal ladder task, where dI3 ON sessions demonstrated the most slips during MEC treatment trials and the least during L-AC and saline treatment trials, with an average number of slips of 1.92 ± 0.67, 0.63 ± 0.37, and 0.51 ± 0.21, respectively (Fig. 3.20A; $N = 12$). After dI3 silencing, MEC treatment trials demonstrated the largest number of average slips once again, however all three treatment groups presented no statistical difference from one another with an average number of slips of 2.71 ± 0.70 (MEC), 2.01 ± 0.40 (L-AC), and 2.40 ± 0.90 (saline), respectively (Fig. 3.20A; Table 3.14; $N = 12$). When comparing the average number of paw slips per attempt from dI3 ON to dI3 OFF trials, all combined treatments demonstrated a nearly two-fold increase. While MEC treatment had the smallest increase of 0.89 ± 0.23 slips per attempt, L-AC and saline increased more significantly in terms of average slips with 1.43 ± 0.40 and 1.95 ± 0.55, respectively (Fig. 3.20B; $N = 12$; Tukey's multiple comparison test, $p \leq 0.001$ for MEC treatment, $p \leq 0.0001$ for L-AC and saline treatment). Overall, for both ladder and beam tasks, the difference in average slips per attempt between dI3 OFF and dI3 ON treatment was lowest in MEC trials and highest in saline trials (Fig. 3.19, 3.20; $N = 12$). All p-values from Tukey's multiple comparisons test are presented below in Table 3.14.

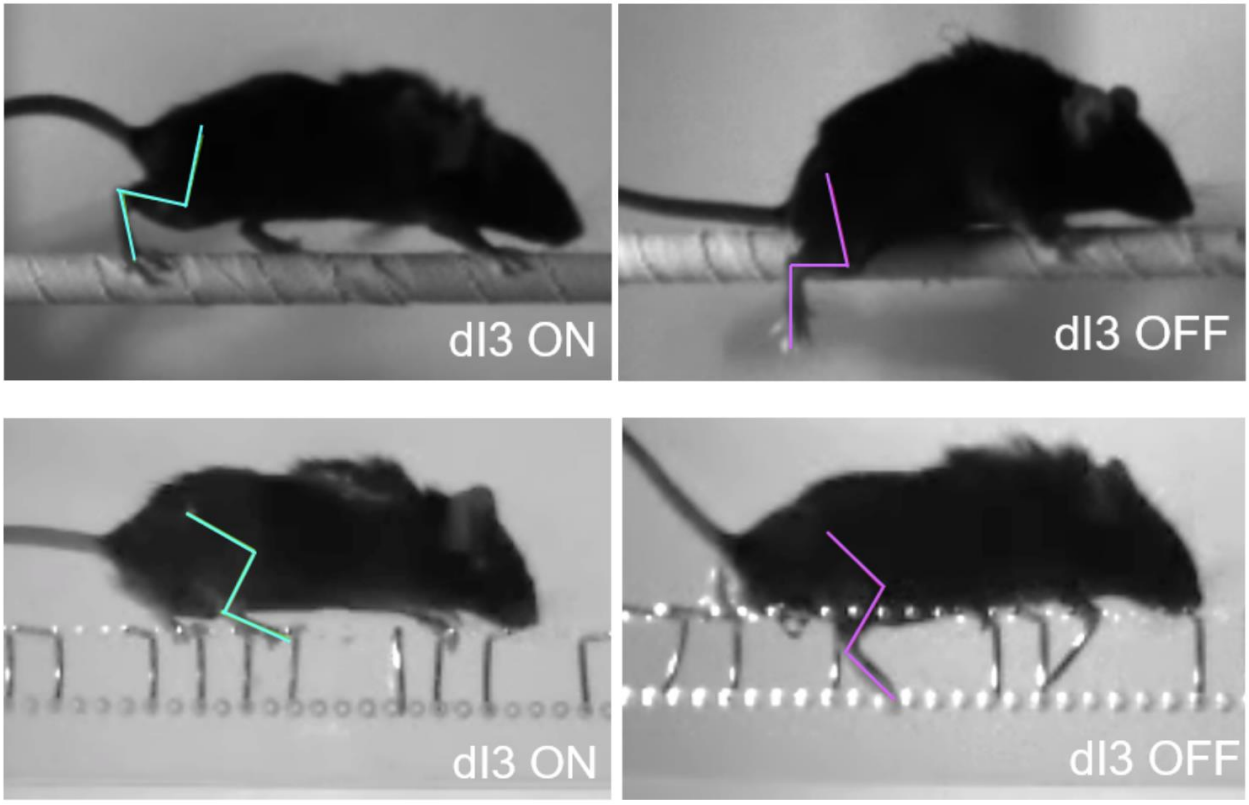

Figure 3.18 Images capturing paw slips of the hindlimb during attempts on the horizontal ladder and vibrating beam task in saline conditions. Cyan-colored kinematic hindlimb skeletons represent dI3 ON conditions; magenta-colored kinematic skeletons represent dI3 OFF conditions. Upper panels depict the vibrating balance beam task; lower panels depict the horizontal ladder task.

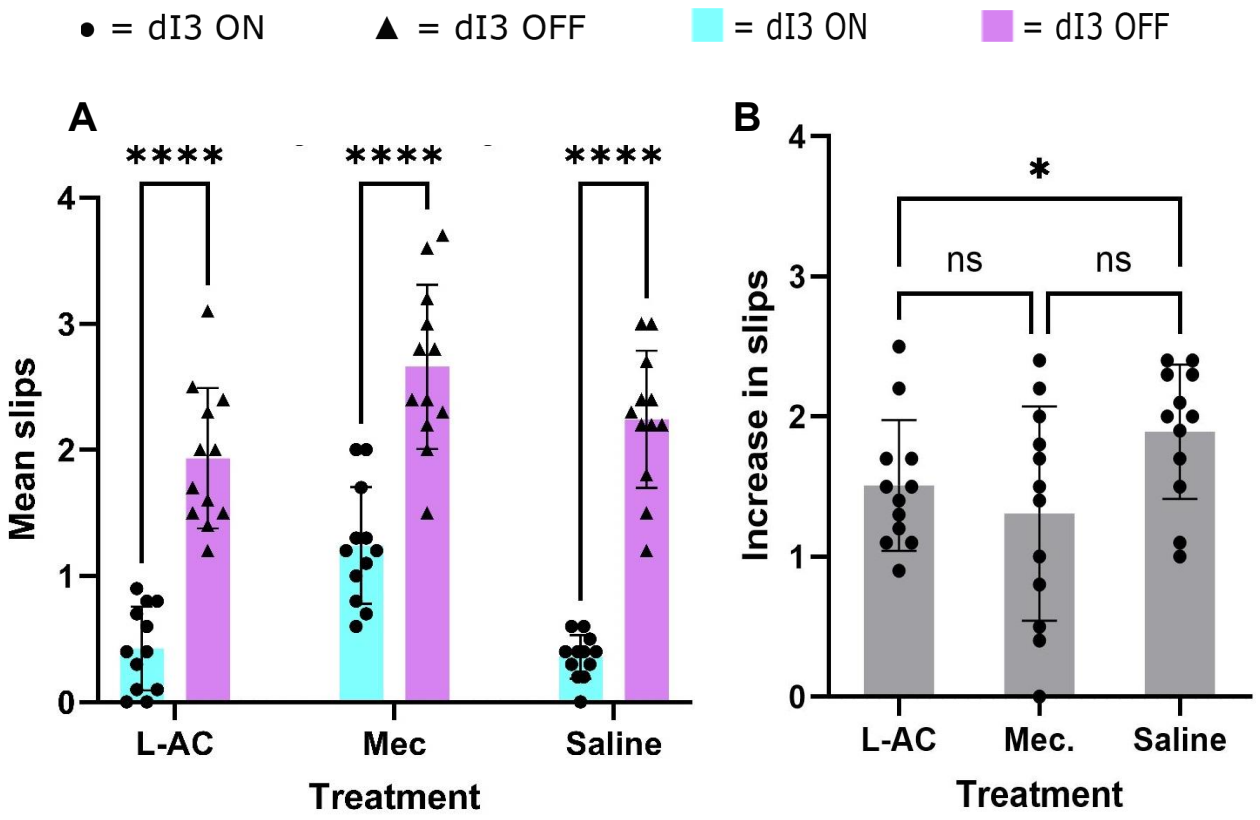

Figure 3.19. Slips during the vibrating beam task. A) The average number of paw slips per attempt on the vibrating beam task between dI3 ON and dI3 OFF trials. Bars colored in cyan with circular data points represent dI3 ON trials while bars colored in magenta with triangular data points represent dI3 OFF trials. B) Increase in slips from dI3 ON to dI3 OFF trials. Data are presented as means ± SD. $N = 12$. The resulting increase in the incidence of slips between dI3 ON and dI3 OFF treatment trials, as well as between the three combined treatments, was analyzed using a two-way ANOVA and Tukey's multiple comparisons test: *$p \leq 0.05$, ****$p \leq 0.0001$.

A) Comparisons between dI3 ON and dI3 OFF	P-Value	Significance
dI3 ON + L-AC vs. dI3 OFF + L-AC	<0.0001	****
dI3 ON + MEC vs. dI3 OFF + MEC	<0.0001	****
dI3 ON + Saline vs. dI3 OFF + Saline	<0.0001	****
dI3 ON + L-AC vs. dI3 ON + MEC	<0.0001	****
dI3 ON + L-AC vs. dI3 ON + Saline	0.7633	ns
dI3 ON + MEC vs. dI3 ON + Saline	0.0002	***
dI3 OFF + L-AC vs. dI3 OFF + MEC	0.0061	**
dI3 OFF + L-AC vs. dI3 OFF + Saline	0.1275	ns
dI3 OFF + MEC vs. dI3 OFF + Saline	0.1850	ns
B) Comparisons between treatments	**P-Value**	**Significance**
L-AC vs. MEC	0.6387	ns
L-AC vs. Saline	0.0272	*
MEC vs. Saline	0.0915	ns

Table 3.13 Table of *p*-value results of Tukey's multiple comparisons test after a two-way ANOVA comparing the incidence of paw slips from the vibrating beam task. A) Statistical test results (*p*-values) represent the difference between the average number of slips per attempt from dI3 ON to dI3 OFF trials, as well as between the three treatments (L-AC, MEC, and saline) in the beam task. B) *p*-values represent the difference in increased slips after dI3 silencing between the three treatments (L-AC, MEC, and saline). $N = 12$. *$p \leq 0.05$, **$p \leq 0.01$, ***$p \leq 0.001$, ****$p \leq 0.0001$.

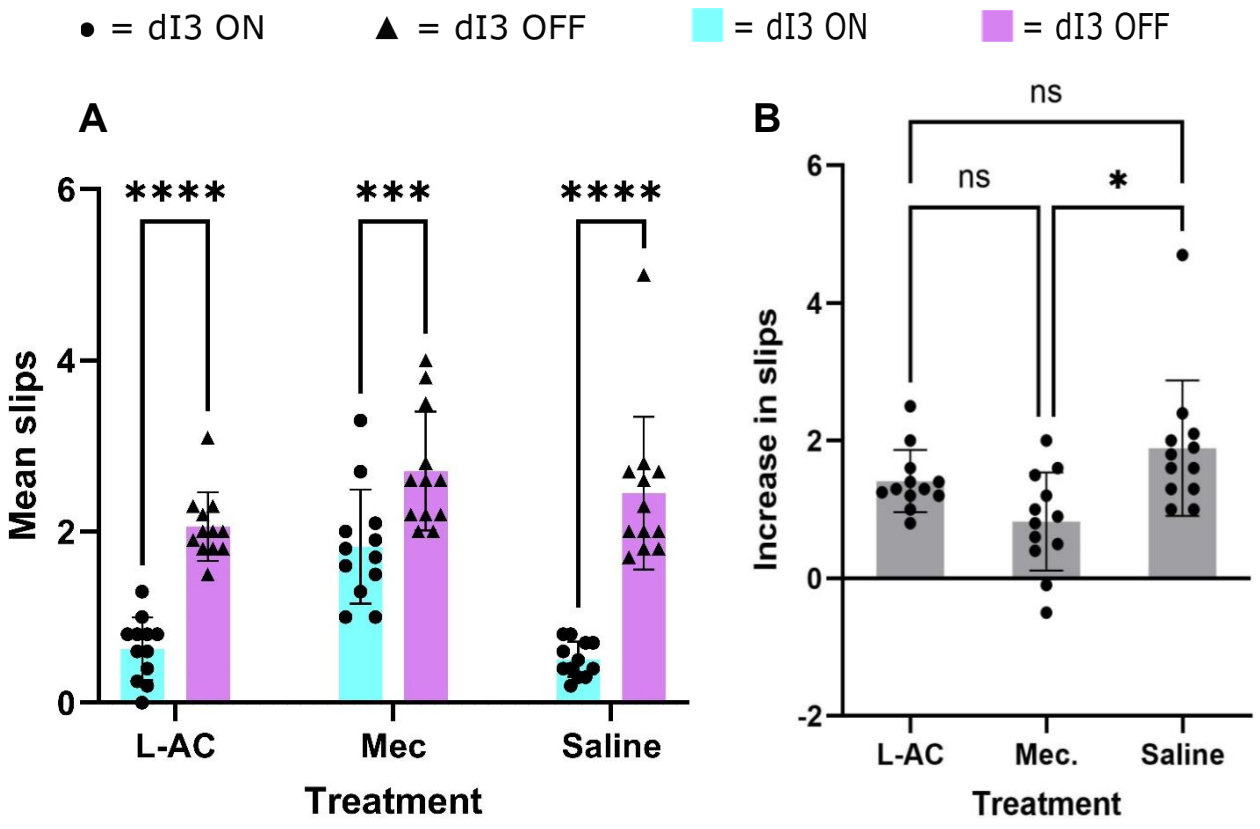

Figure 3.20 Slips during the horizontal ladder task. A) The average number of paw slips per attempt on the horizontal ladder task between dI3 ON and dI3 OFF trials. Bars colored in cyan with circular data points represent dI3 ON trials while bars colored in magenta with triangular data points represent dI3 OFF trials. B) Mean increase in slips from dI3 ON to dI3 OFF trials. Data are presented as means ± SD. $N = 12$. The resulting increase in the incidence of slips between dI3 ON and dI3 OFF treatment trials, as well as between the three combined treatments, was analyzed using a two-way ANOVA and Tukey's multiple comparisons test: *$p \leq 0.05$, ***$p \leq 0.001$, ****$p \leq 0.0001$.

A) Comparisons between dI3 ON and dI3 OFF	P-Value	Significance
dI3 ON + L-AC vs. dI3 OFF + L-AC	<0.0001	****
dI3 ON + MEC vs. dI3 OFF + MEC	0.0009	***
dI3 ON + Saline vs. dI3 OFF + Saline	<0.0001	****
dI3 ON + L-AC vs. dI3 ON + MEC	<0.0001	****
dI3 ON + L-AC vs. dI3 ON + Saline	0.4746	ns
dI3 ON + MEC vs. dI3 ON + Saline	<0.0001	****
dI3 OFF + L-AC vs. dI3 OFF + MEC	0.0609	ns
dI3 OFF + L-AC vs. dI3 OFF + Saline	0.4422	ns
dI3 OFF + MEC vs. dI3 OFF + Saline	0.7358	ns
B) Comparisons between treatments	**P-Value**	**Significance**
L-AC vs. MEC	0.0815	ns
L-AC vs. Saline	0.3423	ns
MEC vs. Saline	0.0265	*

Table 3.14 Table of *p*-value results of Tukey's multiple comparisons test after a two-way ANOVA comparing the incidence of paw slips from the horizontal ladder task. A) Statistical test results (*p*-values) represent the difference between the average number of slips per attempt from dI3 ON to dI3 OFF trials, as well as between the three treatments (L-AC, MEC, and saline) in the ladder task. B) *p*-values represent the difference in increased slips after dI3 silencing between the three treatments (L-AC, MEC, and saline). $N = 12$. *$p \leq 0.05$, ***$p \leq 0.001$, ****$p \leq 0.0001$.

CHAPTER 4: DISCUSSION

Many of the spinal circuits involved in reflexive and corrective behaviours remain to be characterized. Reflexes in mammalian locomotion help to prevent disruption during a wide array of motor behaviours, and although we understand the general basis of reflex initiation, we have yet to identify the neural populations involved. With respect to spinal reflexes, motor activity begins with output from sensory afferents (like mechanoreceptors and muscle afferents) which project to motor neurons within the dorsal horn (Rexed, 1952, 1954). Many reflexes, like the SCR, utilize spinal circuits that rapidly initiate some type of muscle activation, whether that be flexion or extension, triggered by nociceptive, proprioceptive or cutaneous signals to the spinal cord (Hamilton et al., 2018; Pearcey & Zehr, 2020; Radhakrishnan & Sluka, 2005; Zehr, 2006). Additionally, many cutaneous afferents, specifically those conveying mechanical stimuli, terminate within laminae III-V of the spinal cord in rodents and cats (Brown et al., 1981; Levinsson et al., 2002; Molander & Grant, 1986; Panneton et al., 2005). Given what we know of reflexes in movement and the diverse populations of spinal dorsal interneurons, dI3 neurons have features that make them ideal for participating in reflexive and corrective behaviours. They receive sensory inputs from cutaneous and muscle afferents, and they project direct glutamatergic synapses onto spinal motoneurons. With the present study, we aimed to investigate whether dI3 neurons are involved in motor circuits beyond their identified roles in grasping and recovery after spinal cord injury. Using our existing knowledge of the inputs and projections to and from dI3s to silence their activity and examine the effects on behaviour, we discovered that these excitatory neurons may present an important role as a contributing neural mediator to the stumbling corrective response and other types of corrective behaviours requiring balance and coordination.

4.1 dI3s modulate the stumbling corrective response and reflex activation

We first examined whether dI3s were an important neural component in the initiation and execution of a specific hindlimb reflex, known as the stumbling corrective response (SCR). By acutely silencing dI3 activity using the inhibitory DREADD receptor, *hM4DI*, in lumbar dI3s through AAV injection or endogenous transgenic expression, we were able to investigate if a lower level of dI3 activity would result in corrective motor deficits. After administration of the DREADD agonist, JHU37160, mice were tested on a horizontal treadmill wherein the hindlimb would receive some type of perturbation to disrupt the step cycle. We were able to elicit the SCR from both electrical and mechanical perturbations to determine the effects, if any, of dI3 silencing on the SCR.

While there have been numerous studies investigating this reflex in various mammalian models (Mayer & Akay, 2018; McVea & Pearson, 2007; Merlet et al., 2022; Potocanac et al., 2016; Quevedo et al., 2005a), few of the spinal neurons involved have been identified. It is understood that this corrective reflex is triggered by mechanoreceptors of the ventral aspect of the paw when perturbed by an obstacle in the walking path; this stimulus, when detected during the swing phase of the walking cycle, triggers a rapid activation of flexor muscles in the hindlimb to lift the paw or limb in effort to clear the obstacle (Forssberg, 1979). Studies applying local anesthesia to the foot skin and observing an abolished SCR (Forssberg et al., 1975; Wand et al., 1980) highlight the role of mechanoreceptors on the dorsal aspect of the paw. The SCR has also been studied in decerebrate animals through stimulation of the superficial peroneal nerve (Quevedo et al., 2005a), as well as through stimulation of the tibial and saphenous nerve in intact animals (Mayer & Akay, 2018; Zehr et al., 1997). No spinal interneuron has been specifically implicated in the SCR.

Here we present a chemogenetic model to understand the neuronal circuitry of the SCR where this reflex can be blunted through silencing of dI3s. Quevedo and colleagues (2005) proposed a circuit involving several layers of unidentified spinal interneurons communicating to hindlimb flexors and extensors during this type of rapid and adaptive locomotion (Quevedo et al., 2005b; Figure 4.1). We propose that dI3s may be one of the unknown excitatory spinal neurons within this reflex pathway that are partly responsible for interpreting these cutaneous inputs and concurrently exciting the corresponding motor neurons of agonist muscles, such as the knee and ankle flexors, during the swing phase of locomotion.

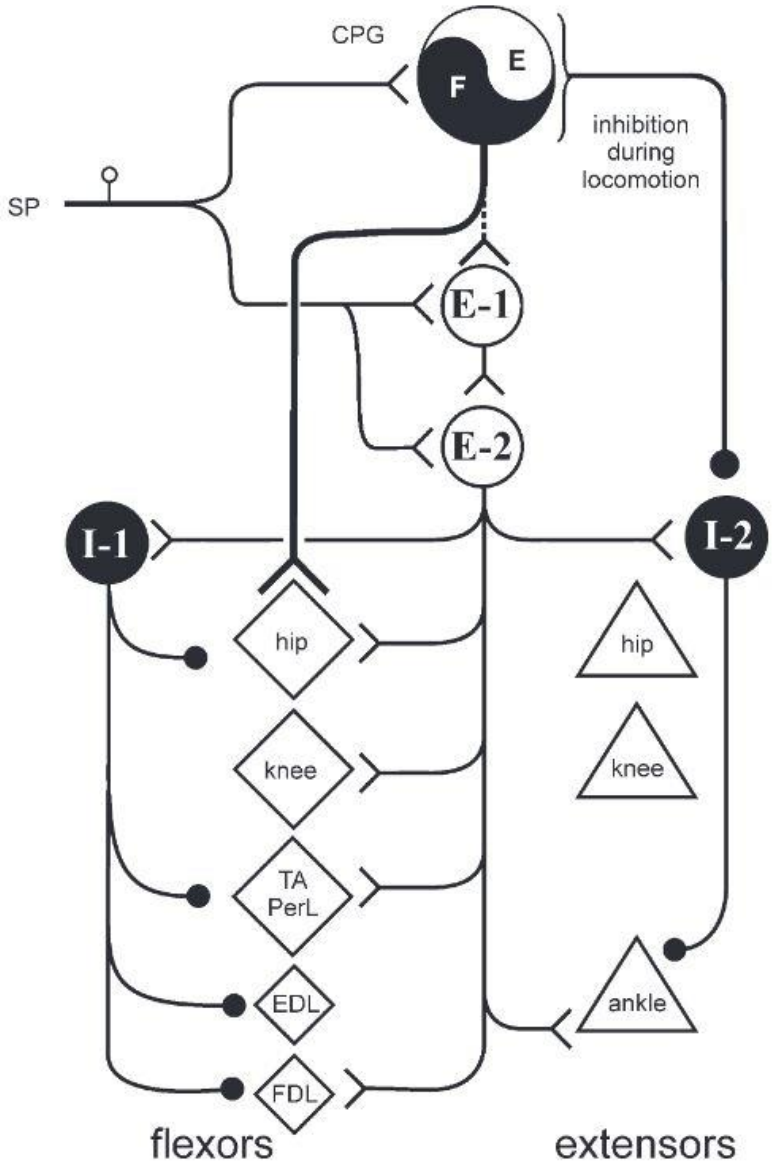

Figure 4.1 Interneuronal pathways involved in the stumbling corrective reaction (sourced from Quevedo et al., 2005b). Circuitry proposed by Quevedo and colleagues to define the synaptic connections between hindlimb flexor/extensor muscles and spinal neurons during the initiation of corrective reflexes, specifically the SCR. Filled circles denote inhibitory interneurons, while empty circles denote excitatory interneurons. Based upon our work's findings, we suggest that the previously unknown excitatory interneuron, E-2, may be dI3s within this pathway.

Overall, the effects of dI3 silencing did not abolish the SCR but rather resulted in a blunted response wherein the hindlimb flexion to clear the perturbation was blunted in comparison with control trials. Specifically, dI3 silencing resulted in a significantly reduced step height during the peak of an SCR and increased the likelihood of dragging events wherein the paw would drag over the mechanical perturbation rather than reflexively attempting to clear it. The percentage of mechanical perturbations resulting in a dragging event at least doubled after dI3 silencing in saline and L-acetyl carnitine treatment groups, with around 10-20% of perturbation attempts resulting in dragging in most mice. The increased rate of failed SCRs suggests that dI3s may play a role in setting the threshold for activation of this corrective response, where dI3 silencing reduces the excitation of motoneurons that is necessary for initiating the rapid activation of knee and ankle flexors.

The effect of increased dragging on the treadmill after mechanical perturbation attempts was seen in all treatment groups except for those given mecamylamine, the nicotinic acetylcholine receptor antagonist, wherein the amount of dragging remained relatively consistent between dI3 ON and dI3 OFF trials. Since mecamylamine putatively reduces Renshaw cell excitation by motoneuron collaterals, this would suggest that Renshaw cell activity reduced the SCR as well or that reducing Renshaw cell activity compensated for the negative effects of turning off dI3s in the dI3 OFF trials. The fact that the effects of mecamylamine in dI3 ON trials resembled those of dI3 OFF in saline suggests that turning off Renshaw cell activity by mecamylamine disrupted the SCR, and that there was no compounding effect of turning off dI3s using JHU37160 and reducing Renshaw cell activity by mecamylamine. The same trend was observed with respect to the peak step height of SCRs, wherein mecamylamine administration resulted in similar step heights for both dI3 ON and dI3 OFF trials. We observed no statistical difference between dI3 ON and dI3

OFF treatment groups when mecamylamine was administered; the same trend was observed between dI3 ON with mecamylamine trials and dI3 OFF with saline trials. This suggests that perhaps dI3s and Renshaw cells operate together within the same or converging circuits that control the activation of corrective motor behaviours. Moreover, given the observed increase in the rate of failure to clear perturbations and a general blunting of the SCR, it also appears likely that dI3s may play a role in modulating the threshold for activation of this behaviour.

Furthermore, our analysis of EMG activity from the ankle flexor (tibialis anterior, TA) during the SCR further supports this idea, as we observed longer duration and lower amplitude bursts from the TA after a perturbation, thus indicating a weaker ankle flexor response and increased time to reach the threshold required to elicit this reflex. While recordings from the ankle extensor (medial gastrocnemius, MG) did not demonstrate any overt differences in bursting activity between the different treatments, we can suggest that the dI3s are not the sole population of spinal neurons involved in the activation of the SCR, specifically since the reflex observed was mostly blunted and not completely abolished during dI3 silencing.

4.2 dI3s modulate sensorimotor integration during complex tasks requiring error prediction

We also investigated the effects of dI3 silencing on other skilled types of locomotion requiring balance, error prediction and rapid correction. Using the same combinations of pharmacological treatments, we observed the effects of Renshaw cell manipulation and dI3 silencing during a horizontal ladder walk and balance beam task. To increase the difficulty of the two tasks, ladder rungs were removed and spaced irregularly while a vibrating motor was placed on each end of the beam to reduce stability. Similarly to our previous set of experiments on the

treadmill, we observed an overall blunting in the ability to correct the hindlimb trajectory as evidenced by increases in errors and footfalls when crossing the ladder and beam. During L-acetyl carnitine and saline trials, we observed that the number of paw slips tripled on average when comparing dI3 OFF to dI3 ON treatment for both ladder and beam tasks. In mecamylamine trials, however, we observed a smaller increase in the number of slips in dI3 OFF treatment, as the baseline number of slips in dI3 ON sessions was generally double of what was observed in dI3 ON + L-acetyl carnitine and saline treatment trials. With the greatest average of slips in dI3 ON trials with mecamylamine treatment, and a lack of a compounding effect to slips in dI3 OFF trials with mecamylamine treatment, this suggests that Renshaw cells may participate in similar or shared spinal circuits with dI3s. The silencing of dI3s and reduced activation of Renshaw cells appears to result in similar effects to corrective motor deficit, thus supporting the idea that Renshaw cells likely contribute to the activation of corrective behaviours alongside dI3s.

While dI3 silencing did not induce motor changes so significant that mice were unable to successfully cross the ladder and beam, we did observe subtle changes to gait and an overall increased difficulty when crossing these apparatuses. Not only did mice demonstrate significantly increased numbers of paw slips off the ladder and beam, but mice also demonstrated occasional whole-body destabilizing events wherein one or both hindlimbs and posterior chain hung off the balance beam with forelimbs supporting the body (Figure 4.2). These posterior-end destabilizing events were rarely observed within any of the combined dI3 ON treatment trials, with the exception of a few instances in dI3 ON + mecamylamine treatment trials. Although these events did not occur within every attempt during dI3 OFF treatment trials, they only occurred after dI3 silencing or with mecamylamine treatment. This suggests that dI3s may be more involved in proprioceptive integration than previously understood, as a lack of dI3 signaling appears to prevent mice from

consistently predicting error and ensuring appropriate hindlimb placement and movement when navigating complex environments. Although error correction and paw recovery during more complex tasks may require additional supraspinal processing, we suggest that dI3 spinal circuits are likely to be involved in modulating these rapidly adaptive movements required for smooth locomotion, and perhaps may have more involvement in balance than previously thought. Given that dI3s receive monosynaptic input from proprioceptive and cutaneous afferents (Bui et al., 2013), as well as the newly discovered inputs from Renshaw cells (Brownstone lab collaboration, 2025), it appears that dI3s may perform more than just sensory processing and relay but rather additional error computation using active monitoring of both proprioceptive and cutaneous inputs to adjust motoneuron firing.

Additionally, we observed subtle gait changes after dI3 silencing specifically for mice navigating a complex environment. During attempts to cross the ladder and beam, mouse tail posture appeared to have changed in dI3 OFF trials. In control sessions, we observed an active and upright tail posture as a form of counterbalance when walking. Conversely, in dI3 OFF trials, the tail was more often laying flat against the ladder rungs or hanging off the balance beam, thus no longer providing the same balance and stability when crossing the apparatus. Mice after dI3 silencing also demonstrated a lower center of mass when crossing the ladder and beam, with the body residing closer to the ground. This suggests that without dI3 activity, spinal circuits may be receiving less information on body position through reduced integration of sensory and proprioceptive signals, thus impeding locomotion and requiring compensatory mechanisms to make up for a lack of stability and balance.

Overall, through dI3 silencing we observed a reduction in successful error prediction and slip correction for both the horizontal ladder and balance beam task. This supports our idea of potential converging spinal circuits comprising dI3 spinal neurons and Renshaw cells, operating together to process sensory changes rapidly and adjust motoneuron excitation appropriately to ensure locomotor adjustment. Although disruption of function to these spinal neurons through mecamylamine and JHU37160 did not completely inhibit successful crossing and hindlimb correction, we observed significant motor deficits and compensatory behaviours to make up for the lack of Renshaw cell and dI3 activity. While few other studies have investigated the locomotor effects of developmental disruption of dI3 and Renshaw cell circuits (Bui et al., 2013; Enjin et al., 2017; Laliberte et al., 2022), transgenic mouse studies have demonstrated the presence of compensatory behaviours to locomotion after dI3 circuit disruption, thus indicating that these spinal neurons are important to corrective motor output but are not the sole contributors. Similarly with Renshaw cells, while their disruption can induce subtle changes to various spinal circuits, it appears they are not the sole contributors to these circuits as the movements they control remain mostly intact (Hilaire et al., 1986; Noga et al., 1987).

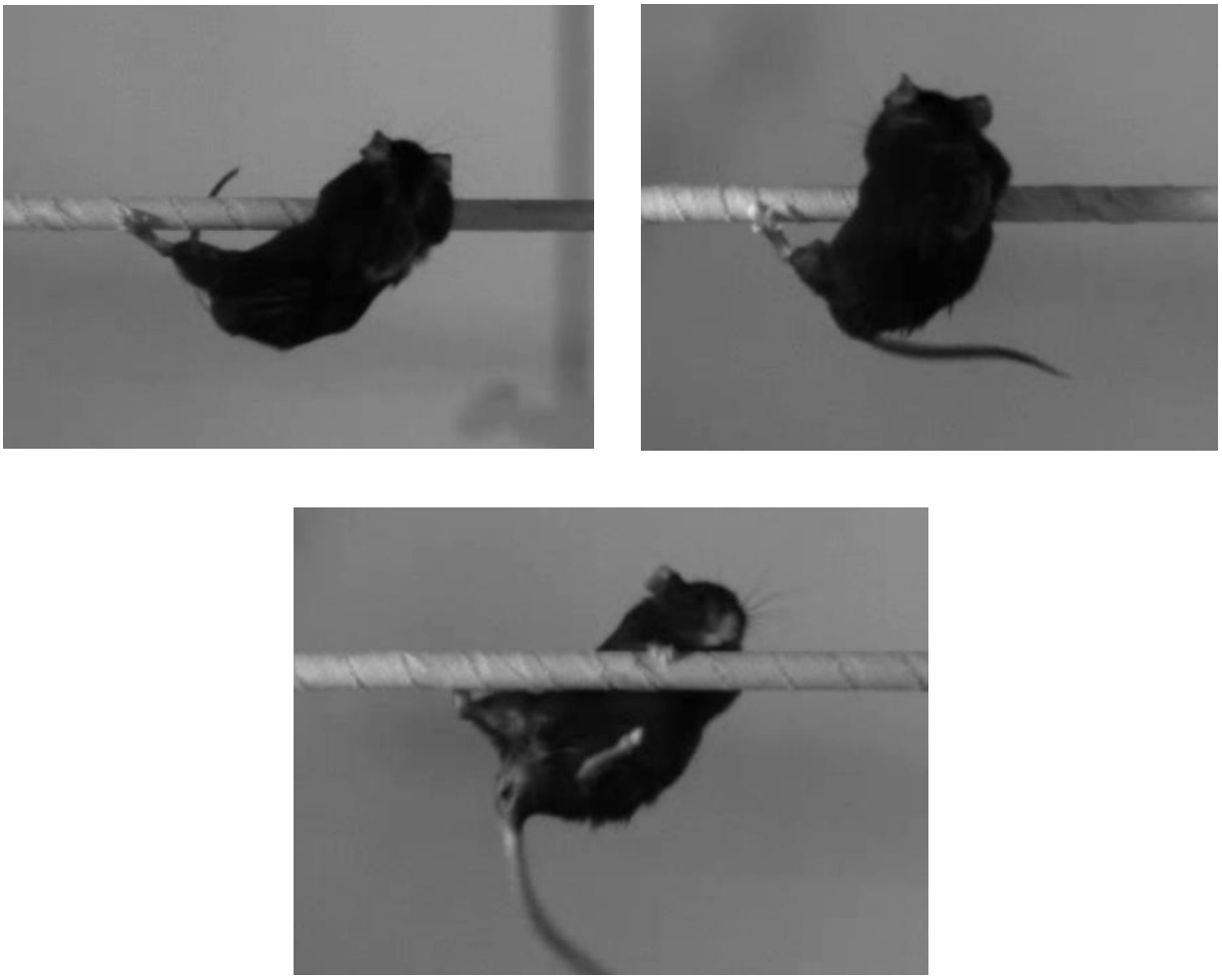

Figure 4.2 Images capturing destabilizing events on the balance beam during dI3 OFF treatment trials. Destabilizing events resulted from paw slips of one or both hindlimbs inducing a significant loss of stability of the posterior end of the body.

4.3 dI3s and Renshaw cells as part of a spinal comparator module

While our current understanding of the spinal cord's role in motor learning and error prediction remains obscure, there is reason to believe that the spinal cord may contribute to these processes more than is currently believed. Neural circuits involved in motor learning are typically associated with neural populations within the cerebellum, however, given the properties of cerebellar learning networks it may be plausible that similar circuits are present within the spinal cord. Cerebellar networks, such as those involved in learning and conditioning, are thought to involve a main controller which sends motor commands to an effector to thus initiate an action (Freeman & Steinmetz, 2011). Between controller and effector, there are other key components that allow for processing beyond motor intention translation, such as the neural comparator. To allow for the execution of complex motor behaviours, the cerebellum is thought to compare incoming motor commands with active sensory feedback, thus performing additional sensorimotor processing to determine how successful motor execution is (Brownstone et al., 2015). For many skilled motor behaviours, particularly in a rapidly changing environment, the feedback and feed-forward circuitry of a neural comparator is necessary to predict error, sensory consequences, and to instruct the required action accordingly (Brownstone et al., 2015; Freeman & Steinmetz, 2011). Within the comparator module specifically, it is thought to receive input on both motor prediction and instruction to allow for motor learning and correction.

With respect to spinal motor learning, it is hypothesized that motoneurons may function as fundamental comparator neurons due to their contributions as the controller to muscle contraction and direct inputs from sensory afferents (Brownstone et al., 2015). Considering other spinal neurons, Renshaw cells have also been hypothesized to be part of this module due to their involvement in recurrent inhibition. The excitation they receive from motoneurons would suggest

that they receive a feed-forward copy of motor commands. Given the dI3's extensive cutaneous and proprioceptive inputs and their direct projections to motoneurons, we suggest that dI3s would receive sensory feedback and that together with Renshaw cells, these two neuron populations form the core of a comparator. We suggest that a dI3 comparator module may function wherein sensory inputs are integrated and compared to ongoing motoneuron activity that is conveyed by Renshaw cells, which are the only known spinal neurons to receive excitation from motoneurons through their central axon collaterals. This comparator module would compare sensory inputs processed by dI3s (what the body is doing) and motoneuron activity monitored by Renshaw cells (what the nervous system is trying to do) to rapidly adjust ongoing movements through direct excitation of motoneurons by dI3s and direct inhibition of dI3s by Renshaw cells (Figure 4.3). Given our knowledge of comparator modules within the cerebellum, we suggest that a spinal comparator module comprising dI3 circuits may operate in a similar fashion with dI3s receiving both outgoing motor command from Renshaw cells and active sensory feedback from sensory afferents, thus providing sufficient information to allow for error calculation and prediction. Based upon our findings of increased motor deficits to corrective behaviours after dI3 silencing and reduced Renshaw cell activation, it appears that a dI3 comparator module may have significant contribution to the regulation of reflexes, error prediction, and rapid motor adaptation.

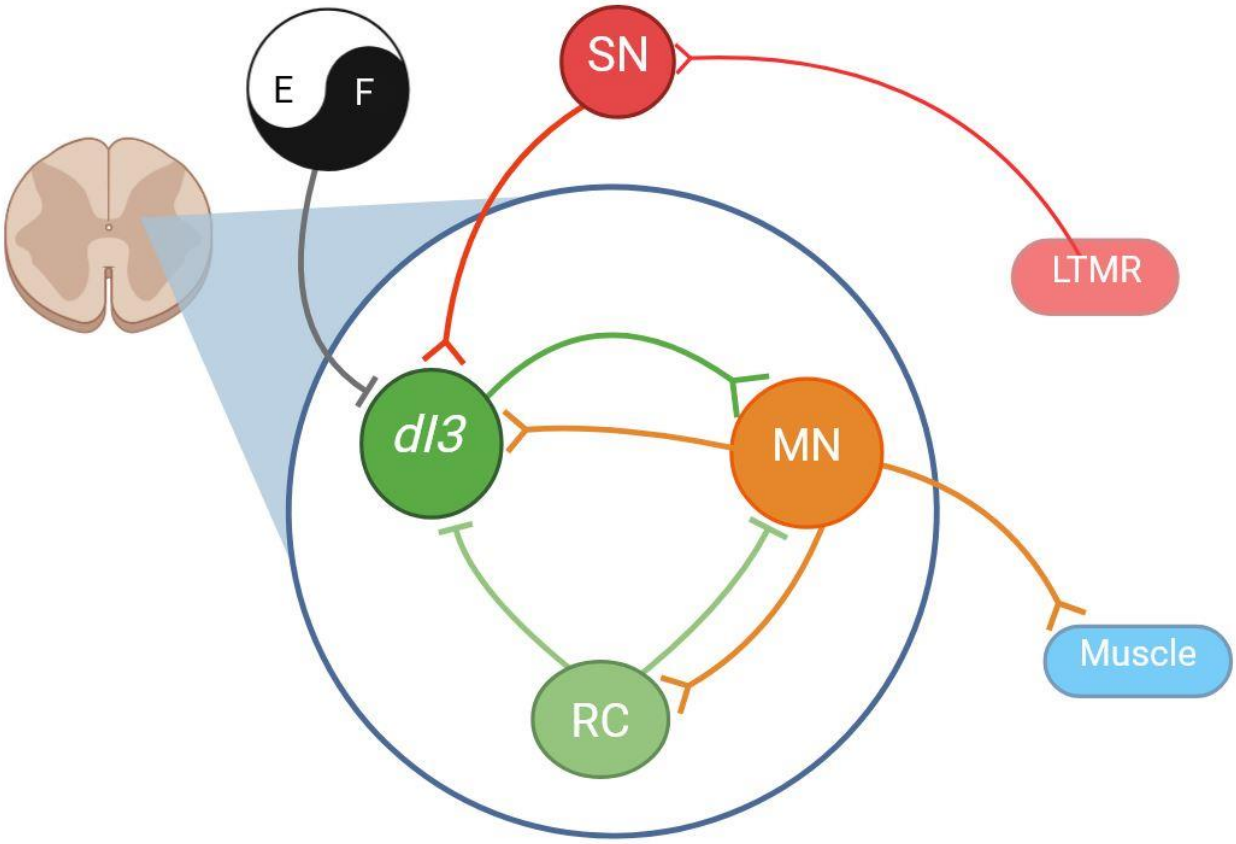

Figure 4.3 A summary of the proposed spinal circuitry of dI3 and Renshaw cell sensory integration, forming a spinal comparator module to adjust motoneuron excitation for the activation of adaptive and corrective motor behaviours, such as the stumbling corrective reaction. dI3 = dorsal interneuron 3; E/F = Central pattern generator (extensor/flexor); LTMR = low-threshold mechanoreceptor; SN = sensory neuron; MN = motoneuron; RC = Renshaw cell. Flathead arrows indicate inhibition, branched arrows indicate excitation. Diagram created with *BioRender*.

4.4 Study limitations

The goal of our study was to determine the potential impacts to corrective motor behaviours upon silencing dI3 spinal neurons in adult mice. For this purpose, we utilized two different mouse models to manipulate dI3 activity, each presenting their own potential limitations. With the use of our AAV-transduced *hM4Di* line, the expression of the inhibitory DREADD *hM4Di* was induced through spinal injection of the viral construct into various sites of the spinal cord. While the use of a high-quality microinjector and skilled technician can allow for precise targeting of landmarks of the spinal cord, it is possible that the injection of virus may bleed and spread to areas of the spinal cord beyond the desired target area, thus potentially reducing the concentration of virus in target areas and resulting in reduced DREADD receptor expression. Alternatively, with our transgenic *hM4Di* mouse line, wherein the DREADD receptor is endogenously expressed in dI3s, there is the possibility of receptor expression in spinal neurons beyond dI3s. Prior research has demonstrated the expression of Isl1 and Vglut2 transcription factors to define the differentiation of some sensory neurons (Fremeau et al., 2004; Scherrer et al., 2010; Sun et al., 2008), thus there is the possibility of *hM4Di* receptor expression in select sensory neurons as well as dI3s. While the two mouse models demonstrate advantages and disadvantages, the use of both within this study was intentional to determine if any significant differences would be seen in terms of impact to locomotion and overall levels of DREADD receptor expression. Fortunately, we did not observe any significant differences in terms of the severity or strength of impacts to corrective behaviours between the two mouse lines, thus suggesting both as reliable models for dI3 circuit manipulation.

Additionally, there is the possibility of sex differences to present an impact on the results within this study. Due to the nature of selective breeding and requiring specific genotypes from a given litter, it was not possible to obtain equal numbers of male and female mice for these

experiments. Thus, a majority of female mice was utilized (8 females, 4 males) for surgical procedures and behavioural testing. There are some physiological contexts demonstrated within the literature wherein females can present a slightly different phenotype, such as increased pain prevalence after spinal cord injury (Burke et al., 2019) or lower performance in behavioural tasks such as the Rotarod after brain lesioning (Antzoulatos et al., 2010). However, the likelihood of sex differences within intact animals in a motor control context is likely to be lower without the presence of injury. Indeed, stride length and walking gait may demonstrate slight differences between male and female mice (Antzoulatos et al., 2010), however we did not observe any statistically significant differences between male and female groups.

It is also important to note that some of the pharmacological interventions used within this study also demonstrate some limitations. While our *hM4Di* agonist, JHU37160, was designed specifically for targeted DREADD manipulation and presents robust specificity, the interventions used for Renshaw cell manipulation are slightly less specific. Without the use of a transgenic mouse line designed to genetically target Renshaw cells, we relied upon nicotinic acetylcholine receptor antagonist mecamylamine to blunt the activation of Renshaw cells. While many studies have demonstrated the direct effects of mecamylamine upon Renshaw cell excitation and firing, showing that Renshaw cells behave like nicotinic cholinergic synapses and exhibit depressed activity after mecamylamine administration (Noga et al., 1987; Ueki et al., 1961), it is possible that this nicotinic antagonist may also depress cholinergic signaling on a more global scale. To determine if additional impacts to motor control were present from mecamylamine administration, preliminary testing was conducted in control mice, prior to behavioural testing, using a range of mecamylamine dosages. With a range from low to high dosages, we did not observe any significant changes to basic locomotor function (i.e., basic stepping, alertness, motivation, etc.) after

mecamylamine administration. Similarly with L-acetyl carnitine, this cholinergic compound has been demonstrated to enhance the activation of Renshaw cells through increasing synaptic drive of motoneuron collaterals (Mazzocchio & Rossi, 1997). While we performed the same dosage range preliminary testing with L-acetyl carnitine and saw no observable changes to basic behaviour, it is still possible that the administration of this compound could potentially have had broader effects in other cholinergic cells.

4.5 Implications for future research

To date, there are very few studies investigating motor circuits in the scope of dI3s specifically. Here we present two unique models for manipulating dI3 spinal circuitry with targeted chemogenetic techniques like DREADDs. The mouse lines and designer drugs utilized within our experiments for investigating dI3 function present an effective method for inducing temporary changes to neuron activity, rather than inducing permanent ablations or knockouts from birth. With the ability to transiently alter dI3 excitation, the role of these spinal neurons can be investigated under a broad range of conditions, developmental stages, and behavioural tests. A more thorough investigation of dI3 function and motor contribution could be useful for not only clarifying unknown spinal circuits, but also for creating new transgenic or optogenetic models for manipulating other spinal neurons operating within dI3 circuits. Future work could involve investigation of the synaptic connections between dI3s and Renshaw cells to determine how sensory information is processed within this neuronal comparator module; studies mapping the full synaptic connections between Renshaw cells and dI3s would present a greater understanding of the synaptic properties of this module. Investigation into other reflexes and corrective behaviours after dI3 circuit manipulation would also prove valuable, such as examining

performance on tests like the Rotarod, inclined ladder climb, or balance beam with varying beam diameters to assess how strongly dI3s are involved with motor parameters like coordination, balance, and even forelimb function.

With respect to the stumbling corrective reaction, there is little research identifying specific spinal neurons associated with the activation and modulation of this reflex. Our findings are among the first to identify dI3s as contributors to this corrective behaviour. While many studies have described interneuronal pathways that propose unknown spinal neurons as sensorimotor integrators for the SCR, we now have a better understanding of this spinal circuit in which dI3s are likely to be an important integrator within this pathway. Future work with similar mouse models and methodology could determine what other, if any, spinal neurons are involved in modulating the threshold of this reflex. With this broader knowledge, many further experiments could be conducted using diverse and complex locomotor tasks to obtain a more detailed understanding of other motor behaviours in which dI3s regulate.

Given our hypothesis of a dI3 comparator module, it may even suggest a potential role for dI3s in spinal learning. Although motor learning is often thought to be regulated by supraspinal processes, our work suggests that the spinal cord may have more involvement in learning and motor control than previously understood. Future experiments examining motor learning, such as the pellet grab or maze tests, after dI3 circuit manipulation could uncover more significant and complex functions of spinal neurons and enhance our understanding of spinal learning. Motor learning within the spinal cord could even be investigated within the scope of spinal cord injury, investigating possible involvement in recovering motor function after injury with the manipulation of dI3 spinal circuits. Given their functional role in recovery after spinal cord injury (Bui et al.,

2016; Goltash et al., 2023), research investigating dI3s as a potential target for future therapies to improve motor deficits resulting from spinal cord injury or disease would be useful. Investigating a potential role for enhancing spinal learning could point to the dI3 comparator module as a key target for the regulation of motor control and spinal plasticity.

4.6 Concluding thoughts

Despite the significant advancements in chemogenetic and molecular genetic techniques in animal research, we have yet to fully understand the roles and functions of many spinal neurons. dI3 neurons have been of interest for many years due to their projections to motoneurons and, recently, their projections from Renshaw cells. Within this study we have investigated various corrective behaviours, including the stumbling corrective reaction, and have discovered dI3s to have significant influence in the ability to predict error and perform motor corrections in a mouse model. While a lack of dI3 activity does not result in a complete inhibition of corrective behaviours, it does appear to impair the ability to integrate proprioceptive and cutaneous information whilst moving through more complex environments, thus resulting in poor motor adaptation and poor motor recovery after error. Specifically with the SCR, we observed a blunted reaction to both electrical and mechanical perturbations after dI3 silencing. For other tasks such as the horizontal ladder and balance beam, an increased instability and paw slipping was observed with reduced dI3 activity. Overall, this suggests that dI3 spinal neurons are an important modulator of corrective behaviours by actively processing sensory inputs to thereby modulate motoneuron excitation accordingly.

Additionally, we discovered that dI3s appear to operate alongside Renshaw cells to compare various sensory inputs for rapid initiation of motor correction. Given their newly identified projections to dI3s through a collaboration with the Brownstone lab, reduced Renshaw cell activity appears to induce similar changes to corrective behaviours as dI3 silencing, wherein rapid motor adaptation is blunted. Interestingly, despite having similar effects on locomotion, the combination of both dI3 silencing and decreased Renshaw cell excitation did not produce a compounded effect in terms of motor deficits. When the two conditions were combined, corrective behaviours were impaired to a similar degree as to what was observed after only dI3 silencing. We suggest that this finding indicates a type of shared or parallel circuitry between dI3s and Renshaw cells, wherein the two spinal neurons form a type of comparator module. This neuronal module appears to likely be involved in sensorimotor processing (both proprioceptive and cutaneous inputs) which allows for error prediction and rapid adjustment to motoneuron excitation, thus actively comparing and adjusting motor output for smooth locomotion. Conversely, we did not observe the opposite effect when enhancing Renshaw cell activation. Despite our predictions, the combination of increased Renshaw cell excitation and dI3 silencing did not compensate for the lack of dI3 activity and thus motor correction remained mostly impaired with this pharmacological treatment.

Overall, my thesis reveals new functional roles relating to dI3 spinal circuits. Until now, it was unclear whether dI3 spinal neurons were involved in reflexes beyond grasping and even other types of motor behaviours. With our transgenic mouse lines, we were able to experimentally test two chemogenetic models that allowed for consistent and robust silencing of dI3 spinal neurons to influence observable changes in locomotion. This invaluable model presents future promise for further investigation into dI3 spinal circuits, beyond corrective behaviours and reflexes. While the

complete role of dI3s in movement remains largely unclear, in this thesis we have demonstrated that dI3 spinal neurons are an important contributor to not only corrective behaviours and skilled locomotion, but also in motor error prediction and avoidance.

Bibliography

Akay, T. (2014). Long-term measurement of muscle denervation and locomotor behavior in individual wild-type and ALS model mice. *Journal of Neurophysiology*, *111*(3), 694–703. https://doi.org/10.1152/jn.00507.2013

Akay, T., Acharya, H. J., Fouad, K., & Pearson, K. G. (2006). Behavioral and Electromyographic Characterization of Mice Lacking EphA4 Receptors. *Journal of Neurophysiology*, *96*(2), 642–651. https://doi.org/10.1152/jn.00174.2006

Aljovic, A., Zhao, S., Chahin, M., De La Rosa, C., Van Steenbergen, V., Kerschensteiner, M., & Bareyre, F. M. (2022). A deep learning-based toolbox for Automated Limb Motion Analysis (ALMA) in murine models of neurological disorders. *Communications Biology*, *5*(1), 131. https://doi.org/10.1038/s42003-022-03077-6

Alvarez, F. J., Dewey, D. E., McMillin, P., & Fyffe, R. E. W. (1999). Distribution of cholinergic contacts on Renshaw cells in the rat spinal cord: A light microscopic study. *The Journal of Physiology*, *515*(3), 787–797. https://doi.org/10.1111/j.1469-7793.1999.787ab.x

Antzoulatos, E., Jakowec, M. W., Petzinger, G. M., & Wood, R. I. (2010). Sex differences in motor behavior in the MPTP mouse model of Parkinson's disease. *Pharmacology Biochemistry and Behavior*, *95*(4), 466–472. https://doi.org/10.1016/j.pbb.2010.03.009

Berger, W., Dietz, V., & Quintern, J. (1984). Corrective reactions to stumbling in man: Neuronal co-ordination of bilateral leg muscle activity during gait. *The Journal of Physiology*, *357*(1), 109–125. https://doi.org/10.1113/jphysiol.1984.sp015492

Bermingham, N. A., Hassan, B. A., Wang, V. Y., Fernandez, M., Banfi, S., Bellen, H. J., Fritzsch, B., & Zoghbi, H. Y. (2001). Proprioceptor Pathway Development Is Dependent on MATH1. *Neuron*, *30*(2), 411–422. https://doi.org/10.1016/S0896-6273(01)00305-1

Betley, J. N., Wright, C. V. E., Kawaguchi, Y., Erdélyi, F., Szabó, G., Jessell, T. M., & Kaltschmidt, J. A. (2009). Stringent Specificity in the Construction of a GABAergic Presynaptic Inhibitory Circuit. *Cell*, *139*(1), 161–174. https://doi.org/10.1016/j.cell.2009.08.027

Bhumbra, G. S., Bannatyne, B. A., Watanabe, M., Todd, A. J., Maxwell, D. J., & Beato, M. (2014). The Recurrent Case for the Renshaw Cell. *Journal of Neuroscience*, *34*(38), 12919–12932. https://doi.org/10.1523/JNEUROSCI.0199-14.2014

Bouyer, L. J. G., & Rossignol, S. (2003). Contribution of Cutaneous Inputs From the Hindpaw to the Control of Locomotion. II. Spinal Cats. *Journal of Neurophysiology*, *90*(6), 3640–3653. https://doi.org/10.1152/jn.00497.2003

Brown, A. G., Fyffe, R. E. W., Rose, P. K., & Snow, P. J. (1981). Spinal cord collaterals from axons of Type II slowly adapting units in the cat. *Journal of Physiology*, *316*, 469–480.

Brownstone, R. M., & Bui, T. V. (2010). Spinal interneurons providing input to the final common path during locomotion. In *Progress in Brain Research* (Vol. 187, pp. 81–95). Elsevier. https://doi.org/10.1016/B978-0-444-53613-6.00006-X

Brownstone, R. M., Bui, T. V., & Stifani, N. (2015). Spinal circuits for motor learning. *Current Opinion in Neurobiology*, *33*, 166–173. https://doi.org/10.1016/j.conb.2015.04.007

Bui, T. V., Akay, T., Loubani, O., Hnasko, T. S., Jessell, T. M., & Brownstone, R. M. (2013). Circuits for Grasping: Spinal dI3 Interneurons Mediate Cutaneous Control of Motor Behavior. *Neuron*, *78*(1), 191–204. https://doi.org/10.1016/j.neuron.2013.02.007

Bui, T. V., Stifani, N., Akay, T., & Brownstone, R. M. (2016). Spinal microcircuits comprising dI3 interneurons are necessary for motor functional recovery following spinal cord transection. *eLife*, *5*, e21715. https://doi.org/10.7554/eLife.21715

Bui, T. V., Stifani, N., Panek, I., & Farah, C. (2015). Genetically identified spinal interneurons integrating tactile afferents for motor control. *Journal of Neurophysiology*, *114*(6), 3050–3063. https://doi.org/10.1152/jn.00522.2015

Burke, D., Fullen, B. M., & Lennon, O. (2019). Pain profiles in a community dwelling population following spinal cord injury: A national survey. *The Journal of Spinal Cord Medicine*, *42*(2), 201–211. https://doi.org/10.1080/10790268.2017.1351051

Capelli, P., Pivetta, C., Soledad Esposito, M., & Arber, S. (2017). Locomotor speed control circuits in the caudal brainstem. *Nature*, *551*(7680), 373–377. https://doi.org/10.1038/nature24064

Chapman, P. D., Kulkarni, A. S., Trevisan, A. J., Han, K., Hinton, J. M., Deltuvaite, P., Fenno, L. E., Ramakrishnan, C., Patton, M. H., Schwarz, L. A., Zakharenko, S. S., Deisseroth, K., & Bikoff, J. B. (2024). A brain-wide map of descending inputs onto spinal V1 interneurons. *Neuron*, S0896627324008766. https://doi.org/10.1016/j.neuron.2024.11.019

Cullheim, S., & Kellerth, J. O. (1981). TWO KINDS OF RECURRENT INHIBITION OF CAT SPINAL a-MOTONEURONES AS DIFFERENTIATED PHARMACOLOGICALLY. *Journal of Physiology*, *312*, 209–224.

DeVries, K. L., & Goshgarian, H. G. (1989). Spinal cord localization and characterization of the neurons which give rise to the accessory phrenic nerve in the adult rat. *Experimental Neurology*, *104*(1), 88–90. https://doi.org/10.1016/0014-4886(89)90013-7

Dietz, V. (2003). Spinal cord pattern generators for locomotion. *Clinical Neurophysiology*, *114*(8), 1379–1389. https://doi.org/10.1016/S1388-2457(03)00120-2

Dietz, V., Quintern, J., & Berger, W. (1984). Corrective reactions to stumbling in man: Functional significance of spinal and transcortical reflexes. *Neuroscience Letters*, *44*(2), 131–135. https://doi.org/10.1016/0304-3940(84)90070-3

Dougherty, K. J., Zagoraiou, L., Satoh, D., Rozani, I., Doobar, S., Arber, S., Jessell, T. M., & Kiehn, O. (2013). Locomotor Rhythm Generation Linked to the Output of Spinal Shox2 Excitatory Interneurons. *Neuron*, *80*(4), 920–933. https://doi.org/10.1016/j.neuron.2013.08.015

Dyck, J., Lanuza, G. M., & Gosgnach, S. (2012). Functional characterization of dI6 interneurons in the neonatal mouse spinal cord. *Journal of Neurophysiology*, *107*(12), 3256–3266. https://doi.org/10.1152/jn.01132.2011

Eccles, J. C., Eccles, R. M., & Iggo, A. (1961). Distribution of recurrent inhibition among motoneurones. *Journal of Physiology*, *159*, 479–499.

Eccles, J. C., Fatt, P., & Koketsu, K. (1954). Cholinergic and inhibitory synapses in a pathway from motor-axon collaterals to motoneurones. *The Journal of Physiology*, *126*(3), 524–562. https://doi.org/10.1113/jphysiol.1954.sp005226

Enjin, A., Perry, S., Hilscher, M. M., Nagaraja, C., Larhammar, M., Gezelius, H., Eriksson, A., Leão, K. E., & Kullander, K. (2017). Developmental Disruption of Recurrent Inhibitory Feedback Results in Compensatory Adaptation in the Renshaw Cell–Motor Neuron Circuit. *The Journal of Neuroscience*, *37*(23), 5634–5647. https://doi.org/10.1523/JNEUROSCI.0949-16.2017

Forssberg, H. (1979). Stumbling corrective reaction: A phase-dependent compensatory reaction during locomotion. *Journal of Neurophysiology*, *42*(4), 936–953. https://doi.org/10.1152/jn.1979.42.4.936

Forssberg, H., Grillner, S., & Rossignol, S. (1975). Phase dependent reflex reversal during walking in chronic spinal cats. *Brain Research*, *85*(1), 103–107. https://doi.org/10.1016/0006-8993(75)91013-6

Forssberg, H., Grillner, S., & Rossignol, S. (1977). Phasic gain control of reflexes from the dorsum of the paw during spinal locomotion. *Brain Research*, *132*(1), 121–139. https://doi.org/10.1016/0006-8993(77)90710-7

Freeman, J. H., & Steinmetz, A. B. (2011a). Neural circuitry and plasticity mechanisms underlying delay eyeblink conditioning. *Learning & Memory*, *18*(10), 666–677. https://doi.org/10.1101/lm.2023011

Freeman, J. H., & Steinmetz, A. B. (2011b). Neural circuitry and plasticity mechanisms underlying delay eyeblink conditioning. *Learning & Memory*, *18*(10), 666–677. https://doi.org/10.1101/lm.2023011

Fremeau, R. T., Voglmaier, S., Seal, R. P., & Edwards, R. H. (2004). VGLUTs define subsets of excitatory neurons and suggest novel roles for glutamate. *Trends in Neurosciences*, *27*(2), 98–103. https://doi.org/10.1016/j.tins.2003.11.005

Fyffe, R. E. (1991). Spatial distribution of recurrent inhibitory synapses on spinal motoneurons in the cat. *Journal of Neurophysiology*, *65*(5), 1134–1149. https://doi.org/10.1152/jn.1991.65.5.1134

Goetz, C., Pivetta, C., & Arber, S. (2015). Distinct Limb and Trunk Premotor Circuits Establish Laterality in the Spinal Cord. *Neuron*, *85*(1), 131–144. https://doi.org/10.1016/j.neuron.2014.11.024

Goltash, S., Stevens, S. J., Topcu, E., & Bui, T. V. (2023). Changes in synaptic inputs to dI3 INs and MNs after complete transection in adult mice. *Frontiers in Neural Circuits*, *17*, 1176310. https://doi.org/10.3389/fncir.2023.1176310

Granit, R., Pascoe, J. E., & Steg, G. (1957). The behaviour of tonic alpha and gamma motoneurones during stimulation of reucrrent collaterals. *Journal of Physiology*, *138*, 381–400.

Griener, A., Zhang, W., Kao, H., Haque, F., & Gosgnach, S. (2017). Anatomical and electrophysiological characterization of a population of dI6 interneurons in the neonatal mouse spinal cord. *Neuroscience*, *362*, 47–59. https://doi.org/10.1016/j.neuroscience.2017.08.031

Gross, M. K., Dottori, M., & Goulding, M. (2002). Lbx1 Specifies Somatosensory Association Interneurons in the Dorsal Spinal Cord. *Neuron*, *34*(4), 535–549. https://doi.org/10.1016/S0896-6273(02)00690-6

Hamilton, L. D., Mani, D., Almuklass, A. M., Davis, L. A., Vieira, T., Botter, A., & Enoka, R. M. (2018). Electrical nerve stimulation modulates motor unit activity in contralateral biceps brachii during steady isometric contractions. *Journal of Neurophysiology*, *120*(5), 2603–2613. https://doi.org/10.1152/jn.00235.2018

Harrison, M., O'Brien, A., Adams, L., Cowin, G., Ruitenberg, M. J., Sengul, G., & Watson, C. (2013). Vertebral landmarks for the identification of spinal cord segments in the mouse. *NeuroImage*, *68*, 22–29. https://doi.org/10.1016/j.neuroimage.2012.11.048

Harrison, P. J., Jankowska, E., & Zytnicki, D. (1986). Lamina VIII interneurones interposed in crossed reflex pathways in the cat. *The Journal of Physiology*, *371*(1), 147–166. https://doi.org/10.1113/jphysiol.1986.sp015965

Hilaire, G., Khatib, M., & Monteau, R. (1986). Central drive on Renshaw cells coupled with phrenic motoneurons. *Brain Research*, *376*(1), 133–139. https://doi.org/10.1016/0006-8993(86)90907-8

Hoover, J. E., & Durkovic, R. G. (1992). Retrograde Labeling of Lumbosacral Interneurons Following Injections of Red and Green Fluorescent Microspheres into Hindlimb Motor Nuclei of the Cat. *Somatosensory & Motor Research*, *9*(3), 211–226. https://doi.org/10.3109/08990229209144772

Hultborn, H., Lindstrom, S., & Wigstrom, H. (1979). On the function of recurrent inhibition in the spinal cord. *Experimental Brain Research*, *37*(2). https://doi.org/10.1007/BF00237722

Kaneko, S., Niki, Y., Yamada, K., Nasukawa, D., Ujihara, Y., & Toda, K. (2022). Systemic injection of nicotinic acetylcholine receptor antagonist mecamylamine affects licking, eyelid size, and locomotor and autonomic activities but not temporal prediction in male mice. *Molecular Brain*, *15*(1), 77. https://doi.org/10.1186/s13041-022-00959-y

Kwan, A. C., Dietz, S. B., Webb, W. W., & Harris-Warrick, R. M. (2009). Activity of Hb9 Interneurons during Fictive Locomotion in Mouse Spinal Cord. *The Journal of Neuroscience*, *29*(37), 11601–11613. https://doi.org/10.1523/JNEUROSCI.1612-09.2009

Laliberte, A. M., Farah, C., Steiner, K. R., Tariq, O., & Bui, T. V. (2022). Changes in Sensorimotor Connectivity to dI3 Interneurons in Relation to the Postnatal Maturation of Grasping. *Frontiers in Neural Circuits*, *15*, 768235. https://doi.org/10.3389/fncir.2021.768235

Lam, T., Wolstenholme, C., Van Der Linden, M., Pang, M. Y. C., & Yang, J. F. (2003). Stumbling Corrective Responses During Treadmill-Elicited Stepping in Human Infants. *The Journal of Physiology*, *553*(1), 319–331. https://doi.org/10.1113/jphysiol.2003.043984

Levinsson, A., Holmberg, H., Broman, J., Zhang, M., & Schouenborg, J. (2002). Spinal Sensorimotor Transformation: Relation between Cutaneous Somatotopy and a Reflex Network. *The Journal of Neuroscience*, *22*(18), 8170–8182. https://doi.org/10.1523/JNEUROSCI.22-18-08170.2002

Liem, K. F., Tremml, G., & Jessell, T. M. (1997). A Role for the Roof Plate and Its Resident TGFb-Related Proteins in Neuronal Patterning in the Dorsal Spinal Cord. *Cell Press*, *91*, 127–138.

Maltenfort, M. G., McCurdy, M. L., Phillips, C. A., Turkin, V. V., & Hamm, T. M. (2004). Location and Magnitude of Conductance Changes Produced by Renshaw Recurrent Inhibition in Spinal Motoneurons. *Journal of Neurophysiology*, *92*(3), 1417–1432. https://doi.org/10.1152/jn.00874.2003

Mathis, A., Mamidanna, P., Cury, K. M., Abe, T., Murthy, V. N., Mathis, M. W., & Bethge, M. (2018). DeepLabCut: Markerless pose estimation of user-defined body parts with deep learning. *Nature Neuroscience*, *21*(9), 1281–1289. https://doi.org/10.1038/s41593-018-0209-y

Mayer, W. P., & Akay, T. (2018). Stumbling corrective reaction elicited by mechanical and electrical stimulation of the saphenous nerve in walking mice. *Journal of Experimental Biology*, jeb.178095. https://doi.org/10.1242/jeb.178095

Mazzocchio, R., & Rossi, A. (1997). A method for potentiating Renshaw cell activity in humans. *Brain Research Protocols*, *2*(1), 53–58. https://doi.org/10.1016/S1385-299X(97)00028-7

Mazzocchio, R., Schieppati, M., Scarpini, C., & Rossi, A. (1990). Enhancement of recurrent inhibition by intravenous administration of L-acetylcarnitine in spastic patients. *Journal of Neurology*, *53*, 321–326.

McVea, D. A., & Pearson, K. G. (2007). Long-Lasting, Context-Dependent Modification of Stepping in the Cat After Repeated Stumbling-Corrective Responses. *Journal of Neurophysiology*, *97*(1), 659–669. https://doi.org/10.1152/jn.00921.2006

Merlet, A. N., Jéhannin, P., Mari, S., Lecomte, C. G., Audet, J., Harnie, J., Rybak, I. A., Prilutsky, B. I., & Frigon, A. (2022). Sensory Perturbations from Hindlimb Cutaneous Afferents Generate Coordinated Functional Responses in All Four Limbs during Locomotion in Intact Cats. *Eneuro*, *9*(6), ENEURO.0178-22.2022. https://doi.org/10.1523/ENEURO.0178-22.2022

Molander, C., & Grant, G. (1986). Laminar distribution of somatotopic organization of primary afferent fibers from hindlimb nerves in the dorsal horn. A study by transganglionic transport of horseradish peroxidase in the rat. *Neuroscience*, *19*, 297–312.

Müller, T., Anlag, K., Wildner, H., Britsch, S., Treier, M., & Birchmeier, C. (2005). The bHLH factor Olig3 coordinates the specification of dorsal neurons in the spinal cord. *Genes & Development*, *19*(6), 733–743. https://doi.org/10.1101/gad.326105

Müller, T., Brohmann, H., Pierani, A., Heppenstall, P. A., Lewin, G. R., Jessell, T. M., & Birchmeier, C. (2002). The Homeodomain Factor Lbx1 Distinguishes Two Major Programs of Neuronal Differentiation in the Dorsal Spinal Cord. *Neuron*, *34*(4), 551–562. https://doi.org/10.1016/S0896-6273(02)00689-X

Nakada, Y., Hunsaker, T. L., Henke, R. M., & Johnson, J. E. (2004). Distinct domains within Mash1 and Math1 are required for function in neuronal differentiation versus neuronal cell-type specification. *Development*, *131*(6), 1319–1330. https://doi.org/10.1242/dev.01008

Nakada, Y., Parab, P., Simmons, A., Omer-Abdalla, A., & Johnson, J. E. (2004). Separable enhancer sequences regulate the expression of the neural bHLH transcription factor neurogenin 1. *Developmental Biology*, *271*(2), 479–487. https://doi.org/10.1016/j.ydbio.2004.04.021

Nath, T., Mathis, A., Chen, A. C., Patel, A., Bethge, M., & Mathis, M. W. (2019). Using DeepLabCut for 3D markerless pose estimation across species and behaviors. *Nature Protocols*, *14*(7), 2152–2176. https://doi.org/10.1038/s41596-019-0176-0

Noga, B. R., Shefchyk, S. J., Jamal, J., & Jordan, L. M. (1987). The role of Renshaw cells in locomotion: Antagonism of their excitation from motor axon collaterals with intravenous mecamylamine. *Experimental Brain Research*, *66*(1). https://doi.org/10.1007/BF00236206

Panneton, W. M., Gan, Q., & Juric, R. (2005). The central termination of sensory fibers from nerves to the gastrocnemius muscle of the rat. *Neuroscience*, *134*(1), 175–187. https://doi.org/10.1016/j.neuroscience.2005.02.032

Pearcey, G. E. P., & Zehr, E. P. (2020). Repeated and patterned stimulation of cutaneous reflex pathways amplifies spinal cord excitability. *Journal of Neurophysiology*, *124*(2), 342–351. https://doi.org/10.1152/jn.00072.2020

Pearson, K. G., Acharya, H., & Fouad, K. (2005). A new electrode configuration for recording electromyographic activity in behaving mice. *Journal of Neuroscience Methods*, *148*(1), 36–42. https://doi.org/10.1016/j.jneumeth.2005.04.006

Pivetta, C., Esposito, M. S., Sigrist, M., & Arber, S. (2014). Motor-Circuit Communication Matrix from Spinal Cord to Brainstem Neurons Revealed by Developmental Origin. *Cell*, *156*(3), 537–548. https://doi.org/10.1016/j.cell.2013.12.014

Potocanac, Z., Pijnappels, M., Verschueren, S., Van Dieën, J., & Duysens, J. (2016). Two-stage muscle activity responses in decisions about leg movement adjustments during trip recovery. *Journal of Neurophysiology*, *115*(1), 143–156. https://doi.org/10.1152/jn.00263.2015

Puskár, Z., & Antal, M. (1997). Localization of last-order premotor interneurons in the lumbar spinal cord of rats. *The Journal of Comparative Neurology*, *389*(3), 377–389. https://doi.org/10.1002/(SICI)1096-9861(19971222)389:3<377::AID-CNE2>3.0.CO;2-Y

Quevedo, J., Stecina, K., Gosgnach, S., & McCrea, D. A. (2005). Stumbling Corrective Reaction During Fictive Locomotion in the Cat. *Journal of Neurophysiology*, *94*(3), 2045–2052. https://doi.org/10.1152/jn.00175.2005

Quevedo, J., Stecina, K., & McCrea, D. A. (2005). Intracellular Analysis of Reflex Pathways Underlying the Stumbling Corrective Reaction During Fictive Locomotion in the Cat. *Journal of Neurophysiology*, *94*(3), 2053–2062. https://doi.org/10.1152/jn.00176.2005

Radhakrishnan, R., & Sluka, K. A. (2005). Deep Tissue Afferents, but not Cutaneous Afferents, Mediate Transcutaneous Electrical Nerve Stimulation–Induced Antihyperalgesia. *The Journal of Pain*, *6*(10), 673–680. https://doi.org/10.1016/j.jpain.2005.06.001

Renshaw, B. (1946). Central effects of centripetal impulses in axons of spinal ventral roots. *Journal of Neurophysiology*, *9*(3), 191–204. https://doi.org/10.1152/jn.1946.9.3.191

Rexed, B. (1952). The cytoarchitectonic organization of the spinal cord in the cat. *Journal of Comparative Neurology*, *96*(3), 415–495. https://doi.org/10.1002/cne.900960303

Rexed, B. (1954). A cytoarchitectonic atlas of the spinal coed in the cat. *Journal of Comparative Neurology*, *100*(2), 297–379. https://doi.org/10.1002/cne.901000205

Scherrer, G., Low, S. A., Wang, X., Zhang, J., Yamanaka, H., Urban, R., Solorzano, C., Harper, B., Hnasko, T. S., Edwards, R. H., & Basbaum, A. I. (2010). VGLUT2 expression in primary afferent neurons is essential for normal acute pain and injury-induced heat hypersensitivity. *Proceedings of the National Academy of Sciences*, *107*(51), 22296–22301. https://doi.org/10.1073/pnas.1013413108

Sun, Y., Dykes, I. M., Liang, X., Eng, S. R., Evans, S. M., & Turner, E. E. (2008). A central role for Islet1 in sensory neuron development linking sensory and spinal gene regulatory programs. *Nature Neuroscience*, *11*(11), 1283–1293. https://doi.org/10.1038/nn.2209

Takeoka, A., Vollenweider, I., Courtine, G., & Arber, S. (2014). Muscle Spindle Feedback Directs Locomotor Recovery and Circuit Reorganization after Spinal Cord Injury. *Cell*, *159*(7), 1626–1639. https://doi.org/10.1016/j.cell.2014.11.019

Talpalar, A. E., Bouvier, J., Borgius, L., Fortin, G., Pierani, A., & Kiehn, O. (2013). Dual-mode operation of neuronal networks involved in left–right alternation. *Nature*, *500*(7460), 85–88. https://doi.org/10.1038/nature12286

Ueki, S., Koketsu, K., & Domino, E. F. (1961). Effects of mecamylamine on the Golgi recurrent collateral—Renshaw-cell synapse in the spinal cord. *Experimental Neurology*, *3*(2), 141–148. https://doi.org/10.1016/0014-4886(61)90064-4

Wand, P., Prochazka, A., & Sontag, K.-H. (1980). Neuromuscular responses to gait perturbations in freely moving cats. *Experimental Brain Research*, *38*(1). https://doi.org/10.1007/BF00237937

Zehr, E. P. (2006). Training-induced adaptive plasticity in human somatosensory reflex pathways. *Journal of Applied Physiology*, *101*(6), 1783–1794. https://doi.org/10.1152/japplphysiol.00540.2006

Zehr, E. P., Komiyama, T., & Stein, R. B. (1997). Cutaneous Reflexes During Human Gait: Electromyographic and Kinematic Responses to Electrical Stimulation. *Journal of Neurophysiology*, *77*(6), 3311–3325. https://doi.org/10.1152/jn.1997.77.6.3311

Zhang, J., Lanuza, G. M., Britz, O., Wang, Z., Siembab, V. C., Zhang, Y., Velasquez, T., Alvarez, F. J., Frank, E., & Goulding, M. (2014). V1 and V2b Interneurons Secure the Alternating Flexor-Extensor Motor Activity Mice Require for Limbed Locomotion. *Neuron*, *82*(1), 138–150. https://doi.org/10.1016/j.neuron.2014.02.013